Title

Neutral and Cationic Vanadium Bisimido Complexes: Their Synthesis, Characterization, and Application in the Binding, Activation, and Catalytic Functionalization of Small Molecules

Author

La Pierre, Henry Storms

Publication Date

2011

Peer reviewed|Thesis/dissertation

Neutral and Cationic Vanadium Bisimido Complexes: Their Synthesis, Characterization, and Application in the Binding, Activation, and Catalytic Functionalization of Small Molecules

By

Henry Storms La Pierre

A dissertation submitted in partial satisfaction of the

requirements for the degree of

Doctor of Philosophy

in

Chemistry

in the

Graduate Division

of the

University of California, Berkeley

Committee in charge:

Professor John Arnold, Co-Chair
Professor F. Dean Toste, Co-Chair
Professor Alexander Katz

Fall 2011

Abstract

Neutral and Cationic Vanadium Bisimido Complexes: Their Synthesis, Characterization, and Application in the Binding, Activation, and Catalytic Functionalization of Small Molecules

by

Henry Storms La Pierre

Doctor of Philosophy in Chemistry

University of California, Berkeley

Professor John Arnold, Co-Chair

Professor F. Dean Toste, Co-Chair

Chapter 1: The syntheses of neutral (halide and aryl) and cationic vanadium bisimides are described. Characterization of the complexes by X-ray diffraction, ^{13}C NMR, ^{51}V NMR, and V $L_{2,3}$-edge NEXFAS provide a description of the electronic structure in comparison to group 6 bisimides and the bent metallocene isolobal analogs.

Chapter 2: Under 1 atm of H_2, $[V(N\textit{t}Bu)_2(PMe_3)_3][Al(PFTB)_4]$, **1.10**, (PFTB = perfluoro-*tert*-butoxide), was shown to catalytically semihydrogenate alkynes to (*z*)-alkenes. Synthetic and DFT studies, in combination with H_2/D_2 crossover and PHIP NMR experiments, indicate that H_2 is activated by [1,2]-addition to **1.10** and upon the insertion of alkyne into the V-H bond of the vanadium hydrido amide **A**, the product alkene and **1.10** are generated by the [1,2]-α-NH-elimination of the alkenyl ligand.

Chapter 3: A series of carbon monoxide, isocyanide, and nitrile complexes of $[V(PR_3)_2(N^tBu)_2][Al(PFTB)_4]$, (R = Me, Et) were prepared. $[V(PMe_3)_3(N^tBu)_2][Al(PFTB)_4]$, (PFTB = perfluoro-*tert*-butoxide) reacts with 2,6-xylylisocyanide (CNXyl) or acetonitrile to afford complexes **3.1** and **3.2**. Complex **3.1** was crystallographically characterized revealing a C-N bond length of (1.152(4) Å), and IR studies showed a C-N stretching frequency of 2164 cm^{-1}. Treatment of $[V(PEt_3)_2(N^tBu)_2][Al(PFTB)_4]$ with CNXyl yielded the desired isocyanide complex in 60% yield with a C-N stretching frequency of 2156 cm^{-1}. The desired d^0 vanadium bisimido, carbonyl complex was achieved *via* the exposure of **1.11** to 1 atm of CO. Complex **3.4** has a C-O stretching frequency of 2015 cm^{-1} (CaF_2 solution cell). Isotopic labeling with ^{13}CO reveals a stretching frequency of 1970 cm^{-1}, which confirms the assignment of the complex as a terminal η^1-CO complex and which is also implied by its NMR data in comparison to the other crystallographically characterized compounds presented here. The $^{13}C\{^{31}P\}\{^1H\}$ NMR spectrum of **3.4-^{13}C** reveals a broad singlet at 228.36 ppm implying deshielding of the carbonyl carbon. This datum, in conjunction with the shielded vanadium NMR shift of -843.71 ppm, suggests π back-bonding is

operative in the bond between carbon monoxide and **1.11**. This model was further confirmed by DFT analysis of the model complex $[V(\eta^1\text{-}CO)(PMe_3)_2(N^tBu)_2]^+$, **3.5**, which reveals that the basis of the reduced stretching frequency in **3.4** is π back-bonding from the $2b_1$ and $1b_2$ orbitals of **1.11**.

Neutral and Cationic Vanadium Bisimido Complexes: Their Synthesis, Characterization, and Application in the Binding, Activation, and Catalytic Functionalization of Small Molecules

Table of Contents

Acknowledgements

Graduate school was definitely not what I expected. The challenges I found most frustrating were actually outside of lab. That frustration and, at times anxiety, would occasionally find its way back to work. Fortunately I had the advising team of John Arnold, Bob Bergman, and Dean Toste to point me back to the quite enjoyable (but still frustrating) problems of my thesis. While I did not achieve all the work I could have, what I did produce would have been absolutely impossible without their patient guidance. I am deeply indebted to them for focusing and fine-tuning my scientific approach and allowing me to pursue the problems that were particularly interesting to me.

I would not have been able to navigate Berkeley without the help of Roger Sender, who tirelessly kept the Arnold and Toste labs running smoothly and kept me out of trouble with the bureaucracy. Anneke Runtapalit taught me the ropes of writing a grant with Bob and made sure the work got done – hopefully we will finally hear good news on that endeavor soon. Drs. Antonio G. DiPisquale, Chris Canlas, and Jamin Krinsky were three corner stones of my education here. As much of the details of data acquisition are not taught in class, the heavy lifting of making efficient and productive graduate students falls on their shoulders – thank you for the very large amount of time you all spent on teaching me X-ray, NMR, and DFT methods. As should be evident, this thesis would not exist otherwise.

My undergraduate research advisors, Profs. Jared T. Shaw and Masahiro Murakami, were essential in my development into a chemist. When I first joined Jared's lab I was photography major, a concentration also known as "Visual and Environmental Studies," at Harvard. Jared, your patience with my intellectual attention deficit in college (I changed majors at least once a semester) and careful cajoling allowed me to find a home for my creative instincts in synthetic chemistry. Your insistence on the development of technique has also paid great dividends in my graduate work. Prof. Murakami took quite a gamble on an American undergraduate student. Without him I would not have learned organometallic chemistry – thank you Masahiro for fostering my initial interest in the field that has captured my imagination for the last five years and will hopefully provide the basis of a career.

I have taken a rather circuitous route through the Berkeley department but my first and lasting home was the Toste lab. While my intellectual interests moved from the core of the group, your support in executing my work has been essential. I owe particular thanks to my cohort in the Toste lab – Greg, Asa, and Steve – I am sure you all be successful in your next endeavors. Hopefully Greg, you and I can get back to our brainstorming sessions.

My physical and intellectual home of the last four years was the Arnold lab. It is hard to capture how important all of you are to me. I should start with Sergio – you and I have been the core of the group through many changes – including a short while where it was just you and I running all of the lab – isn't it great to have some help now? I wish you and Tanya the best – I am already looking forward to lab reunions, it will be great to socialize more without the lab as the constant backdrop. Stefan – my labmate of three years – you have taught me many things essential for the rest of my life: a new intellectual interest in the actinides, efficiency (in theory), and productivity, as well as providing a real example of a successful career balanced with a satisfying personal life. I

am very glad our friendship survived being labmates. Hopefully Thomas and I will have a similar post – did you 'borrow' my lab gear – boost. Neil, your direct influence on the ideas contained in this thesis is immense – our collaboration was essential and extremely enjoyable. You said that I taught you 'big ideas,' well, you taught me how to do real, detailed chemistry and the methods to create narratives that actually make some progress towards those original, motivating 'big ideas.' Don't worry, I have kept the floppy-haired cabal going – at the end of my thesis I have shoulder length hair. Wayne, you and I did not have a frictionless relationship, but I would be remiss in not acknowledging and thanking you for pushing me to be a better student. Of course the lab has changed substantially since I first joined and I leave the floppy-haired cabal to Dan, Ashleigh, Thomas, and Heather. I hope that I have been helpful – your contributions to the group have been significant. I am sure you will be successful in the coming years. Make sure The Long Johns (aka Los Juanes Largos) survive and prosper.

I was fortunate enough in my last two years here to have Thomas join my project, and quite rapidly become a very good friend. While I have may have mentored you when you first joined, you quickly surpassed my abilities in many ways. It has been wonderful sharing ideas and a lab with you (despite the frequent thievery!). Greg, as the unofficial Arnold group postdoc and mentor, you have made the last year and half wonderful. You may not have noticed, but you have been a much-needed foil for all matters intellectual and personal. While you may disagree, you are actually an excellent wingman. I am always available to return the favor – I look forward to seeing you in Europe next year. Mark – thank you for joining my project. You synthetic skill and commitment to work the same crazy hours as I are much appreciated. You'll be great in graduate school – just get the application submitted! I am sure there are those I have forgotten to mention: I apologize. Thank you for your help as well.

Mom and Dad, you have been absolutely amazing. Thank you supporting me. It is difficult to summarize our relationship in a paragraph or a longer form, but it is easy to do in a few words: I love you both. Always remember that simple fact – it is the basis of all we have achieved. I have been fortunate to share my last 27 years with a large, wonderful, but geographically separated family. Unfortunately three very important people are not here at the end of my Ph.D.: Jacqui, Grandpa Bill and Grandpa Doug. I miss you all and wish I could share this accomplishment with you.

Sara – I am so happy I found you: I love you. You center my life and keep me calm, and this thesis would not be without you. Thank you for putting up with the many moods and anxieties this work has produced. While the next stage presents new challenges for us, I am sure we will find a way through them together.

Henry Storms La Pierre

Education

Ph.D., Inorganic Chemistry, **University of California** – Berkeley, CA 2006 – 2011
A.B., *magna cum laude*, Chemistry, **Harvard University** – Cambridge, MA 2002 – 2006
Honors Degree, **John Burroughs School** – Saint Louis, MO 1998 – 2002

Research Experience

University of Erlangen – *with Prof. Karsten Meyer* 2011 –
- Coordination chemistry and pnictogen activation/transfer reactions of uranium complexes.

University of California – *with Profs. John Arnold, Robert G. Bergman, and F. Dean Toste* 2006 – 2011
- Synthesis, characterization, and reactivity studies of vanadium bisimido complexes.

Broad Institute of Harvard and MIT – *with Prof. Jared T. Shaw* 2004 – 2006
- Synthesis of asymmetrically benzylated derivatives of pinocembrin.

Kyoto University – *with Prof. Masahiro Murakami* 2005
- Synthesis and reactivity studies of 3-(1-silacyclobutyl)cyclobutene.

Distinctions

William G. Dauben Memorial Fellowship (Departmental Award for Distinguished Academic Achievement) 2009 – 2010
Outstanding Graduate Student Instructor Award for exceptional achievements as a teacher in Chemistry 3a, Spring 2008 2009
National Science Foundation (NSF) Pre-Doctoral Fellowship 2006 – 2011
Herchel Smith Harvard Summer Undergraduate Research Fellowship for organometallic chemistry at Kyoto University with Prof. Masahiro Murakami 2005
National Merit Scholar 2002

Publications

3. "Carbon Monoxide, Isocyanide, and Nitrile Complexes of a d^0 Vanadium Bisimide: Pi-Back Bonding Derived from the Pi Symmetry, Bonding Bisimido Ligand Orbitals," Henry S. La Pierre, John Arnold, Robert G. Bergman, and F. Dean Toste *J. Am. Chem. Soc.,* **Submitted.**

2. "(Z)-Selective, Semihydrogenation of Alkynes Catalyzed by a Cationic, Vanadium Bisimido Complex," Henry S. La Pierre, John Arnold, and F. Dean Toste, *Angew. Chem., Int. Ed.* **2011**, 50(*17*), 3900-3903.

1. "Synthesis of Antimicrobial Natural Products Targeting FtsZ: (+/-)-Dichamanetin and (+/-)-2"'-hydroxy-5"-benzylisouvarinol," Sameer Urgaonkar, Henry S. La Pierre, Israel Meir, Heinrik Lund, Debabrata RayChaudhuri, and Jared T. Shaw, *Org. Lett.* **2005**, *7*, 5609-5612.

Invited Seminars

5. "Catalytic Hydrogenation of Alkynes by a Cationic Vanadium Bisimido Complex," Presented at the 239th ACS National Meeting, San Francisco, CA, March 24, 2010.

4. Alexander Pines Group Seminar; Presented at University of California, Berkeley, CA, February 12, 2010.

3. "Synthesis of a Cationic Vanadium Bisimido Complex and its Reversible Addition of H_2," Presented at the International Symposium on Bio-Environmental Chemistry, Osaka University, Osaka, JP, December 19-20, 2009.

2. "Synthesis of Vanadium Bisimido Complexes: Progress Towards a C-H Bond Functionalization Reaction," Presented at the UC-Berkeley Graduate Research Seminar Series, University of California, Berkeley, CA, January 24, 2008.

1. "Synthesis and Thermal Ring-opening Reaction of 3-(1-silacyclobutyl)cyclobutene." Presented at the Herchel Smith Undergraduate Science Research Symposium, Harvard University, Cambridge, MA, February 27, 2006.

Poster Presentations

5. "Group 5 Imides: Two Methods for Directing Selective Hydrogenation." Thomas L. Gianetti, Henry S. La Pierre, Robert G. Bergman, F. Dean Toste, and John Arnold. Presented at the Gordon Research Conference on Organometallics, Salve Regina, Rhode Island, July, 2011.

4. "Catalytic Hydrogenation *via* [1,2]-addition of H_2 to an Imido Ligand of a Cationic Vanadium Bisimido Complex," Henry S. La Pierre, John Arnold, and F. Dean Toste. Presented at CaRLa Winter School 2010, Catalysis Research Laboratory (CaRLa) at University of Heidelberg, Heidelberg, DE, March 6-12, 2010.

3. "Group 14 Element Substituent Effect on Cyclobutene Ring-Opening." Usui, Ippei; Konno, Soichiro; La Pierre, Henry Storms; Hasegawa, Munehiro; Murakami,* Masahiro. Presented at Nippon Kagakkai Koen Yokoshu (Conference of the Chemical Society of Japan), Nihon University, Tokyo, JP, March 27-30, 2006.

2. "Synthesis and Thermal Ring-opening Reaction of 3-(1-silacyclobutyl)cyclobutene." Ippei Usui, Henry S. La Pierre, and Masahiro Murakami. Presented at the Herchel Smith Undergraduate Science Research Symposium, Harvard University, Cambridge, MA, February 27, 2006.

1. "Studies in the Synthesis and Mechanism of Action of Antimicrobial Phenolic Natural Products." H. S. La Pierre, M. L. Fingerhood, I. Meir and J. T. Shaw*. Presented at the Gordon Research Conference on Natural Products, Tilton School, New Hampshire, July, 2004.

Patents

1. "Synthesis of Inhibitors of FtsZ." J. T. Shaw. S. Urgaonkar, H. S. La Pierre, D. RayChaudhuri, US Patent application (No. 60/733,543) filed on Nov. 4, 2005, by Harvard and Tufts Universities.

Chapter 1:

Synthesis and Characterization of Neutral – Halo and Aryl – and Cationic Vanadium Bisimido Complexes: A Combined Vanadium $L_{2,3}$-Edge NEXAFS and ^{51}V and ^{13}C NMR Study

Introduction

The chemistry of transition metal bisimido complexes has received only intermittent attention by the chemical community over the last 50 years.[1-3] This lack of sustained interest is initially surprising in that bisimido complexes represent the union of the two major driving concepts in organometallic chemistry during this period:[4-7] metallocenes and reactive metal-ligand multiple bonds. A brief historical analysis reveals the reason for this indifference.[3] Unlike the wealth of important and varied chemistry derived from transition metal metallocene complexes and reactive metal-ligand multiple bond complexes, bisimido complexes have been demonstrated to catalyze few industrially, and no biologically, relevant transformations.

Notwithstanding the absence of compelling, applied reactivity, their fundamental chemistry has been explored. In fact, a large body of bisimido complexes have been isolated and characterized for Groups 5-8, and a significant body of coordination and reactivity chemistry has been produced by a number of prominent research groups.[2,3,8] Group 6 represents the largest body of compounds. Nugent and Wilkinson extensively developed their coordination chemistry.[3,9-17] These studies illuminated the fundamentals of bonding in these systems and provided access to model systems for propylene ammoxidation via the [3,3] rearrangement of allylic alcohols to allylic amines (Scheme 1.1).[18,19] Schrock and co-workers further developed the chemistry of d^2 Group 6 and 7 complexes affording the first examples of bisimido complexes that give access to their metal frontier orbitals which are isolobal to the bent-metallocene frontier orbitals (this concept is developed fully in Chapter 3).[4,20-22] These complexes bind, small unsaturated molecules such as alkynes, olefins, and organic carbonyls. The d^4 Group 8 complexes present similar reactivity.[23] The d^0 Group 8 bisimides developed by Sharpless have led to the development of stoichiometric diamination of alkenes and alkynes.[24] The much more limited chemistry of Group 5 bisimide chemistry presents two key seminal examples of σ

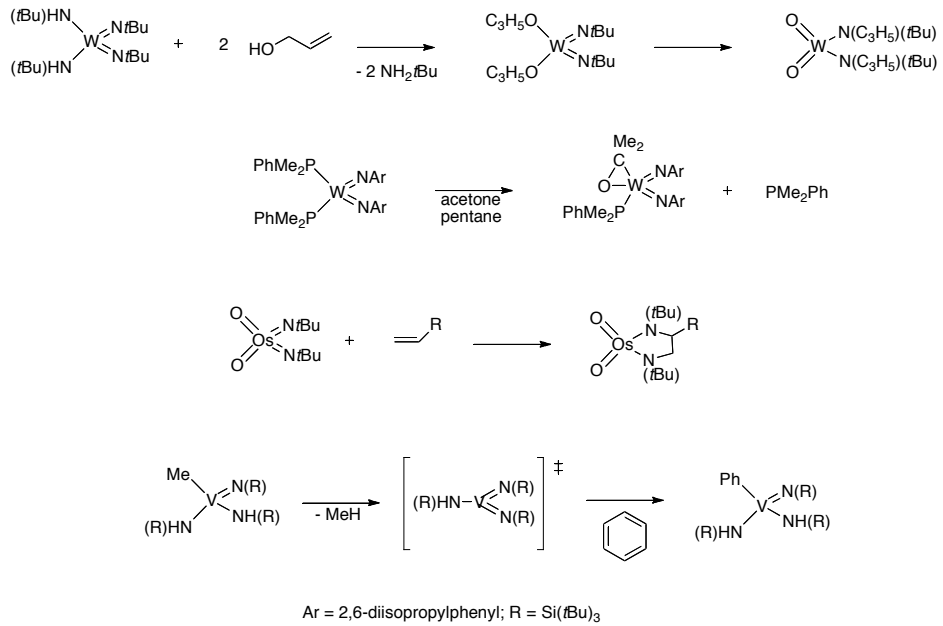

Ar = 2,6-diisopropylphenyl; R = Si(*t*Bu)$_3$

Scheme 1.1: Selected group 5-8 bisimide reactivity.

C-H bond addition to transient vanadium or tantalum bisimides supported by the bulky ~Si(^{t}Bu)$_3$ imido capping group.[25,26]

This stoichiometric σ C-H bond activation chemistry drove our reexamination of Group 5 bisimido chemistry. The Toste lab has recently developed the $ReIO_2(PPh_3)_2$ catalyzed hydrosilylation of ketones and imines.[27-30] This reaction proceeds via the net [1,2]-addition of a silane σ Si-H bond across a rhenium oxo. We hypothesized that a properly ligated Group 5 bisimide analog of $ReIO_2(PPh_3)_2$ would allow the activation of less polarized H-H and C-H σ bonds. Such stoichiometric reactivity is well-precedented for properly ligated Group 4 and 5 imido complexes.[25,26,31-39] Furthermore, Nikonov and co-workers have shown that d^2 Group 6 bisimides and Group 5 Cp/imido complexes are competent catalysts for hydrosilylation.[40-44] While these systems depend on the d^0/d^2 redox couple to activate silanes, they serve as a significant guidepost for developing catalytic reactivity based on bent metallocene analogs.

The first significant challenge in developing vanadium bisimido complexes for the activation σ bonds is largely synthetic – very few Group 5 bisimides are described (V,[26,45-49] Nb,[50,51] Ta[25,50]). Herein we report the synthesis and characterization of neutral and cationic vanadium bis-*tert*-butyl imido complexes supported by monodentate phosphines and pyridine. These studies lay the basis for further reactivity studies presented in Chapters 2 and 3 and provide a rare opportunity for the evaluation of bisimido electronic structure by four complementary methods: ^{13}C NMR, ^{51}V NMR, X-Ray crystallography, and vanadium $L_{2,3}$-edge NEXAFS. This detailed analysis of these complexes is important because it illuminates the dominant features of the electronic structure of the bisimides which are formal structural analogs of bent-metallocenes. ^{13}C NMR reveals qualitatively that the degree of electron localization at the imido nitrogens decreases on the formation of 4 coordinate cations but increases on the formation of 5 coordinate cations. ^{51}V NMR shifts are striking in that chemical shift is essentially invariant for all 5 coordinate complexes both neutral and cationic, which suggests that local electron denisty at vanadium is dominated by the π bonding to the bisimides. This result stands in stark contrast to the sheilding trends observed for the well studied mixed imido, Cp system $CpVNRX_2$ (where X = Cl, Br, I, and Me).[52-54] Vanadium L-edge X-ray absorption spectra from total electron yield (TEY) and scanning transmission X-ray microscopy (STXM) measurements confirm the presence of V^{5+}, and it is sensitive enough to discriminate between subtle differences in the steric environments imposed by supporting ligands as revealed by the crystallographic studies.

Results

Synthesis of Neutral Chloro Vanadium Bisimides. At the start of our studies there were just three extant vanadium bisimido complexes, and during the course of our studies two more examples appeared in the literature. These complexes are either supported as their anionic –ate complexes[47] or employ bulky supporting ligands to enforce kinetic stability.[26,45,46,48,49] Although these syntheses defined reliable methods to vanadium bisimides, they did not provide modular access to sterically unencumbered complexes. These complexes also are not supported by labile ligands, and they do not afford access to the frontier molecular orbitals of the bisimido moiety. Therefore they were not amenable to the development of catalytic reactions. Three general approaches

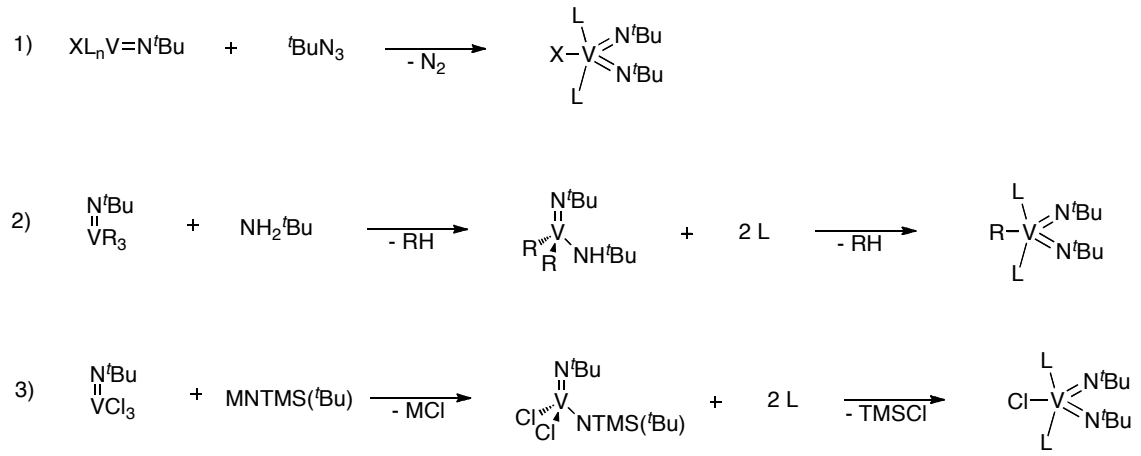

Scheme 1.2: Synthetic approaches to vanadium bisimides.

for the synthesis vanadium bisimides were considered (Scheme 1.2): (1) reduction of organic azides by a d^2 imide, (2) base induced α-NH elimination of a mixed alkyl, primary amide, vanadium imide, and (3) base induced α-NTMS elimination of a mixed halo, silyl amide, vanadium imide.

The first approach was not pursued as it required employing bulky supporting ligands for the low valent imide and would not have provided a modular synthesis. The second approach required the synthesis of triakyl vanadium imides. In the case of aryl imides, these complexes are well-known and readily produced. However, in the case of *tert*-butyl vanadium imides, there is little literature precedent and, in our hands, treatment of $V(N^tBu)Cl_3$ with common alkylating agents such as KCH_2Ph, $LiCH_2TMS$ (TMS = trimethylsilyl), and $LiCH_2C(CH_3)_3$ yielded only intractable mixtures presumably due to complications from reduction of V(V) to V(IV), as has been noted by other researchers. The third approach, however, was successful. The use of a Lewis base-induced elimination of TMSCl was inspired by the methodology for installing Cp* to $TiCl_4$ via Cp*TMS, which avoids the reduction of $TiCl_4$ to $TiCl_3$. Thus, treating Preuss's $V(N^tBu)Cl_3$[55] with Et_2O•LiNTMS(^{t}Bu), **1.1**, gave $VCl_2(N^tBu)(NTMS(^tBu)$, **1.2**, in 68% yield as red/orange crystals (Scheme 1.3). This reaction is very sensitive to reaction conditions and stoichiometry. Any excess Et_2O•LiNTMS(^{t}Bu) or the use of LiNTMS(^{t}Bu) gives the deep blue vanadium (IV) dimer $(V(NTMS(^tBu))Cl)_2(\mu\text{-}N^tBu)_2$, which was originally described by Preuss.[47] In order to achieve best results it is advisable to recrystallize Et_2O•LiNTMS(^{t}Bu) from Et_2O twice to ensure a 1:1 ratio of Et_2O to lithium amide. In the case that the reduced side-product is formed it can be separated via fractional crystallization from pentane at -80 °C. At room temperature in C_6D_6,$VCl_2(N^tBu)(NTMS(^tBu))$ is a mixture of two isomers about the V-N amide bond and is extremely soluble in hydrocarbons. This latter property has hindered its crystallographic characterization as it readily dissolves in Paratone-N oil. While $VCl_2(N^tBu)(NTMS(^tBu))$ is best purified by crystallization, it can be distilled at 120 °C at ~0.1 mmHg without decomposition or loss of TMSCl.

However, in contrast to this observed thermal stability, the addition of 2.0 - 2.2 equivalents small Lewis bases induces the elimination of TMSCl in refluxing toluene. Pyridine, trimethyl phosphine (PMe_3), triethyl phosphine (PEt_3), and dimethylphenyl

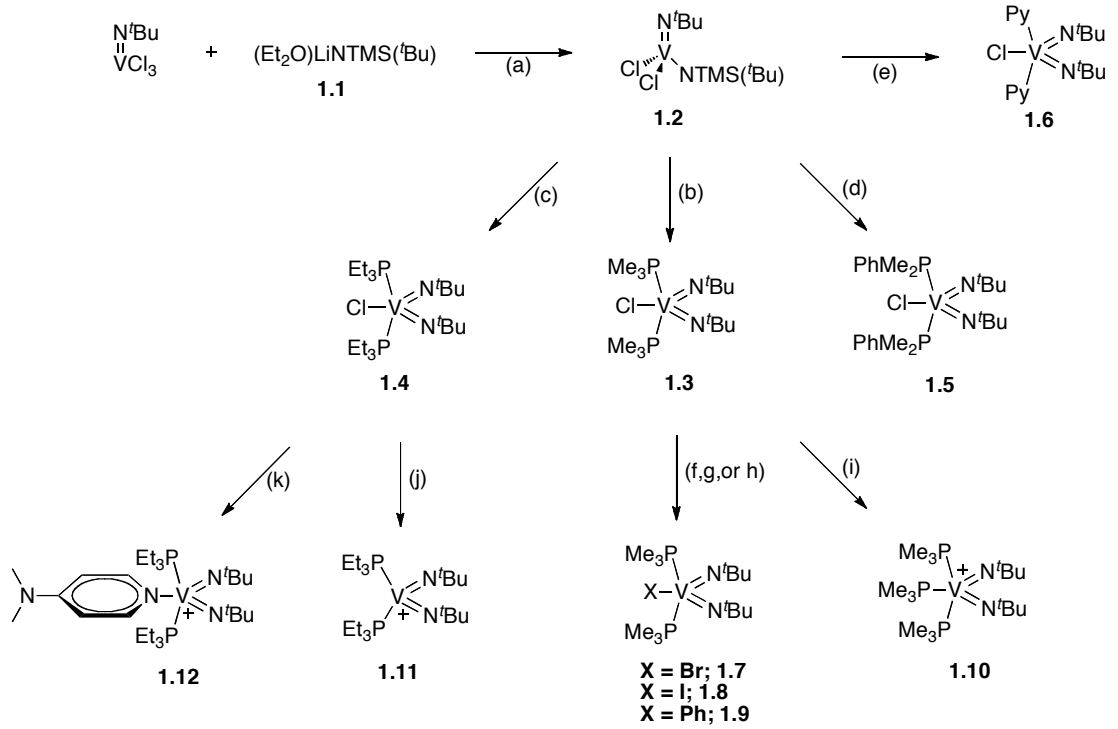

Scheme 1.3: Synthesis of neutral and cationic vanadium bisimides. In complexes **1.10** – **1.12** the counteranion, $[Al(PFTB)_4]^-$, is not depicted for clarity. Conditions: (a) pentane, -42 °C, 1h, rt, 6 d, 68 %; (b) 2.2 equiv. PMe_3, toluene, reflux, ovn., 77 %; (c) 2.0 equiv. PEt_3, toluene, reflux, ovn. 83 %; (d) 2.0 equiv. PMe_2Ph, toluene, reflux, ovn., 74 %; (e) 2.0 equiv. pyridine, toluene, reflux, ovn., 33 %; (f) 1.1 equiv. TMSBr, toluene, reflux, ovn., 31 %; (g) 1.0 equiv. TMSI, toluene, reflux, ovn., 39 %; (h) 1.2 equiv. Ph2Mg, -72 °C 1h, rt 4h, 18%; (i) 3 equiv. PMe_3; 1 equiv. $Li[Al(PFTB)_4]$, PhCl, 75%; (j) 1 equiv. $Li[Al(PFTB)_4]$, DCE, 47%; (k) 1 equiv. DMAP, 1 equiv. $Li[Al(PFTB)_4]$, $PhCF_3$, 50%.

phosphine (PMe_2Ph) all produce stable 5-coordinate distorted trigonal bipyramidal complexes in low to good yield (33-84%) after crystallization (Scheme 1.3). The geometric parameters for complexes **1.3**-**1.6** are presented in Figures **1.1**-**1.4** and the details of their spectroscopic characterization are presented in the following discussion. This Lewis base induced TMSCl elimination is not general. No reaction occurs with phosphines with cone angles larger than that of PEt_3 (132°): diphenylmethyl phosphine (PPh_2Me), di-*tert*-butylphenyl phosphine (P^tBu_2Ph), triphenylphosphine (PPh_3), triisopropyl phosphine ($PiPr_3$), and tricyclohexyl phosphine (PCy_3) do not react with **1.2**.

Derivatization of Neutral Vanadium Bisimides. The parent *bis*-PMe_3 complex **1.3** is readily transformed into its heavier halide cogners. Treatment of **1.3** in toluene with one equivalent of either TMSBr or TMSI gives the corresponding complexes **1.7** and **1.8** in reasonable yields (31 and 39 %) after refluxing the solution overnight and

crystallization from hexane (Scheme 1.3). As will be described in detail later, this halide series possesses very similar ^{51}V NMR shifts. As such, clean conversion of the equatorial halides was confirmed by elemental and crystallographic analysis. The ORTEP representation of **1.8** is shown in Figure 1.5, and, like its chloride precursor, it has a distorted trigonal bipyramidal structure with $\tau = .77$. The bromide also crystallizes readily from hexane, but suffers from whole molecule disorder in the solid state. Further work on disorder modeling is ongoing. Attempts to complete the halo series with the synthesis of the fluoride derivative were unsuccesful – trimethyltinfluoride did not undergo exchange with the chloride in refluxing toluene.

In order to access simple organometallic derivatives – alkyl, hydride, and aryl – of **1.3**, the reactivity of **1.3** with common alkylating reagents was pursued. As with other high valent vanadium systems, these reactions gave intractable mixtures presumably due to the ready reduction of V(V) to V(IV).[47,56] While one equivalent of KCH_2Ph, $LiCH_2TMS$ (TMS = trimethylsilyl), $LiCH_2C(CH_3)_3$, and MeLi failed to give the monoalkyl derivatives, the dialkyl magnesium reagent, Me_2Mg, gave no reaction, which is surprising given that similar reagents have been shown to give d^0 vanadium alkyls without significant reduction. All attempts to synthesize a vanadium hydride using ionic reagents ($NaBH_4$, $LiAlH_4$, or Red-Al®) gave similar intractable reaction mixtures. Drawing inspiration from the synthesis of the V-Br and V-I complexes, **1.7** and **1.8**, triethylsilane was employed, however no net reaction was observed despite a color change from green to yellow at reflux. One explanation for this lack of reactivity may be that the formation of a Si-Cl bond does not provide a significant enough driving force for the formation of a very weak V-H bond.[57] While the reactivity of **1.3** with aryl lithium and Grignard reagents was similar to that of their alkyl equivalents, **1.3** under went salt methathesis with one equivalent of Ph_2Mg to give $VPh(PMe_3)_2(N^tBu)_2$, **1.9**, in low yield (18%, Scheme 1.3). The complex crystallizes from hexane as yellow plates. The ORTEP of **1.9** is presented in Figure 1.6. Like the halide derivatives, **1.9** is also a distorted trigonal bipyramid with $\tau = 0.56$. Crystallographically characterized d^0 vanadium, σ bonded phenyl complexes are rare, but the metrical parameters of **1.9** match well with the only previously reported complex.[58]

Synthesis of Cationic Vanadium Bisimides. The cationic bisimides can be readily formed via chloride abstraction. Addition of a solution of $VCl(PMe_3)_2(N\textit{t}Bu)_2$, **1.3**, and 3 equivalents of PMe_3 in chlorobenzene (PhCl) to a slurry of $Li[Al(PFTB)_4]$ in PhCl afforded **1.10** as bright yellow crystals in 75% yield after crystallization (Scheme 1.3). Complex **1.10**, like the chloride precursor, is a distorted trigonal bipyramid with $\tau = 0.62$. This complex, like many complexes supported by the $[Al(PFTB)_4]^-$ anion, suffered from significant disorder in the anion (See experimental section for details), but provides sufficient resolution to confirm connectivity (Figure 1.7).

The four coordinate, cationic vanadium bisimide was then prepared by the addition of a DCE solution of **1.4** to a slurry of $Li[Al(PFTB)_4]$ in DCE at room temperature. This addition resulted in a shift in color from light green to a very deep red. While this complex is generated quantitatively on mixing in several solvents (d_2-DCM, DCE, $PhCF_3$), reasonable preparative yields (*ca.* 40-60%) can only be achieved by crystallization from DCE as red blades. Complex **1.11** prepared by this method can be used directly within hours, but storage at -40 °C in the solid state under N_2 leads to *ca.* 10% loss per week. In comparison to the chloride precursor, **5** has a ^{51}V NMR resonance

of δ -278.99 ppm ($\Delta\nu_{1/2}$ = 80.78 Hz, in $PhCF_3$ (C_6D_6 insert)). Like all the complexes presented here, the ^{31}P NMR is largely uninformative as unresolved V-P coupling gives broad peaks: **1.11** has single ^{31}P resonance at δ 26.69 ppm ($\Delta\nu_{1/2}$ = 2674.50 Hz, in $PhCF_3$ (C_6D_6 insert)).

As all attempts to obtain a crystal structure of **1.11** were unsuccessful, we sought to derivatize **1.11** in order to confirm NMR assignments and molecular geometry. This goal was achieved by generating **1.11** in the presence of DMAP in $PhCF_3$. After workup the desired complex, **1.12,** was obtained in 50% yield by crystallization from $PhCF_3$ (Scheme 1.3) as yellow blocks. The NMR characteristics of this complex are very similar to those of **1.10**. The ^{51}V NMR resonance is shifted from **1.11** at δ -278.99 ppm to δ -728.16 similar to that observed for **1.10** of -792.29 ppm. The molecular structure was determined by X-ray diffraction (Figure 1.8). This complex, like **1.10**, suffered from significant disorder in the anion (See experimental section for details). Nonetheless, the molecular geometry was confirmed and demonstrates that the four-coordinate cation is successfully generated. Complex **1.5**, supported by PMe_2Ph, unlike **1.3** and **1.4,** did not undergo clean halide abstraction and no tractable products were isolated. Other non-coordinating anions were considered for the synthesis of complexes **1.10** and **1.11**. The use $Na[BPh_4]$, $K[B(ArF_{20})_4]$, or $Na[B(ArF_{24})]$ under analogous reaction conditions lead to decomposition of the anion and intractable reaction mixtures. Only the very non-basic $[Al(PFTB)_4]^-$ anion provided access to stable complexes.

NEXAFS Analysis of Neutral and Cationic Bisimides by Vanadium $L_{2,3}$-edge Spectroscopy. In an effort to evaluate electronic structure and corroborate geometric trends in the vanadium bisimido compounds, vanadium L-edge X-ray absorption spectra were obtained by total electron yield (TEY) and scanning transmission X-ray microscopy (STXM) for samples of **1.3**, **1.4**, **1.5**, and **1.11**. The position and splitting of bands in L-edge (2p) spectra, which are sensitive to oxidation state, ligand field, and local geometry,[59] have been used to characterize a variety of vanadium oxides,[60-70] particularly V_2O_5.[71-79] However, few applications of V L-edge spectroscopy have been reported for molecular systems.[80,81] Metal K-edge spectroscopy is, nonetheless, an increasingly important tool for the characterization of molecular transition metal complexes. A detailed Ti K-edge study of $CpTiCl_3$ and Cp_2TiCl_2 is the point of comparison for this study as it provides a measure of metal-ligand covalency for the formally isolobal bent-metallocenes.[82]

The normalized L-edge spectra for **1.3**, **1.4**, **1.5**, and **1.11**, from TEY are shown in Figure 1.9 and, for comparison, those of for other well-known V^{5+} standards, Na_3VO_4 and V_2O_5 are in Figure 1.10 (see Figure 1.11 for STXM spectra of **1.4**, **1.5**, and **1.11**). Except for **1.3**, V L-edge XAS were obtained by both TEY and STXM to ensure that each spectrum was correct for the sample and did not represent qualities of the particle-based (STXM) or surface-sensitive (TEY) measurements. For each d^0 V complex, the L-edge absorptions arise from dipole allowed $2p^63d^0 \rightarrow 2p^53d^1$ transitions, which are split by roughly 7 eV into L_3 ($2p_{3/2}$) and L_2 ($2p_{1/2}$) edges due to spin-orbit coupling of the core-hole.[83,84] The L_2 edge is broadened due to Coster–Kronig Auger decay processes,[73,85,86] and is not discussed further.

The presence or absence of individual features in the L_3 edges was determined by inspection of a plot of the 2nd derivative of the absorption, as described previously (Figure 1.12 and Table 1.1).[87-89] Although the STXM and TEY detection methods have

different energy resolutions of *ca*. 0.2 eV and 0.08 eV, respectively, there is excellent agreement with regard to the maximum absorption energy of the L_3 edge. While no structure was observed in the TEY spectra, the STXM spectra for **1.4**, **1.5**, and **1.11**each contains well-resolved shoulders (and a peak for **1.5**) on the low-energy side of the L_3 edge. The peak energies in the L_3 edge for **1.3**, **1.4**, **1.5**, and **1.11** compare well with those in spectra of V_2O_5 and Na_3VO_4 (Table 1.1) and are consistent with V^{5+} formal oxidation states for the bisimido compounds.

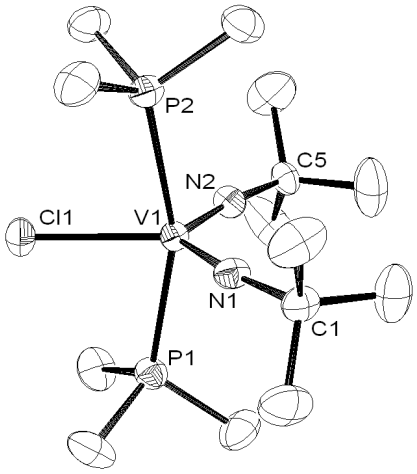

Figure 1.1: Molecular structure of **1.3.** Thermal ellipsoids are drawn at 50% probability level. Hydrogen atoms have been removed for clarity. Selected bond lengths (Å) and angles (deg): V(1)-N(1), 1.6888(19); V(1)-N(2), 1.6839(19); V(1)-Cl(1), 2.4387(6); V(1)-P(1), 2.4507(7); V(1)-P(2), 2.4546(7); N(2)-V(1)-N(1), 115.88(10); Cl(1)-V(1)-P(1), 80.44(2); Cl(1)-V(1)-P(2), 80.52(2); P(1)-V(1)-P(2), 160.93(2); C(1)-N(1)-V(1), 168.82(17); C(5)-N(2)-V(1), 169.64(17).

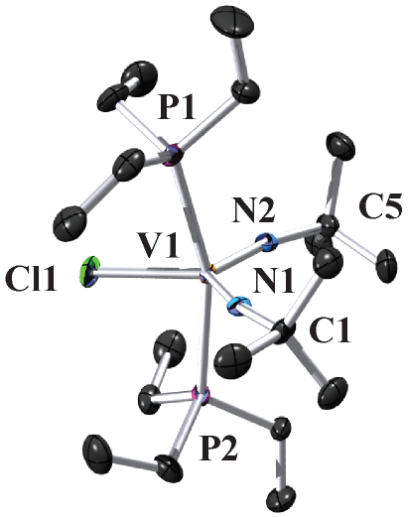

Figure 1.2: Molecular structure of **1.4.** Thermal ellipsoids are drawn at 50% probability level. Hydrogen atoms have been removed for clarity. Selected bond lengths (Å) and angles (deg): N(1)-V(1), 1.687(4); N(2)-V(1), 1.681(4); P(1)-V(1), 2.4999(14); P(2)-V(1), 2.5006(14); Cl(1)-V(1), 2.4296(14); N(2)-V(1)-N(1), 114.0(2); C(1)-N(1)-V(1), 167.8(4); C(5)-N(2)-V(1), 164.6(4); N(2)-V(1)-Cl(1), 120.65(15); N(1)-V(1)-Cl(1), 125.40(15); N(2)-V(1)-P(1), 99.09(13); N(1)-V(1)-P(1), 91.14(13); N(2)-V(1)-P(2), 96.08(13); N(1)-V(1)-P(2), 92.89(13); P(1)-V(1)-P(2), 161.14(5); Cl(1)-V(1)-P(1), 80.96(5); Cl(1)-V(1)-P(2), 81.69(5).

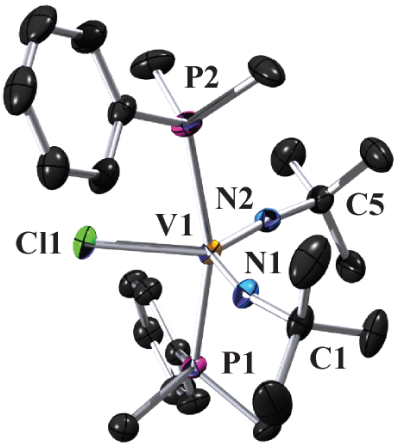

Figure 1.3: Molecular structure of **1.5.** Thermal ellipsoids are drawn at 50% probability level. Hydrogen atoms have been removed for clarity. Selected bond lengths (Å) and angles (deg): N(1)-V(1), 1.696(2); N(2)-V(1), 1.685(2); P(1)-V(1), 2.4756(7); P(2)-V(1), 2.4646(8); Cl(1)-V(1), 2.4175(7); C(1)-N(1)-V(1), 161.2(2); C(5)-N(2)-V(1), 173.21(19); N(2)-V(1)-N(1), 116.14(10); N(2)-V(1)-Cl(1), 123.21(7); N(1)-V(1)-Cl(1), 120.65(8); N(2)-V(1)-P(2), 93.00(7); N(1)-V(1)-P(2), 98.28(7); Cl(1)-V(1)-P(2), 78.79(3); N(2)-V(1)-P(1), 92.58(7); N(1)-V(1)-P(1), 95.82(7); Cl(1)-V(1)-P(1), 82.67(2); P(2)-V(1)-P(1), 160.67(3).

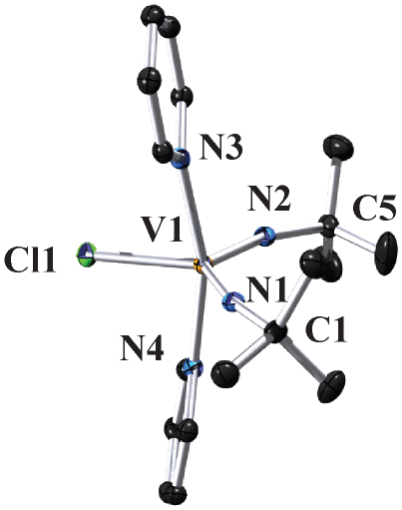

Figure 1.4: Molecular structure of **1.6.** Thermal ellipsoids are drawn at 50% probability level. Hydrogen atoms have been removed for clarity. Selected bond lengths (Å) and angles (deg): N(1)-V(1), 1.6852(17); N(2)-V(1), 1.6873(17); N(3)-V(1), 2.1626(17); N(4)-V(1), 2.1662(17); Cl(1)-V(1), 2.4329(7); C(1)-N(1)-V(1), 167.73(15); C(5)-N(2)-V(1),161.83(15); N(1)-V(1)-N(2), 113.83(8); N(1)-V(1)-N(3), 93.64(7); N(2)-V(1)-N(3), 97.51(7); N(1)-V(1)-N(4), 93.03(7); N(2)-V(1)-N(4), 94.45(7); N(3)-V(1)-N(4), 162.60(6); N(1)-V(1)-Cl(1), 127.55(6); N(2)-V(1)-Cl(1), 118.57(6); N(3)-V(1)-Cl(1),

82.14(5); N(4)-V(1)-Cl(1), 81.05(5).

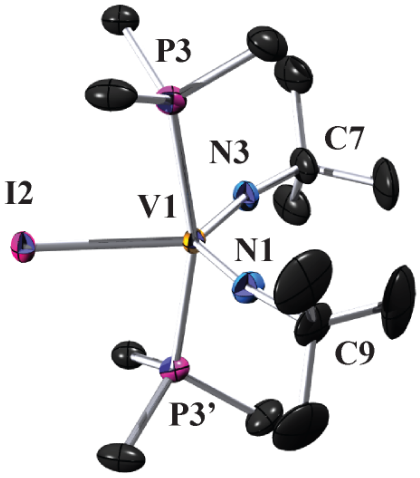

Figure 1.5: Molecular structure of **1.8.** Thermal ellipsoids are drawn at 50% probability level. Hydrogen atoms have been removed for clarity. Selected bond lengths (Å) and angles (deg) for both molecules in asymmetric unit: N(1)-V(1), 1.669(5); N(2)-V(2), 1.684(4); N(3)-V(1), 1.687(5); P(1)-V(2), 2.4548(16); P(2)-V(2), 2.4703(16); P(3)-V(1), 2.4545(11); V(1)-I(2), 2.8370(11); V(2)-I(1), 2.8201(12); C(9)-N(1)-V(1), 168.5(5); C(8)-N(2)-V(2), 168.1(3); C(7)-N(3)-V(1), 166.5(4); N(1)-V(1)-N(3), 116.4(2); N(1)-V(1)-P(3), 95.73(4); N(3)-V(1)-P(3), 93.07(4); N(1)-V(1)-I(2), 118.58(18); N(3)-V(1)-I(2), 124.97(18); P(3)-V(1)-I(2), 81.73(4); N(2)-V(2)-P(1), 93.33(11); N(2)-V(2)-P(2), 93.05(11); P(1)-V(2)-P(2), 167.77(7); N(2)-V(2)-I(1), 121.48(13); P(1)-V(2)-I(1), 83.77(5); P(2)-V(2)-I(1), 84.00(5).

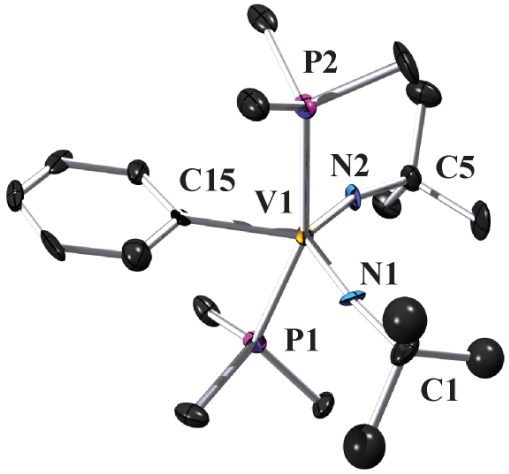

Figure 1.6: Molecular structure of **1.9.** Thermal ellipsoids are drawn at 50% probability level. Hydrogen atoms have been removed for clarity. Selected bond lengths (Å) and angles (deg): C(15)-V(1), 2.175(5); N(1)-V(1), 1.707(5); N(2)-V(1), 1.718(5); P(1)-V(1), 2.4264(18); P(2)-V(1), 2.4375(19); C(1)-N(1)-V(1), 172.0(40; C(5)-N(2)-V(1), 160.6(4); N(1)-V(1)-N(2), 119.6(2); N(1)-V(1)-C(15), 116.4(2); N(2)-V(1)-C(15), 124.0(2); N(1)-V(1)-P(1), 95.50(16); N(2)-V(1)-P(1), 93.96(15); C(15)-V(1)-P(1), 79.39(15); N(1)-V(1)-

P(2), 96.78(16); N(2)-V(1)-P(2), 95.47(16); C(15)-V(1)-P(2), 79.09(15); P(1)-V(1)-P(2), 158.26(6).

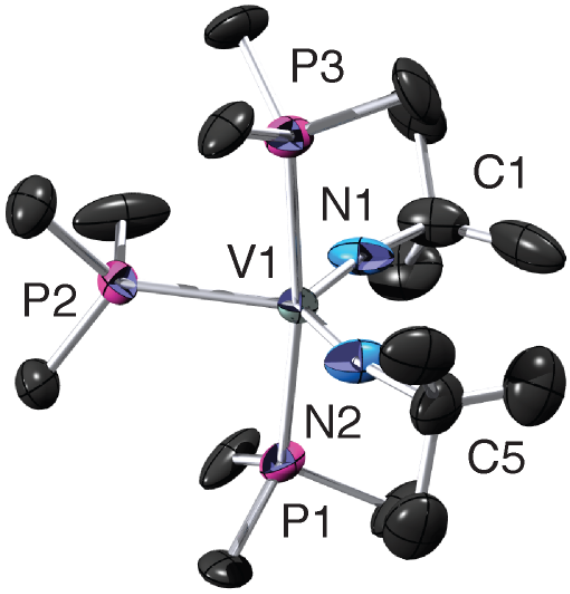

Figure 1.7: Molecular structure of **1.10.** Thermal ellipsoids are drawn at 50% probability level. Hydrogen atoms and the counteranion ($[Al(PFTB)_4]^-$) have have been removed for clarity. Selected bond lengths (Å) and angles (deg): V(1)-N(1), 1.652(10); V(1)-N(2), 1.647(6); V(1)-P(2), 2.611(3); V(1)-P(1), 2.4839(16); V(1)-P(3), 2.4887(17); N(1)-V(1)-N(2), 118.1(4); P(1)-V(1)-P(2), 86.00(7); P(3)-V(1)-P(1), 171.57(8); C(1)-N(1)-V(1), 164.6(8); C(5)-N(2)-V(1), 165.3(6).

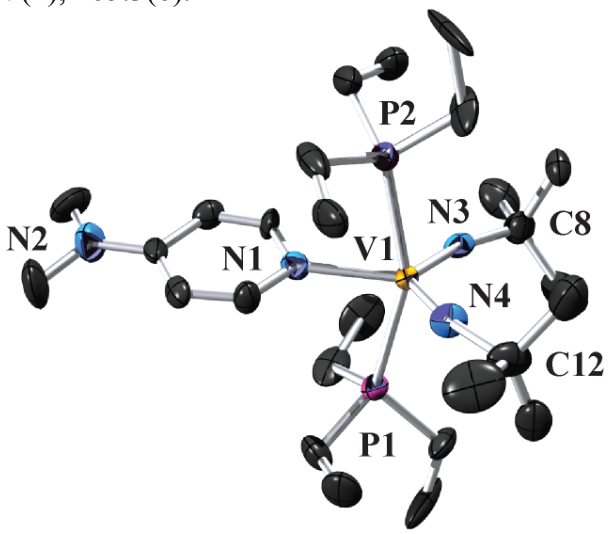

Figure 1.8: Molecular structure of **1.12.** Thermal ellipsoids are drawn at 50% probability level. Hydrogen atoms and the counteranion ($[Al(PFTB)_4]^-$) have have been removed for clarity. Selected bond lengths (Å) and angles (deg): N(3)-V(1), 1.682(6); N(4)-V(1), 1.683(5); P(1)-V(1), 2.532(2); P(2)-V(1), 2.526(2); N(1)-V(1), 2.207(5); N(3)-V(1)-N(4), 112.9(3); C(8)-N(3)-V(1), 162.3(5); C(12)-N(4)-V(1), 161.1(6); N(3)-V(1)-N(1), 121.6(2); N(4)-V(1)-N(1), 125.5(3); N(3)-V(1)-P(2), 97.57(17), N(4)-V(1)-P(2), 95.3(2);

N(3)-V(1)-P(1), 95.69(18); N(4)-V(1)-P(1), 98.1(2); P(2)-V(1)-P(1), 155.75(7); N(1)-V(1)-P(2), 78.13(14); N(1)-V(1)-P(1), 77.64(14).

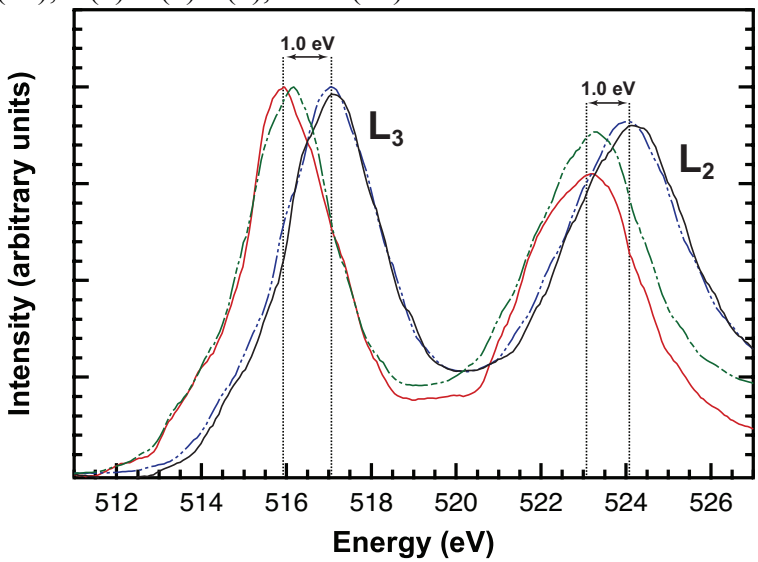

Figure 1.9: V L-edge spectra obtained by total electron yield (TEY) for **1.3** (blue dashes), **1.5** (black line), **1.4** (green dashes), and **1.11** (red line).

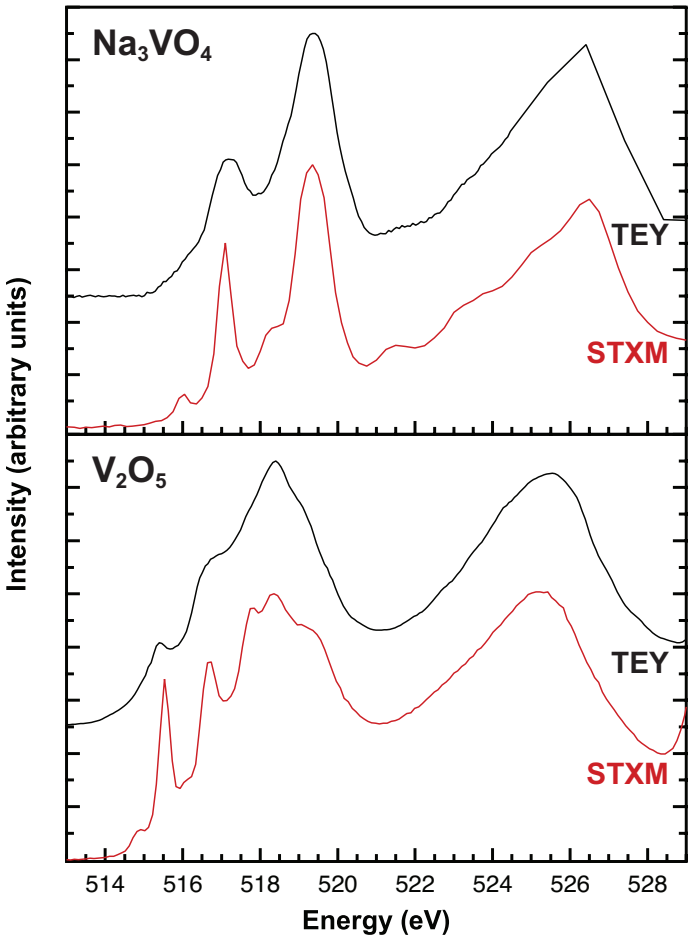

Figure 1.10: V L-edge spectra obtained by total electron yield (black line) and STXM (red line) for V^{5+} standards Na_3VO_4 (above) and V_2O_5 (below).

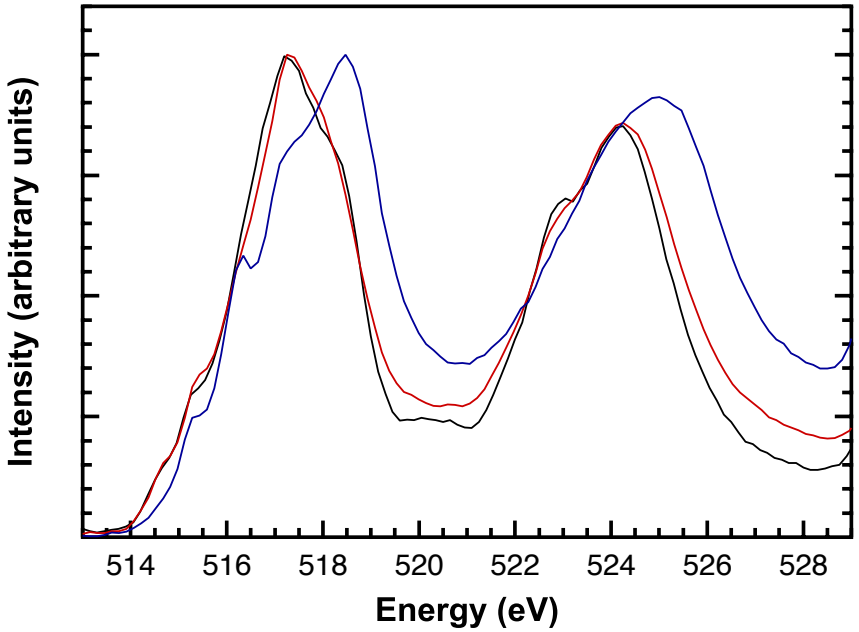

Figure 1.11: V L-edge spectra obtained by scanning transmission X-ray microcopy (STXM) for **1.5** (blue line), **1.4** (red line), and **1.11** (black line).

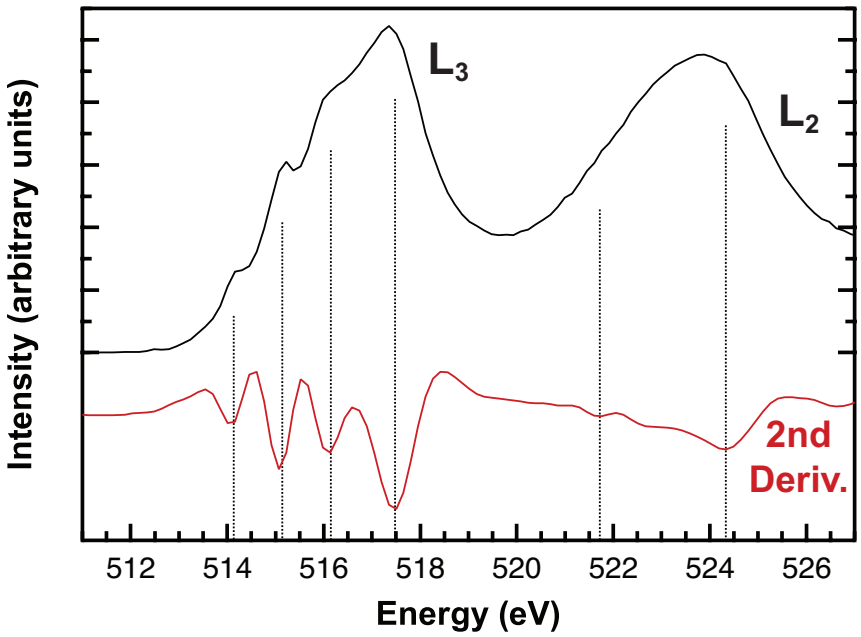

Figure 1.12: The data reduction of a V L-edge spectrum of **1.5** obtained by scanning transmission X-ray microscopy (STXM, black line) showing the smoothed second derivative of the normalized data (red line) and energy of resolved features.

Table 1.1: Experimental L-edge energies (eV) determined from the minima in the second derivative of spectra.

Cmpd	Method	L3 edge energies[a]	L2 edge energies[a]
Na_3VO_4	STXM	515.9 (p), 517.1 (p), 518.2 (p), 519.4* (p)	521.6 (p), 523.3 (sh), 525.0 (sh), 526.5* (p)
	TEY	515.8 (sh), 517.0 (p), 518.0 (sh), 519.4* (p)	526.7* (p)
1.5	STXM	515.2 (sh), 516.6 (p), 517.6 (sh), 518.9* (p)	523.3 (sh), 525.8* (p)
	TEY	518.6* (p)	525.6* (p)
1.3	TEY	518.5* (p)	525.5* (p)
V_2O_5	STXM	514.7 (p), 515.5 (p), 516.7 (p), 517.7 (p), 518.4* (p), 519.5 (sh)	525.2* (p)
	TEY	515.4 (p), 516.5 (sh), 517.7 (sh), 518.4* (p), 519.8 (sh)	525.5* (p)
1.4	STXM	514.9 (s), 515.7 (sh), 516.7 (sh), 517.7* (p), 518.6 (sh)	523.1 (sh), 524.7* (p)
	TEY	517.7* (p)	524.7* (p)
1.11	STXM	514.9 (sh), 515.6 (sh), 517.5* (p), 518.8 (sh)	523.1 (sh), 524.7* (p)
	TEY	517.4* (p)	524.7* (p)

[a] Labels "p" = peak and "sh" = shoulder. The energy of absorption maxima for the L_3 and L_2 edges are followed by an asterisk (*).

Discussion

X-Ray Crystallography. Solid-state structures for complexes **1.3** – **1.6**, **1.8** – **1.10**, and **1.12** have been determined by X-ray crystallographic studies. All compounds are distorted trigonal bipyramids with τ between 0.50 and 0.77. For the chloride series $VCl(N^tBu)_2(L)_2$, where L = PMe_3, PEt_3, PMe_2Ph, and Py, the vanadium chloride bond lengths are essentially invariant (2.43 Å; for **1.5**, 2.41 Å). Likewise, the V-N_{im} bond lengths change little from 1.68 Å. However, there are subtle, but significant changes in the V-P bond lengths, and P-V-P (or N_{py}), N_{im}-V-N_{im}, and V-N_{im}-C bond angles. In the three phosphine supported complexes **1.3** – **1.5**, the length of the V-P bonds corresponds to the measured cone angle for the corresponding phosphine, (*i.e.* the cone angles (Θ) for PMe_3 (118°),[90] PMe_2Ph (122°),[91] and PEt_3 (132°).[90] In other words, the shortest are for the PMe_3 complex **1.3** at 2.4507(7) and 2.4546(7) Å, **1.5** follows with 2.4756(7) and 2.4646(8) Å, and finally **1.4** with 2.4999(14) and 2.5006(14) Å. The P-V-P angles for the complexes follow nearly the same trend (**1.3**, 160.93(2)°; **1.5**, 160.67(3)°; **1.4**, 161.14(5)°). The N_{im}-V-N_{im} angles follow the inverse trend and decrease with increasing cone angle (**1.4**, 114.0(2)°; **1.5**, 116.14(10)°; **1.3**, 115.88(10)°). All of these N_{im}-V-N_{im} angles lie below the ideal angle of 120°, a feature which is common to Group 5 bisimides,[25] regardless of the nature of the imido R group. This feature has been rationalized based on an electronic argument, whereby the imido ligands are better both σ

and π donors than the axial supporting ligands. Therefore the contraction of the N_{im}-V-N_{im} angle serves to increase effective overlap with the metal atomic orbitals.[25] As such the contraction of this angle with increasing cone angle of the supporting phophine implies that the contraction is the result of less effective donation of electron density to the metal center by the more sterically hindered phosphine. There is no apparent trend in the V-N_{im}-C bond angles for the four chloride complexes. On average these angles are 168°. However, they cover the range of 160° to 171°, and none of the complexes have equivalent V-N_{im}-C angles. This phenomenon is not surprising in that deformation energy of *tert*-butyl imides is quite small, and likely caused by crystal packing forces rather the intrinsic electronic properties of the complexes.[8]

The substitution of phenyl or iodide for chloride in **1.3** results in noticable changes in the key parameters of the bisimido complexes. In complex **1.9**, the phenyl ring lies in the equatorial plane of the trigonal bipyramid. As a result, the steric profile of the phenyl substituent is reduced in comparison to the parent chloride. This phenomenon allows for the relation of the P-V-P angle to 158.26(6)°, the contraction of the V-P bonds to 2.4264(18) and 2.4375(19) Å, and the expansion of the N_{im}-V-N_{im} angle to 119.6(2)°. These changes combine to give a $\tau = 0.56$. In the iodide complex **1.8**, the larger size of the iodide substituent (despite the longer V-I than V-Cl bond) leads to the expansion of the P-V-P angle to 167.77(7)°. However, the V-P bonds lengths are nearly identical to those of the chloride precursor at 2.4548(16) and 2.4703(16) Å (2.4545(11), second phosphine generated by a mirror plane). As a result the N_{im}-V-N_{im} angle is expanded to 116.4(2) and gives an overall $\tau = 0.77$ and 0.63 for each molecule in the asymmetric unit. While the structures of the two cationic complexes confirm connectivity and characterization assignments (Figures 1.7 and 1.8), the data quality is insufficient for a comparative discussion. Chapter 3 contains a detailed discussion of a related cationic bisimide.

Table 1.2: A comparison of $\Delta\delta_{\alpha\beta}$ values for complexes **1.3** – **1.12**.

Compound	$\Delta\delta_{\alpha\beta}$ in ppm
1.3	34.4
1.4	34.4
1.5	36.2
1.6	27.1
1.7	35.4
1.8	36.4
1.9	a
1.10	a
1.11	29.8
1.12	39.9

a = The α-*t*Bu resonance was not located.

^{13}C NMR Spectroscopy. The $\Delta\delta_{\alpha\beta}$ of the C_α and C_β has been shown to be qualitatively indicative of the degree of charge localization at the imido nitrogen and, hence, the nucleophilicity of the imide.[92] A decrease in electron density at nitrogen leads to a downfield shift in C_α and an upfield shift in C_β. Therefore, an increase in the

difference in the shifts of the resonances indicates a decrease in the localization of electron density at nitrogen. Table 1.2 contains the $\Delta\delta_{\alpha\beta}$ for the complexes reported in Chapter 1. Several trends can be delineated. Other studies have correlated $\Delta\delta_{\alpha\beta}$ with the electronegativity of the metal or the ligand set.[8] In these systems $\Delta\delta_{\alpha\beta}$ increases with increasing electronegativity of the metal or ligand set. However, in the series of halide complexes **1.3 – 1.5**, $\Delta\delta_{\alpha\beta}$ decreases with increasing electronegativity of the equatorially bound halide. In other words, the chloride complex has lowest $\Delta\delta_{\alpha\beta}$, and the greatest localization of charge density at nitrogen. This effect implies that chloride more effectively donates electron density to vanadium. The basis of this trend is likely the more effective overlap of chloride 3*p* orbitals with the vanadium 3*d* based fragment orbitals than that of the bromide 4*p* or iodide 5*p* orbitals. For the chloride series supported by different phosphines, the $\Delta\delta_{\alpha\beta}$ is sensitive to the electron donating ability of the corresponding phosphine. Both the PMe_3 complex, **1.3**, and the PEt_3 complex, **1.4**, have a similar $\Delta\delta_{\alpha\beta}$ (34.4 and 34.4) as both are electron rich trialkyl phosphines. The less electron donating PMe_2Ph complex, **1.5**, has a larger $\Delta\delta_{\alpha\beta}$ presumably because the imide ligands compensate by donating more electron density to the electron deficient metal center. This similar pattern is observed for the two cationic complexes for which the C_α resonance could be observed, **1.11** and **1.12**. The four coordinate complex **1.11** has a $\Delta\delta_{\alpha\beta}$ of 39.9 ppm reflecting the extremely electron poor metal center. On the coordination of DMAP to form complex **1.12**, $\Delta\delta_{\alpha\beta}$ shifts to 29.8 ppm which indicates the strongly localized electron density in the cationic complexes in comparison to the neutral five coordinate complexes.

Table 1.3: A comparison of ^{51}V NMR values for complexes **1.3** – **1.12**.

Compound	δ in ppm
1.3	-782.31
1.4	-757.33
1.5	-766.92
1.6	-485.42
1.7	-770.95
1.8	-778.38
1.9	-801.07
1.10	-792.29
1.11	-278.99
1.12	-728.16
$CpV(N^tBu)Cl_2$ [a]	-457
$CpV(N^tBu)Br_2$ [a]	-329
$CpV(N^tBu)I_2$ [a]	-110
$CpV(N^tBu)Me_2$ [a]	-25

a = Refs. 52-54.

^{51}V NMR Spectroscopy. ^{51}V NMR is a sensitive method for probing the electronic environment of vanadium complexes. The shift range for $\delta(^{51}V)$ spans 5000 ppm from 2500 to -2500 ppm: a reflection of the sensitivity of the vanadium nucleus to its electronic environment.[93] Unlike ^{1}H or ^{7}Li NMR, ^{51}V NMR shifts do not necessarily

correlate directly with electronic shielding of the nucleus and thus do not correlate with oxidation state. However, within an isostructural series, shielding trends can be defined and used rationalize electronic structure. Heretofore, it has been empirically observed that high valent (d^0), open shell systems such as VOX_3, $VN(p\text{-tol})X_3$, and $CpVN^tBuX_2$ follow an 'inverse electronegativity dependence' on the nature of X σ bonded supporting ligands; *i.e.* less electronegative and more polarizable ligands give rise to deshielding.[93] The case of $CpVN^tBuX_2$ is particularly interesting in that it is the mixed Cp/imido isolobal analog of the complexes presented here. The ^{51}V NMR shifts of $CpVN^tBuX_2$ complexes (for X = Cl, Br, I and Me) are shown in Table 1.3 along with the ^{51}V NMR shifts of the complexes presented in this paper. Clearly the trend for $CpVN^tBuX_2$ complexes does not hold for $VX(PMe_3)_2(N^tBu)_2$. In fact no trend is observable for the halo/aryl series, and, by examining the reported shifts for the different phosphine supported vanadium chloride complexes (**1.3**, **1.4**, and **1.5**), it seems ^{51}V NMR shift is dependent on the nature of the phosphorus supporting ligand.

These phenomena can be explained by considering contributions for overall shielding (also defined as σ).[93] It is composed of three parts: the local diamagnetic term, the local paramagnetic term, and the non-local term. The non-local term is very small and can be ignored. The local diamagnetic term is large, but mostly invariant as it depends on core electrons and, in discussions of shielding trends, can also be ignored. The key part is the local paramagnetic term. Most pertinent to the question at hand are results of Maatta and co-workers that demonstrate for the similar system $VN(p\text{-tol})X_3$ two types of electronic transitions contribute to local paramagnetic term: π to π* and σ to π*.[56] For a given, isostructural imide or bisimide system the π to π* transition changes little, but changing X changes the energy of the σ to π* transition and hence the magnitude of the local paramagnetic term. Assuming that this model holds for the similar bisimide system presented in this paper, the non-dependence of chemical shift on the electronegativity of the supporting ligand can be explained. In the case of $VX(PMe_3)_2(N^tBu)_2$ complexes, the V-X σ bond is orthogonal to the π* system (see Chapter 3 for a full MO description) and there is little overlap. Therefore there is no defined electronegativity trend observed. In the case of the supporting phosphine, the deshielding, local paramagnetic term increases with increasing cone angle of the phosphine and the corresponding V-P bond length. The longer the V-P bond the greater σ to π* transition.

NEXAFS. The overall spectral profile observed for each compound, by both detection methods, was quite similar (Figure 1.9), however, there are significant differences in energy. The position of the TEY absorption maximum for the L_3 edges in **1.3** and **1.5** is, on average, 518.6 eV, which is very close to that determined using STXM. For **1.4** and **1.11**, the absorption maximum is *ca*. 1.0 eV lower in energy, at 517.6 eV. This shift in energy is representative of a decrease in the 3d orbital energies in **1.4** and **1.11** due to weaker bonding relative to **1.3** and **1.5**. To understand the origin of this change in bonding, it is instructive to consider differences in the steric and electronic environment provided by the supporting ligands. The PEt_3 ligands in **1.4** and **1.11** should have similar electron donating/withdrawing properties to the PMe_3 ligands in **1.3**. However, the PMe_2Ph ligands in **1.5** are more electron withdrawing than either *tris*-alkyl-substituted phosphine, which is not consistent with the observed spectral trends. Clearly, the intrinsic electronic differences between the phosphine ligands are not responsible for the differences in the 3d orbital energies for **1.3, 1.4, 1.5, and 1.11**.

Examination of the bond distances and angles given in the X-ray crystal structures reveals a P–V–P angle for **1.4** (161.14(5)°) that is slightly wider than those in **1.3** (160.93(2)°) or **1.5** (160.67(3)°). The added steric pressure provided by the PEt_3 ligand also has an effect on the imido ligands, which are *ca*. 2° wider in **1.3** (115.88(10)°) and **1.5** (116.14(10)°) than in **1.4** (114.0(2)°). This trend is also reflected in the cone angles (Θ) for PMe_3 (118°),[90] PMe_2Ph (122°),[91] and PEt_3 (132°).[90] Taken together with the L-edge XAS, these structural data suggest that subtle differences in the steric properties of each phosphine ligand lead to a significant change in electronic structure. ^{51}V NMR and V L-edge spectroscopy are complementary probes of electronic structure. ^{51}V NMR measures the effect of the nature of the phosphine ligand on the σ to π* transition in complex, while V L-edge spectroscopy is sensitive to geometry changes enforced by the steric environment of the phosphine and hence the energy of the π* LUMO via the energy of the $2p^63d^0 \rightarrow 2p^53d^1$ transitions. This study contains the first examples of V L-edge XAS data from high valent vanadium supported by imido ligands. Additional structural and metal L-edge XAS experiments are needed and are currently underway to test the validity of this interpretation.

Conclusion

The synthesis of a series of isostructural vanadium bisimido complexes was accomplished in a modular fashion. The key step was the Lewis base induced TMSCl elimination to form the bisimido core. These compounds served the basis for the synthesis of a variety of neutral halo and aryl complexes and cationic complexes. The characterization of these complexes by XRD, ^{13}C and ^{51}V NMR, and V L-edge spectroscopy provide a basis for comparison of electronic structure among the series. The complementary nature of ^{51}V NMR and V L-edge spectroscopy allowed for the factors controlling the electronic environment at vanadium to be determined.

Experimental Section:

General Considerations. Unless otherwise noted, all reactions were performed using standard Schlenk line techniques or in an MBraun inert atmosphere box under an atmosphere of argon or dinitrogen (<1 ppm O_2/H_2O), respectively. All glassware and cannulae were stored in an oven at ca. 425 K. Pentane, diethyl ether, toluene, tetrahydrofuran, dichloromethane, and dimehtoxyethane were purified by passage through a column of activated alumina and degassed prior to use. C_6D_6 was vacuum-transferred from sodium/benzophenone and degassed with three freeze-pump-thaw cycles. 1,2-$C_2D_4Cl_2$ was vacuum transferred from CaH_2 and degassed with three freeze-pump-thaw cycles. NMR spectra were recorded on Bruker AV-300, AVB-400, AVQ-400, AV-500, and AV-600 spectrometers. ^1H and $^{13}C\{^1H\}$ chemical shifts are given relative to residual solvent peaks. ^{31}P, ^{51}V, ^{19}F, and ^{27}Al chemical shifts were referenced to external standards ($P(OMe)_3$ at 1.67 ppm, $VOCl_3$ at 0.00 ppm, $CFCl_3$ at 0.00 ppm, and 1M Al(NO3)3 in H_2O/D_2O at 0 ppm, respectively). Proton and carbon NMR assignments were routinely confirmed by ^1H-^1H (COSY) or ^1H-^{13}C (HSQC and HMBC) experiments as necessary. Resonances marked with a * were located by HMBC. Infrared (IR) samples were prepared as Nujol mulls and were taken between KBr disks. The following

chemicals were purified prior to use: chlorobenzene and tBuNH$_2$ were distilled from CaH_2 and were degassed by bubbling argon through the liquids for 15 minutes, α, α', α''-trifluorotoluene ($PhCF_3$), was distilled from P_2O_5 and degassed by bubbling argon through the liquid for 15 minutes; Li[AlH_4] was dissolved in Et_2O, filtered, and reduced *in vacuo* and the residue was heated at 80 °C under vacuum for 2 h, perfluoro-*tert*-butyl alcohol was stored over 4 Å seives and degassed by three freeze-pump-thaw cycles. PMe_3,[94] Li[Al(PFTB)$_4$],[95] Ph_2Mg,[96] and $VCl_3(N^tBu)$[97] were prepared using standard literature procedures. All other reagents were acquired from commercial sources and used as received. Elemental analyses were determined at the College of Chemistry, University of California, Berkeley. The X-ray structural determinations were performed at CHEXRAY, University of California, Berkeley, on Bruker SMART, SMART APEX, APEX II Quazar, or MicroSTAR-H X8 APEXII diffractometers.

Et_2O•LiNTMS(^{t}Bu) (1.1) . To a solution of *N-tert*-butyltrimethylsilylamine (30 mL, 157 mmol) in 300 mL of pentane chilled to -42 °C was slowly added *n*BuLi in hexane (98 mL, 1.6 M). The reaction mixture was stirred for 2 h and then allowed to warm to room temperature and stirred a further 1 h. The solution was then reduced to a residue *in vacuo* and extracted with Et_2O and transferred to a Schlenk tube *via* a filter cannula. The volume of the solution was reduced until the product began to crystallize and was then placed in a -40 °C freezer overnight. The resultant crystals were decanted and recrystallized from Et_2O at -40 °C to ensure a 1:1 ratio of Et_2O to the lithium amide. The title compound was afforded in 68% (24.13 g) yield as large white crystals. ^{1}H NMR (C_6D_6, 300 MHz, 298 K) δ 3.31 (q, O(CH_2CH$_3$)$_2$, 4H, J_{HH} = 7.2 Hz), 1.32 (s, *tBu*, 9H), 1.04 (t, O(CH$_2$CH_3)$_2$, 6H, J_{HH} = 7.2 Hz), 0.30 (s, *TMS*, 9H). ^{13}C{^{1}H} NMR (C_6D_6, 100.6 MHz) δ 64.73 (O(*C*H$_2$CH$_3$)$_2$) 53.15 (α-*t*Bu), 37.10 (β-*t*Bu), 14.88 (O(CH$_2$*C*H$_3$)$_2$) 7.02 (*TMS*). Anal. Calcd (%) for $C_{11}H_{28}LiNOSi$: C, 58.62; H, 12.52; N, 6.21. Found: C, 58.49; H, 12.25; N, 6.56. IR (KBr, nujol, cm^{-1}): 1246 (s), 1214 (s), 1184 (s), 1152 (w), 1121 (w), 1096 (w), 1030 (s), 1003 (s), 853 (s), 755 (m), 740 (m), 680 (w), 663 (m), 619 (w), 564 (m). Mp = 225 °C (dec).

Preparation of VCl_2(N*t*Bu)(NTMS(^{t}Bu)) (1.2). To a slurry of Et_2O•LiNTMS(^{t}Bu) (2.76 g, 12.26 mmol) in 200 mL of pentane chilled to -42 °C was added a solution of $VCl_3(N^tBu)$ (2.80 g, 12.26 mmol) in 200 ml of pentane. The mixture was allowed to warm to room temperature with the cooling bath and then stirred for a total of 6 d. The solution was then reduced to a residue *in vacuo* and extracted with pentane and filtered through Celite. The volume of the solution was reduced until the solution became viscous (about 20-25 ml) and was then placed in a -80 °C freezer overnight. The resultant crystals were decanted and remaining solvent was removed *in vacuo* at -80 °C over 4 h. The title compound was afforded in 68% (2.83 g) yield as fine orange/red needles. At room temperature in C_6D_6 VCl_2(N*t*Bu)(NTMS(^{t}Bu)) is a mixture of two isomers about the V-N amide bond (isomer A:B, 1.2:1). ^{1}H NMR (C_6D_6, 400 MHz, 298 K) δ 1.55 (s, B-amide-*tBu*, 9H), 1.52 (s, A-amide-*tBu*, 9H), 1.42 (s, B-imide-*tBu*, 9H), 1.37 (s, A-imide-*tBu*, 9H), 0.58 (s, A-*TMS*, 9H), 0.45 (s, B-*TMS*, 9H). ^{13}C{^{1}H} NMR (C_6D_6, 150.9 MHz) δ 68.22 (A-amide-α-*t*Bu), 66.26 (B-amide-α-*t*Bu), 36.37 (A-amide-β-*t*Bu), 31.62 (B-amide-β-*t*Bu), 30.55 (B-imide-β-*t*Bu), 30.21 (A-imide-β-*t*Bu), 7.31 (B-TMS), 4.78 (A-TMS). The imide C$_\alpha$-*t*Bu carbon resonances could not be observed. ^{51}V{^{1}H} NMR (C_6D_6,

105.2 MHz, 298 K) δ -26.97 (t, $\Delta\nu_{1/2}$ = 282 Hz, J_{VN} = 78.9 Hz), -99.70 (unresolved t, $\Delta\nu_{1/2}$ = 282 Hz). Anal. Calcd (%) for $C_{11}H_{27}Cl_2N_2SiV$: C, 39.17; H, 8.07; N, 8.31. Found: C, 39.37; H, 8.29; N, 8.44. IR (KBr, nujol, cm^{-1}): 1390 (m), 1252 (s), 1212 (s), 1129 (m), 1117 (m), 1030 (m), 951 (s), 926 (m), 914 (m), 849 (s), 808 (s), 769 (s), 737 (m), 699 (w), 680 (m), 637 (m), 620 (w), 530 (s), 494 (w), 421 (s). Mp = 51-53 °C.

Preparation $VCl(PMe_3)_2(N^tBu)_2$ (1.3). To a solution of $VCl_2(NtBu)(NTMS(^tBu)$ (3.54 g, 10.5 mmol) in 150 mL of toluene was added PMe_3 (2.1 equiv., 2.28 mL, 22 mmol) *via* syringe. The reaction mixture was brought to reflux for 18 h. It was cooled and reduced to a residue *in vacuo* and extracted with pentane. The solution was transferred to a Schlenk tube *via* a filter cannula, and the filtrate was reduced until the product began crystallize and was placed into a -40 °C freezer overnight. The title compound was afforded in 77% (3.07 g) yield as olive green blocks after decantation. X-ray quality crystals were grown from a concentrated pentane solution at -40 °C overnight. ^1H NMR (C_6D_6, 400 MHz, 298 K) δ 1.29 (s, *tBu*, 18H), 1.26 (t, P*Me*$_3$, J_{PH} = 3.8 Hz). $^{13}C\{^1H\}$ NMR (C_6D_6, 100.62 MHz, 298 K) δ 68.62 (br s, α-*t*Bu), 34.26 (t, β-*t*Bu, $^4J_{CP}$ = 3.77) 16.65 (t, PMe_3, $^1J_{CP}$ = 9.96). $^{31}P\{^1H\}$ NMR (C_6D_6, 161.96 MHz, 298 K) δ -3.52 (br s, $\Delta\nu_{1/2}$ = 2232.64 Hz). $^{51}V\{^1H\}$ NMR (C_6D_6, 105.2 MHz, 298 K) δ -782.31 (br s, $\Delta\nu_{1/2}$ = 697.20 Hz). Anal. Calcd (%) for $C_{14}H_{36}ClN_2P_2V$: C, 44.16; H, 9.53; N, 7.36. Found: C, 43.88; H, 9.50; N, 7.18. IR (KBr, nujol, cm^{-1}): 2009 (w), 1946 (w), 1348 (s), 1296 (m), 1281 (m), 1275 (m), 1246 (s), 1224 (s), 1205 (s), 1110 (m), 946 (s), 841 (m), 735 (s), 673 (w), 597 (s), 583 (m), 470 (w). Mp = 154-156°C.

Preparation of $VCl(PEt_3)_2(N^tBu)_2$ (1.4). To a solution of $VCl_2(N^tBu)(NTMS(^tBu))$ (2.10 g, 6.2 mmol) in 50 mL of toluene was added triethylphosphine (2.1 equiv., 1.89 mL, 13.1 mmol) *via* syringe. After this addition, the reaction flask was fitted with a reflux condenser and the reaction mixture was stirred for 16 h at reflux with a bath temperature of 125 °C. The reaction mixture was then cooled to room temperature and reduced to a residue *in vacuo*. The residue was extracted with HMDSO, and the combined extracts were filtered *via* cannula and reduced in volume *in vacuo* until the product began to crystallize. After cooling the solution to -40 °C overnight and decantation, the product was recrystallized by the same method to afford analytically pure product in 83% yield (2.42 g) as large, light green blocks. Recrystallization from HMDSO at -40 °C afforded X-ray quality crystals. ^1H NMR (C_6D_6, 600.1 MHz) δ 1.80 (unresolved m, $P(CH_2CH_3)_3$, 12H), 1.40 (s, N*t*Bu), 1.10 (unresolved m, $P(CH_2CH_3)_3$, 18H). $^{13}C\{^1H\}$ NMR (C_6D_6, 150.9 MHz) δ 68.43 (br s, α-N*t*Bu), 33.99 (s, β-*t*Bu), 16.85 (br s, $P(CH_2CH_3)_3$), 8.74 (br s, $P(CH_2CH_3)_3$). $^{31}P\{^1H\}$ NMR (C_6D_6, 242.9 MHz, 298 K) δ 26.79 (br s, $\Delta\nu_{1/2}$ = 2051.66 Hz). $^{51}V\{^1H\}$ NMR (C_6D_6, 157.7 MHz) δ -757.33 (br s, $\Delta\nu_{1/2}$ = 11.78 Hz). Anal. Calcd (%) for $C_{20}H_{48}N_2P_2VCl$: C, 32.91; H, 3.38; N, 2.88. Found: C, 32.67; H, 3.10; N, 2.84. IR (KBr, cm^{-1}): 1413 (s), 1349 (s), 1228 (s), 1208 (s), 1033 (s), 761 (s), 750 (s), 715 (m), 685 (w), 586 (m), 468 (w). Mp = 66-68 °C.

Preparation of $VCl(PMe_2Ph)_2(N^tBu)_2$ (1.5). To a solution of $VCl_2(NtBu)(NTMS(^tBu)$ (1.56 g, 4.6 mmol) in 50 mL of toluene was added PMe_2Ph (2.0 equiv., 1.32 mL, 4.6 mmol) *via* syringe. The reaction mixture was brought to reflux for 18 h. It was cooled and reduced to a residue *in vacuo* and extracted with warm hexane. The solution was

transferred to a Schlenk tube *via* a filter cannula, and the filtrate was reduced until the product began crystallize and was placed into a -40 °C freezer overnight. The title compound was afforded in 74 % (1.73 g) yield as light green blocks after decantation. X-ray quality crystals were grown from a hot hexane solution, which was cooled to room temperature and then stored at -40 °C overnight. ^{1}H NMR (C_6D_6, 600.1 MHz, 298 K) δ 8.01 (br s, *Ar*, 4H), 7.14 (m (overlapping with residual C_6D_5H), *Ar*, 4H), 7.08 (m, *Ar*, 2H), 1.66 (br s, P*Me*$_2$Ph, 12H), 1.31 (s, *tBu*, 18H). ^{13}C{^{1}H} NMR (C_6D_6, 150.9 MHz, 298 K) δ 137.09 (br s, *Ar*), 133.24 (s, *Ar*), 129.33 (s, *Ar*), 69.5* (br s, α-*t*Bu), 33.32 (br s, β-*t*Bu) 16.28 (unresolved t, PMe_3). ^{31}P{^{1}H} NMR (C_6D_6, 242.9 MHz, 298 K) δ 5.55 (br s, $\Delta\nu_{1/2}$ = 1844.93 Hz). ^{51}V{^{1}H} NMR (C_6D_6, 157.7 MHz, 298 K) δ -766.92 (br s, $\Delta\nu_{1/2}$ = 550.33 Hz). $C_{24}H_{40}N_2P_2VCl$: C, 57.09; H, 7.98; N, 5.55. Found: C, 56.92; H, 7.72; N, 5.53. IR (KBr, nujol, cm^{-1}): 1455 (w), 1435 (w), 1350 (w), 1243 (m), 1220 (m), 1205 (m), 1103 (m), 948 (w), 747 (s), 740 (w), 731 (w), 708 (w), 644 (m), 593 (w), 481 (w), 431 (w). Mp = 72-74 °C.

Preparation of VCl(Py)$_2$(N^{t}Bu)$_2$ (1.6). To a solution of VCl_2(N*t*Bu)(NTMS(^{t}Bu) (675 mg, 2.0 mmol) in 25 mL of toluene was added pyridine (2.0 equiv., 161 μL, 2.0 mmol) *via* syringe. The reaction mixture was brought to reflux for 16 h. It was cooled and reduced to a residue *in vacuo* and extracted with toluene. The solution was transferred to a Schlenk tube *via* a filter cannula, and the filtrate was reduced until approximately 1 mL of red solution remained and copious amounts of solid was present. The solid was dissolved by warming the remaining solution to boiling. Cooling this solution to room temperature afforded the title compound in 33 % (253 mg) yield as gold plates after decantation. X-ray quality crystals were grown by the same method. ^{1}H NMR (C_6D_6, 600.1 MHz, 298 K) δ 9.08 (br s, *Ar*, 4H), 6.81 (br s, *Ar*, 2H), 6.53 (br s, *Ar*, 4H), 1.42 (s, N*t*Bu). ^{13}C{^{1}H} NMR (C_6D_6, 150.9 MHz, 298 K) δ 153.54 (s, *Ar*), 136.75 (s, *Ar*), 123.35 (s, *Ar*), 60.2* (α-N*t*Bu), 33.08 (s, β-*t*Bu),. ^{51}V{^{1}H} NMR (C_6D_6, 157.8 MHz, 298 K) δ -485.42 (br s, $\Delta\nu_{1/2}$ = 20.19 Hz) $C_{18}H_{28}N_4VCl$: C, 55.89; H, 7.30; N, 14.48. Found: C, 54.78; H, 7.03; N, 14.16. Carbon was consistently low on 3 attempts. IR (KBr, nujol, cm^{-1}): .1603 (m), 1477 (w), 1438 (s), 1402 (w), 1356 (w), 1349 (w), 1333 (w), 1240 (m), 1215 (s), 1203 (s), 1151 (w), 1072 (w), 1063 (w), 1043 (w), 768 (w), 757 (w), 701 (s), 638 (w), 602 (w), 586 (m), 464 (w), 445 (w), 404 (w). Mp = 155 °C (dec.).

Preparation of VBr(PMe$_3$)$_2$(N^{t}Bu)$_2$ (1.7). To a solution of VCl(PMe_3)$_2$(N^{t}Bu)$_2$ (404 mg, 1.06 mmol) in 25 mL of toluene was added TMSBr (1.1 equiv., 140 μL, 1.17 mmol) *via* syringe. The reaction mixture was brought to reflux for 16 h. It was cooled and reduced to a residue *in vacuo* and extracted with hexane. The solution was transferred to a Schlenk tube *via* a filter cannula, and the filtrate was reduced until the product began crystallize and was placed into a -40 °C freezer overnight. The compound was further recrystalized by the same method to give title compound in 31 % (140 mg) yield as dark green blocks after decantation. X-ray quality crystals were grown by the same method. ^{1}H NMR ($CDCl_3$, 600.1 MHz, 298 K) δ 1.46 (unresolved t, P*Me*$_3$, 18H), 1.23 (s, *tBu*, 18H). ^{13}C{^{1}H} NMR ($CDCl_3$, 150.9 MHz, 298 K) δ 69.0* (α-*t*Bu), 33.56 (t, β-*t*Bu, $^{4}J_{CP}$ = 3.02 Hz) 17.16 (t, PMe_3, $^{1}J_{CP}$ = 10.86 Hz). ^{31}P{^{1}H} NMR ($CDCl_3$, 242.9 MHz, 298 K) δ -5.85 (br s, $\Delta\nu_{1/2}$ = 2223.42 Hz). ^{51}V{^{1}H} NMR ($CDCl_3$, 157.7 MHz, 298 K) δ -770.95 (br

s, $\Delta\nu_{1/2}$ = 871.77 Hz). Anal. Calcd (%) for $C_{14}H_{36}BrN_2P_2V$: C, 39.54; H, 8.53; N, 6.59. Found: C, 39.25; H, 8.53; N, 6.28. IR (KBr, nujol, cm^{-1}): 1419 (m), 1350 (m), 1297 (m), 1279 (m), 1244 (s), 1221 (s), 1205 (s), 1106 (m), 951 (s), 846 (m), 734 (m), 594 (w). Mp = 110-112 °C.

Preparation of VI(PMe$_3$)$_2$(N^{t}Bu)$_2$ (1.8). To a solution of VCl(PMe$_3$)$_2$(N^{t}Bu)$_2$ (381 mg, 1.0 mmol) in 25 mL of toluene was added TMSI (1.0 equiv., 137 μL, 1.0 mmol) *via* syringe. The reaction mixture was brought to reflux for 16 h. It was cooled and reduced to a residue *in vacuo* and extracted with hexane. The solution was transferred to a Schlenk tube *via* a filter cannula, and the filtrate was reduced until the product began crystallize and was placed into a -40 °C freezer overnight. The compound was further recrystalized by the same method to give title compound in 39 % (185 mg) yield as colorless plates after decantation. X-ray quality crystals were grown by the same method. ^{1}H NMR ($CDCl_3$, 600.1 MHz, 298 K) δ 1.55 (unresolved t, P*Me*$_3$, 18H), 1.24 (s, *tBu*, 18H). $^{13}C\{^1H\}$ NMR ($CDCl_3$, 150.09 MHz, 298 K) δ 69.7* (α-*t*Bu), 33.32 (t, β-*t*Bu, $^4J_{CP}$ = 4.50 Hz) 18.35 (t, PMe$_3$, $^1J_{CP}$ = 11.24 Hz). $^{31}P\{^1H\}$ NMR ($CDCl_3$, 242.9 MHz, 298 K) δ -8.70 (br s, $\Delta\nu_{1/2}$ = 2179.95 Hz). $^{51}V\{^1H\}$ NMR ($CDCl_3$, 157.7 MHz, 298 K) δ -778.38 (br s, $\Delta\nu_{1/2}$ = 15.147 Hz). Anal. Calcd (%) for $C_{14}H_{36}IN_2P_2V$: C, 35.61; H, 7.68; N, 5.93. Found: C, 35.54; H, 7.57; N, 5.79. IR (KBr, nujol, cm^{-1}): 1420 (w), 1350 (w), 1296 (w), 1278 (m), 1242 (m), 1219 (s), 1203 (m), 1105 (m), 955 (s), 850 (w), 732 (m), 593 (m). Mp =191-193 °C.

Preparation of VPh(PMe$_3$)$_2$(N^{t}Bu)$_2$ (1.9). A solution of VCl(PMe$_3$)$_2$(N^{t}Bu)$_2$ (400 mg, 1.05 mmol) in 25 mL of diethyl ether was added to a slurry of Ph_2Mg (1.2 equiv., 225 mg, 1.26 mmol) in 25 mL of diethyl ether at -78 °C *via* cannula. The reaction mixture was stirred for 1 h, allowed to warm to rt, and stirred for 4 h. The reaction mixture was then reduced to a residue *in vacuo*, extracted with hexane, and filtered *via* filter cannula. The filtrate was reduced *in vacuo* until the product began to crystallize. The saturated solution was then stored at -40 °C overnight to afford the product as bright yellow plates after decantation. A second crop was obtained by the same method to give 80 mg (18 %) as combined yield. X-ray quality crystals were grown by the same method. ^{1}H NMR (C_6D_6, 600.1 MHz, 298 K) δ 7.84 (m, *Ar*, 2H), 7.25 (t, *Ar*, 2H, J_{HH} = 7.20 Hz) 1.36 (s, *tBu*, 18H), 1.00 (pseudo d, P*Me*$_3$, J_{PH} = 7.20 Hz). $^{13}C\{^1H\}$ NMR (C_6D_6, 150.9 MHz, 298 K) δ 139.82 (t, *Ar*, J_{CP} = 5.28 Hz), 124.93 (t, *Ar*, J_{CP} = 4.83 Hz), 122.60 (t, *Ar*, J_{CP} = 4.38 Hz), 34.15 (t, β-*t*Bu, $^4J_{CP}$ = 3.02 Hz) 16.88 (dd, PMe$_3$, $^1J_{CP}$ = 11.92 Hz, $^3J_{CP}$ = 8.15 Hz). The α-*t*Bu resonance was not located. $^{31}P\{^1H\}$ NMR (C_6D_6, 161.96 MHz, 298 K) δ 1.07 (br s, $\Delta\nu_{1/2}$ = 1954.62 Hz). $^{51}V\{^1H\}$ NMR (C_6D_6, 105.2 MHz, 298 K) δ -801.07 (br s, $\Delta\nu_{1/2}$ = 21.87 Hz). Anal. Calcd (%) for $C_{20}H_{41}N_2P_2V$: C, 56.86; H, 9.78; N, 6.63. Found: C, 5.48; H, 10.10; N, 6.36. IR (KBr, nujol, cm^{-1}): 1347 (m), 1276 (m), 1247 (m), 1219 (s), 1203 (m), 1100 (m), 944 (s), 729 (s), 714 (m), 592 (m). Mp = 65 °C (dec.).

[V(PMe$_3$)$_3$(N^{t}Bu)$_2$][Al(PFTB)$_4$] (1.10). To a slurry of Li[Al(PFTB)$_4$] (1.67 g, 1.7 mmol) in 100 mL chlorobenzene was added PMe$_3$ (3 equiv., 530 μL, 5.1 mmol) *via* syringe. To this mixture was then added *via* cannula a solution of VCl(PMe$_3$)$_2$(N^{t}Bu)$_2$ (1 equiv., 650 mg, 1.7 mmol) in 100 mL of chlorobenzene. The reaction mixture was stirred

for 12 h at room temperature and filtered through Celite. The filtrate was reduced until the product began to crystallize and then chilled at -15 °C overnight. After decantation the title compound was afforded as yellow needles in 75% yield (1.760 g). X-ray quality crystals were grown from a concentrated diethyl ether solution at -40 °C overnight. ^{1}H NMR ($PhCF_3$ (C_6D_6 insert), 600 MHz, 300 K) δ 1.31 (d, axial P*Me*$_3$, 18H, $^{2}J_{PH}$ = 19.2 Hz), 1.13 (d, equatorial P*Me*$_3$, 9H, $^{2}J_{PH}$ = 4.2 Hz), 1.08 (s, *t*Bu, 18H). ^{13}C NMR ($PhCF_3$ (C_6D_6 insert), 150.9 MHz, 300 K) δ 131.10 (q, C(*C*F$_3$)$_3$, $^{1}J_{CF}$ = 32.14 Hz), 32.92 (t, β-*t*Bu, $^{4}J_{CP}$ = 4.07 Hz), 19.07 (t, axial PMe_3, $^{1}J_{CP}$ = 10.26 Hz), 17.18 (t, equatorial PMe_3, $^{1}J_{CP}$ = 13.43 Hz). The imide α-*t*Bu carbon and the α-C(CF_3)$_3$ resonances could not be observed. ^{31}P{^{1}H} NMR ($PhCF_3$ (C_6D_6 insert), 242.9 MHz, 300 K) δ -3.96 (br s, $\Delta\nu_{1/2}$ = 1957.40 Hz), -32.21 (br s, $\Delta\nu_{1/2}$ = 1045.44 Hz). ^{51}V{^{1}H} NMR ($PhCF_3$ (C_6D_6 insert), 157.7 MHz, 300 K) δ -792.29 (br s, $\Delta\nu_{1/2}$ = 823.39 Hz). ^{19}F NMR ($PhCF_3$ (C_6D_6 insert), 376.5 MHz, 298 K) δ -62.72 (s, $\Delta\nu_{1/2}$ = 4.61 Hz). ^{27}Al NMR ($PhCF_3$ (C_6D_6 insert), 104.3 MHz, 298 K) δ 34.70 (s, $\Delta\nu_{1/2}$ = 2.99 Hz). Anal. Calcd (%) for $C_{33}H_{45}AlF_{36}N_2O_4P_3V$: C, 28.55; H, 3.27; N, 2.02. Found: C, 28.68; H, 3.06; N, 1.81. IR (KBr, nujol, cm^{-1}): 1456 (s), 1423 (s), 1262 (s), 1171 (s), 1101 (w), 973 (s), 832 (m), 803 (w), 755 (w), 728 (s), 669 (w), 597 (w), 560 (m), 537 (m), 445 (s). Mp = 140°C (dec.).

Preparation of [V(PEt$_3$)$_2$(N^{t}Bu)$_2$][Al(PFTB)$_4$] (1.11). Method A: To a slurry of Li[Al(PFTB)$_4$] (974 mg, 1 mmol) in 15 mL of DCE was added **1.4** (465 mg, 1 mmol) in 15 mL of DCE. The reaction mixture was stirred overnight at rt, filtered through Celite, and reduced in volume until the product began to crystallize. After cooling the solution to -15 °C overnight, the title compound was afforded in 47% yield (650 mg) after decantation, as deep red blades. ^{1}H NMR ($PhCF_3$ (C_6D_6 insert), 600.1 MHz) δ 1.46 (pseudo quintet (doublet of quartets), P(*CH*$_2$CH$_3$)$_3$, 12H), 1.25 (s, N*tBu,* 18H), 1.01 (pseudo quintet (doublet of triplets), P(CH$_2$*CH*$_3$)$_3$, 18H). ^{13}C NMR ($PhCF_3$ (C_6D_6 insert), 150.9 MHz) δ 131.02 (q, C(*C*F$_3$)$_3$, $^{1}J_{CF}$ = 32.14 Hz), 72.6* (α-N*t*Bu), 32.73 (s, β-*t*Bu), 16.19 (t, P(*CH*$_2$CH$_3$)$_3$, $^{1}J_{PC}$ = 7.39 Hz), 16.04 (t, P(*CH*$_2$CH$_3$)$_3$, $^{1}J_{PC}$ = 8.63 Hz), 7.84 (br s, P(CH$_2$*CH*$_3$)$_3$). The α-C(CF_3)$_3$ resonance could not be observed. ^{31}P{^{1}H} NMR ($PhCF_3$ (C_6D_6 insert), 242.9 MHz) δ 26.69 (vbr s, $\Delta\nu_{1/2}$ = 2674.50 Hz). ^{51}V{^{1}H} NMR ($PhCF_3$ (C_6D_6 insert), 157.7 MHz) δ -278.99 (br s, $\Delta\nu_{1/2}$ = 80.78 Hz). Anal. Calcd (%) for $C_{36}H_{48}AlF_{36}N_2O_4P_2V$: C, 30.96; H, 3.46; N, 2.01. Found: C, 30.75; H, 3.20; N, 2.06. IR (KBr, cm^{-1}): 1417 (s), 1352 (m), 1300 (s), 1219 (s), 1168 (w), 1038 (w), 831 (w), 768 (w), 755 (w), 560 (w), 537 (w), 444 (w). Mp = 150 °C (dec.).

Method B: A scintillation vial was charged with Li[Al(PFTB)$_4$] (21 mg, 0.02 mmol) and ~300 μL of the appropriate solvent. To this slurry was added a solution of **1.4** (10 mg, 0.02 mmol) in ~150 μL of same solvent. On mixing, the solution shifted from green to deep red. The reaction mixture was agitated *via* pipette for 5 min and transferred *via* pipette to a J. Young NMR tube, in the case of a protio-solvent a sealed capillary filled with C_6D_6 was included. The scintillation vials and pipettes were washed with a further ~150 μL of solvent, which was then transferred to the J. Young NMR tube.

Preparation of [V(PEt)$_2$(N^{t}Bu)$_2$(DMAP)][Al(PFTB)$_4$] (1.12). To a slurry of Li[Al(PFTB)$_4$] (400 mg, 0.41 mmol) in 5 mL $PhCF_3$ was added sequentially 4-

dimethylaminopyridine (1 equiv., 50 mg, 0.41 mmol) in 5 mL of $PhCF_3$ and **1.4** (1 equiv., 191 mg, 0.41 mmol)) in 5 mL of $PhCF_3$ *via* cannula. After these additions, the reaction mixture was stirred for 1 h, during which time the solution became bright yellow. The reaction mixture was then filtered through Celite and reduced until the product began to crystallize. After cooling the solution to -15 °C overnight, the title compound was afforded in 50% yield (310 mg) after decantation, as yellow blocks. Recrystallization from $PhCF_3$ afforded x-ray quality crystals. ^{1}H NMR ($PhCF_3$ (C_6D_6 insert), 600.1 MHz) δ 7.95 (d, Ar*H*, 2H, *J* = 4.8 Hz), 6.39 (d, Ar*H*, 2H, *J* = 6.0 Hz), 2.65 (s, *Me*, 6H), 1.28 (s with shoulder, N*tBu* and P(*CH*$_2$CH$_3$)$_3$, 30H), .91 (unresolved m, P(CH$_2$*CH*$_3$)$_3$, 18H). ^{13}C NMR ($PhCF_3$ (C_6D_6 insert), 150.9 MHz) δ 155.23 (s, *Ar*), 149.74 (s, *Ar*), 131.14 (q, C(*C*F$_3$)$_3$, $^1J_{CF}$ = 32.29 Hz), 107.17 (s, *Ar*), 68.0* (α-N*t*Bu), 38.22 (s, DMAP-*Me*), 33.97 (s, β-N*t*Bu), 16.74 (br s, P(*CH*$_2$CH$_3$)$_3$), 8.09 (br s, P(CH$_2$*CH*$_3$)$_3$). The α-C(CF$_3$)$_3$ resonance could not be observed. ^{31}P{^{1}H} NMR ($PhCF_3$ (C_6D_6 insert), 242.9 MHz) δ 24.67 (vbr s, $\Delta\nu_{1/2}$ = 1800.53 Hz). ^{51}V{^{1}H} NMR ($PhCF_3$ (C_6D_6 insert), 157.7 MHz) δ -728.16 (br s, $\Delta\nu_{1/2}$ = 69.00 Hz). Anal. Calcd (%) for $C_{43}H_{58}AlF_{36}N_4O_4P_2V$: C, 34.01; H, 3.85; N, 3.65. Found: C, 33.94; H, 3.74; N, 3.72. IR (KBr, cm^{-1}): 1622 (s), 1398 (s), 1353 (s), 1219 (s), 1169 (s), 1062 (m), 1037 (m), 1011 (m), 832 (m), 817 (m), 760 (m), 584 (w), 560 (w), 537 (m), 445 (m). Mp = 91 °C (dec.).

NEXAFS Spectroscopy.

General. V_2O_5 and Na_3VO_4 were dried at 150 °C and 0.01 mm Hg for at least 24 hr prior to V $L_{2/3}$-edge XAS measurements and handled with rigorous exclusion of air and moisture prior to and during use.

Vanadium L-Edge TEY Measurements. Samples were prepared in an argon filled glovebox by initially grinding into a fine powder using a mortar and pestle. An aliquot (10 mg) was pressed into the center of a 1 cm^2 circular piece of double adhesive conducting tape which had been affixed to an aluminum sample block. The block was transferred with rigorous exclusion of air and moisture to the sample chamber at the Stanford Synchrotron Radiation Lightsource (SSRL) and analyzed at VUV beamline 10.1, utilizing bending magnet radiation and a spherical grating monochromator, under ring conditions of 3.0 GeV and 85-100 mA in high magnetic field mode of 0.9 T. A chamber similar to that previously described[98] was used, with the exception that a carbon window (1200 Å, Luxel) was used to isolate the chamber from the beam pipe. The incident radiation was monitored using a Au grid with 80% transmission. The total electron yield (TEY, total current leaving the sample) was collected under vacuum (10^{-7} Torr) as a function of the incident beam energy. The TEY spectra showed no sign of radiation damage and the spectra were reproduced from multiple samples during two different synchrotron experiments.

Vanadium L-Edge STXM Measurements. STXM methodology was similar to that discussed previously.[99,100] In an argon-filled glovebox, each sample was ground in a mortar and pestle, and the particles were transferred to a Si_3N_4 window (100 nm, Silson). A second window was placed over the sample, essentially sandwiching the particles, and the windows were sealed together using epoxy.

Single-energy images and vanadium L-edge XAS spectra were acquired using the STXM instrument at the Advanced Light Source Molecular Environmental Science

beamline 11.0.2, which is operated in topoff mode at 500 mA, in a ~0.5 atm He filled chamber. For these measurements, the X-ray beam was focused with a zone plate onto the sample, and the transmitted light was detected. The spot size and spectral resolution were determined from characteristics of the 35 nm zone plate. Images at a single energy were obtained by raster-scanning the sample and collecting transmitted monochromatic light as a function of sample position. Spectra at each image pixel or particular regions of interest on the sample image were extracted from the "stack," which is a collection of images recorded at multiple, closely spaced photon energies across the absorption edge.[101] This enabled spatial mapping of local chemical bonding information. Dwell times used to acquire an image at a single photon energy were ~1 ms per pixel. To quantify the absorbance signal, the measured transmitted intensity (I) was converted to optical density using Beer-Lambert's law: $OD = \ln(I/I_0) = \mu\rho d$, where I_0 is the incident photon flux intensity, d is the sample thickness, and μ and ρ are the mass absorption coefficients and density of the sample material, respectively. Incident beam intensity was measured through the sample-free region of the Si_3N_4 windows. Particle spectra were then obtained by averaging over the particles deposited on the substrate.[102] Regions of particles with an absorption of >1.5 OD were omitted to ensure the spectra were in the linear regime of the Beer-Lambert law. The energy resolution (fwhm) was determined to be 0.08 eV, and spectra were collected using circularly polarized radiation. During the STXM experiment, particles showed no sign of radiation damage and each spectrum was reproduced from multiple independent particles.

Data Analysis. In typical data analysis, a first-order polynomial was fit to the pre-edge region (<514 eV) and then subtracted from the experimental data to eliminate the background of the spectrum. The data were then normalized to the intensity of the L_3 feature. The energy calibration for the TEY and STXM data was referenced to the first O K-edge pre-edge feature of $NaReO_4$ at 531.40 eV, based on the reported NRIXS spectrum.[99]

General Remarks on the Determination of Molecular Structure by X-ray Diffraction. X-ray diffraction data were collected using either Bruker AXS three-circle or Bruker AXS Microstar kappa-geometry diffractometers with either graphite-monochromated Mo-Kα radiation (λ = 0.71073 Å) or HELIOS-monochromated Cu-Kα radiation (λ = 1.54178 Å). A single crystal of appropriate size was coated in Paratone-N oil and mounted on a Cryo loop. The loop was transferred to a diffractometer equipped with a CCD area detector,[103] centered in the beam, and cooled by an Oxford Cryostream 700 LT device. Preliminary orientation matrices and cell constants were determined by collection of three sets of 40, 5 s frames or three sets of 30, 10 s frames, followed by spot integration and least-squares refinement. COSMO was used to determine an appropriate data collection strategy, and the raw data were integrated using SAINT.[104] Cell dimensions reported were calculated from all reflections with $I > 10\ \sigma$. The data were corrected for Lorentz and polarization effects; no correction for crystal decay was applied. Data were analyzed for agreement and possible absorption using XPREP.[105] An absorption correction based on comparison of redundant and equivalent reflections was applied using SADABS.[106] Structures were solved by direct methods with the aid of successive difference Fourier maps and were refined on F^2 using the SHELXTL 5.0 software package. All non-hydrogen atoms were refined anistropically; all hydrogen

atoms were included into the model at their calculated positions and refined using a riding model. For all structures, $R_1 = \Sigma(|Fo| - |Fc|)/\Sigma(|Fo|)$; $wR_2 = [\Sigma]^{1/2}$. See Table 1.4 for integration and refinement details.

Notes on the disorder model for 1.10. The poor quality of the data for **1.10** is due to the spherical (S_4 symmetric) $[Al(PFTB)_4]^-$ anion. Two solutions are presented to resolve the disorder in the anion. In the full structure solution, SADI and ISOR restraints are employed to restrict the $-C(CF_3)_3$ groups to reasonable bond lengths, angles and thermal parameters. In the second solution, the $[Al(PFTB)_4]^-$ anion is reduced to the AlO_4 tetrahedral core and treated with the SQUEEZE routine included in PLATON.[107] The final refinement by this approach provides significantly better residuals and, as the two cation models are very nearly super imposable, implies that poor residuals for the full structure determination are due solely to unresolved disorder in the anion and that the X-ray structure connectivity agrees with the spectroscopic and analytical data. Attempts to remove restraints in the full structure determination resulted only in the collapse of the model or in the generation of unrealistic bond parameters in the anion. While higher symmetry is indicated, efforts to solve **1** in Pm were unsuccessful. The equatorial PMe_3 is disordered between two positions. The related carbon electron density could be located in the difference map only for P2.

Notes on the disorder model for 1.12. The poor quality of the data for **1.12** is due to the spherical (S_4 symmetric) $[Al(PFTB)_4]^-$ anion, which is often heavily disordered in the solid state even at 90 K.[108] Two solutions were considered to resolve the disorder in the anion. In the full structure solution, SADI and ISOR restraints are employed to restrict the $-C(CF_3)_3$ groups to reasonable bond lengths, angles and thermal parameters. In the second solution, the $[Al(PFTB)_4]^-$ anion is reduced to the AlO_4 tetrahedral core and treated with the SQUEEZE routine included in PLATON.[107] The final refinement by this approach provides significantly better residuals and, as the two models of the cation are very nearly super imposable, implies that poor residuals for the full structure determination are due solely to unresolved disorder in the anion and that the X-ray structure connectivity agrees with the spectroscopic and analytical data. Attempts to remove restraints in the full structure determination resulted only in the collapse of the model or in the generation of unrealistic bond parameters in the anion.

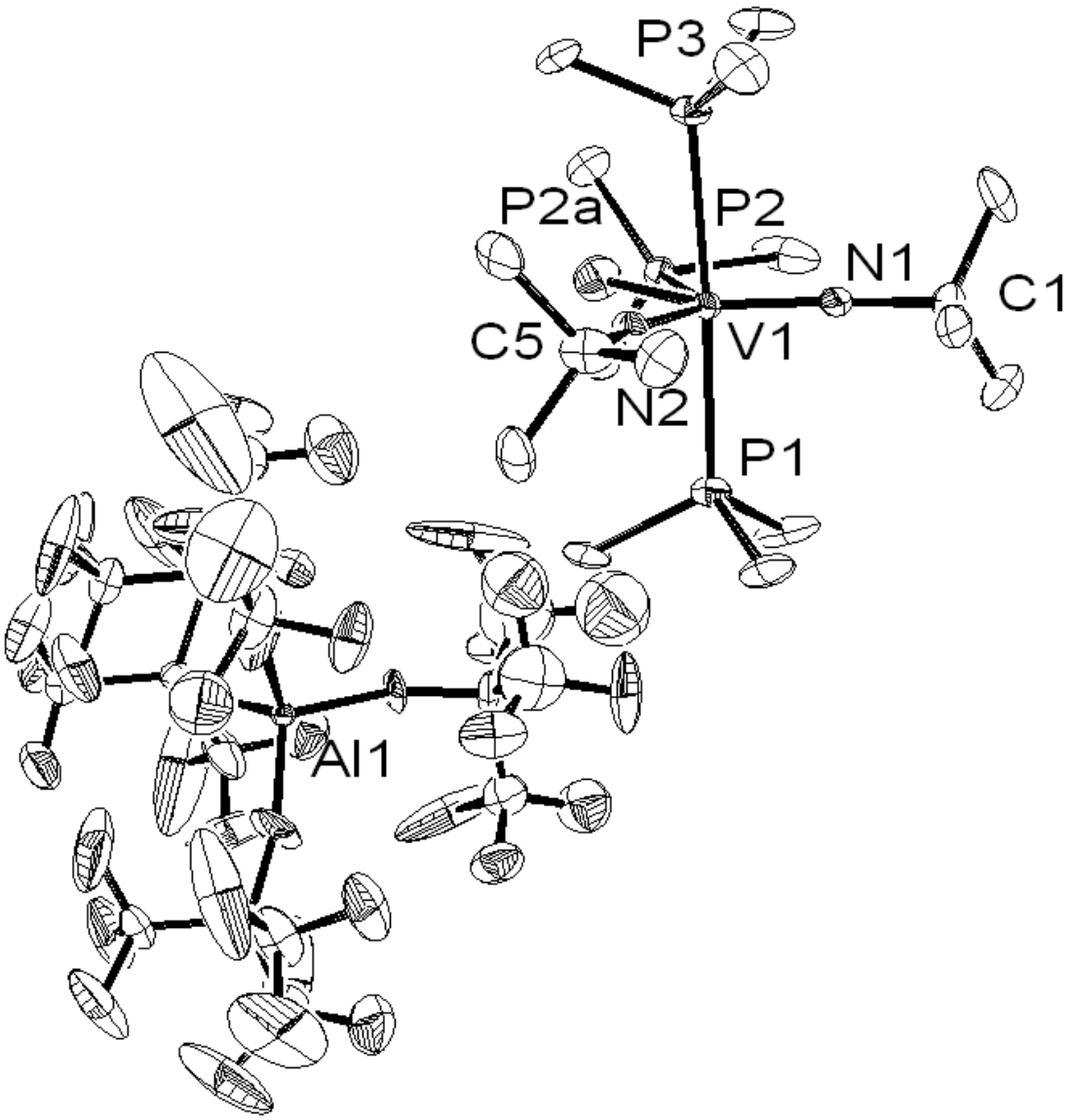

Figure 1.13 ORTEP representation of Complex 1.10 – Full structure determination: Thermal ellipsoids are drawn at 25% probability level. Hydrogen atoms are omitted for clarity. Selected bond lengths (Å) and angles (deg): V(1)-N(1), 1.654(11); V(1)-N(2), 1.651(11); V(1)-P(2), 2.618(5); V(1)-P(1), 2.482(3); V(1)-P(3), 2.490(3); N(1)-V(1)-N(2), 116.6(8); P(1)-V(1)-P(2), 86.23(13); P(3)-V(1)-P(1), 171.96(15); C(1)-N(1)-V(1), 166.6(14); C(5)-N(2)-V(1), 165.2(14).

Table 1.4: Crystal and Refinement Data for Complexes **1.3** – **1.6**, **1.8** – **1.10**, and **1.12**.

	1.3	**1.4**
empirical formula	$C_{14}H_{36}ClN_2P_2V$	$C_{20}H_{48}ClN_2P_2V$
formula weight	380.78	464.93
temp., K	134	100(2)
λ	0.71073	0.71073
crystal system	monoclinic	monoclinic
space group	Cc	$P2_1/c$
a, Å	15.6601(19)	9.658
b, Å	9.4173(12)	14.132
c, Å	15.821(2)	20.637
α, deg	90	90
β, deg	108.731(2)	103.47
γ, deg	90	90
volume, $Å^3$	2209.7(5)	2739.2
Z	4	4
d_{calc}, mg/m^3	1.145	1.127
F_{000}	816	1008
μ, mm^{-1}	.710	0.584
no. rflns measd	6077	20988
no. indep reflns	3395	5033
R_{int}	0.0143	0.0686
Restr/param	2/181	0/235
R_1, wR_2 $[I > 2\sigma(I)]$	0.0265, 0.0661	0.1002, 0.1581
R_1 (all data)	0.0290	0.1292
GOF	1.030	1.363
Resid peak, hole ($e^-/Å^3$)	0.530, -0.163	0.694, -0.443

Table 1.4 Cont'd: Crystal and Refinement Data for Complexes **1.3** – **1.6**, **1.8**, **1.10**, and **1.12**.

	1.5	**1.6**
empirical formula	$C_{24}H_{40}ClN_2P_2V$	$C_{18}H_{28}ClN_4V$
formula weight	504.91	386.83
temp., K	100(2)	100(2)
λ	0.71073	0.71073
crystal system	monoclinic	orthorhombic
space group	$P2_1/c$	Pbca
a, Å	13.374	9.504(2)
b, Å	12.856	18.182(4)
c, Å	16.237	23.174(5)
α, deg	90	90
β, deg	93.16	90
γ, deg	90	90
volume, Å^3	2787.5	4004.7(15)
Z	4	8
d_{calc}, mg/m^3	1.203	1.283
F_{000}	1072	1632
μ, mm^{-1}	0.579	0.635
no. rflns measd	25126	134969
no. indep reflns	5098	3692
R_{int}	0.0301]	0.0636
Restr/param	0/271	0/217
R_1, wR_2 [$I > 2\sigma(I)$]	0.0352, 0.0981	0.0325, 0.0765
R_1 (all data)	0.0504	0.0438
GOF	1.138	1.103
Resid peak, hole (e-/Å^3)	0.736, -0.561	0.486, -0.257

Table 1.4 Con't: Crystal and Refinement Data for Complexes **1.3** – **1.6**, **1.8**, **1.10**, and **1.12**.

	1.8	**1.9**
empirical formula	$C_{14}H_{36}IN_2P_2V$	$C_{20}H_{41}N_2P_2V$
formula weight	472.23	422.43
temp., K	100(2)	100(2)
λ	0.71073	0.71073
crystal system	orthorhombic	monoclinic
space group	Pbcm	$P2_1/c$
a, Å	11.5148(13)	9.485(4)
b, Å	28.109(3)	9.550(4)
c, Å	14.1707(16)	27.830(11)
α, deg	90	90
β, deg	90	95.873(7)
γ, deg	90	90
volume, $Å^3$	4586.7(9)	2507.6(17)
Z	8	4
d_{calc}, mg/m^3	1.368	1.119
F_{000}	1920	912
μ, mm^{-1}	1.914	0.529
no. rflns measd	46440	
no. indep reflns	4422	
R_{int}	0.0808	
Restr/param	0/214	0/240
R_1, wR_2 $[I > 2\sigma(I)]$	0.0342, 0.0572	0.0958, 0.2211
R_1 (all data)	0.0627	0.1068
GOF	1.074	1.158
Resid peak, hole (e-/$Å^3$)	0.952, -0.641	0.617, -1.288

Table 1.4 Con't: Crystal and Refinement Data for Complexes **1.3** – **1.6**, **1.8** – **1.10**, and **1.12**.

	1.10 - full	**1.10 - Platon**
empirical formula	$C_{33}H_{45}AlF_{36}N_2O_4P_3V$	$C_{17}H_{45}N_2P_3V$
formula weight	1388.54	421.40
temp., K	100(2)	100(2)
λ	1.54178	1.54178
crystal system	triclinic	triclinic
space group	P1	1
a, Å	10.5819(7)	10.5819(7)
b, Å	12.2896(9)	12.2896(9)
c, Å	10.6523(8)	10.6523(8)
α, deg	89.984	89.984
β, deg	92.954	92.954
γ, deg	90.043	90.043
volume, $Å^3$	1383.46(17)	1383.46(17)
Z	1	1
d_{calc}, mg/m^3	1.667	0.506
F_{000}	694	229
μ, mm^{-1}	3.964	2.316
no. rflns measd	22314	22314
no. indep reflns	6868	6868
R_{int}	0.0338	0.0338
Restr/param	192 / 732	3/219
R_1, wR_2 $[I > 2\sigma(I)]$	0.1607, 0.4093	0.0878, 0.2268
R_1 (all data)	0.1648	0.0930
GOF	2.062	1.053
Resid peak, hole (e-/$Å^3$)	2.345, -0.929	0.609, -0.490

Table 1.4 Con't: Crystal and Refinement Data for Complexes **1.3** – **1.6**, **1.8** – **1.10**, and **1.12**.

	1.12 - Platon
empirical formula	$C_{27}H_{58}AlN_4O_4P_2V$
formula weight	642.63
temp., K	90(2)
λ	1.5418
crystal system	monoclinic
space group	$P2_1/c$
a, Å	10.849(5)
b, Å	21.033(5)
c, Å	27.038(5)
α, deg	90
β, deg	90.830(5)
γ, deg	90
volume, $Å^3$	6169(3)
Z	4
d_{calc}, mg/m^3	0.692
F_{000}	1384
μ, mm^{-1}	0.247
no. rflns measd	93011
no. indep reflns	11043
R_{int}	0.1339
Restr/param	21/352
R_1, wR_2 $[I > 2\sigma(I)]$	0.1424, 0.3545
R_1 (all data)	0.1737
GOF	1.289
Resid peak, hole (e-/$Å^3$)	1.742, -0.640

Notes and References.

(1) Nugent, W. A.; Haymore, B. L. *Coord. Chem. Rev.* **1980**, *31*, 123.
(2) Nugent, W. A.; Mayer, J. M. *Metal-Ligand Multiple Bonds*; Wiley: New York, NY, 1988.
(3) Wigley, D. E. *Prog. Inorg. Chem.* **1994**, 239.
(4) Williams, D. S.; Schofield, M. H.; Schrock, R. R. *Organometallics* **1993**, *12*, 4560.
(5) Albright, T. A.; Burdett, J. K.; Whangbo, M. H. *Orbital Interactions in Chemistry*; John Wiley & Sons: New York, 1985.
(6) Lauher, J. W.; Hoffmann, R. *J. Am. Chem. Soc.* **1976**, *98*, 1729.
(7) Brintzinger, H. H.; Lohr, L. L.; Wong, K. L. T. *J. Am. Chem. Soc.* **1975**, *97*, 5146.
(8) Ciszewski, J. T.; Harrison, J. F.; Odom, A. L. *Inorg. Chem.* **2004**, *43*, 3605.
(9) Nugent, W. A.; Harlow, R. L. *Inorg. Chem.* **1980**, *19*, 777.
(10) Meijboom, N.; Schaverien, C. J.; Orpen, A. G. *Organometallics* **1990**, *9*, 774.
(11) Leung, W. H.; Danopoulos, A. A.; Wilkinson, G.; Hussainbates, B.; Hursthouse, M. B. *J. Chem. Soc. Dalton Trans.* **1991**, 2051.
(12) Nugent, W. A.; Harlow, R. L. *J. Am. Chem. Soc.* **1980**, *102*, 1759.
(13) Lam, H. W.; Wilkinson, G.; Hussainbates, B.; Hursthouse, M. B. *J. Chem. Soc. Dalton Trans.* **1993**, 1477.
(14) Hursthouse, M. B.; Motevalli, M.; Sullivan, A. C.; Wilkinson, G. *J. Chem. Soc. Chem. Comm.* **1986**, 1398.
(15) Sullivan, A. C.; Wilkinson, G.; Motevalli, M.; Hursthouse, M. B. *J. Chem. Soc. Dalton Trans.* **1988**, 53.
(16) Danopoulos, A. A.; Leung, W. H.; Wilkinson, G.; Hussainbates, B.; Hursthouse, M. B. *Polyhedron* **1990**, *9*, 2625.
(17) Danopoulos, A. A.; Wilkinson, G. *Polyhedron* **1990**, *9*, 1009.
(18) Chan, D. M. T.; Nugent, W. A. *Inorg. Chem.* **1985**, *24*, 1422.
(19) Chan, D. M. T.; Fultz, W. C.; Nugent, W. A.; Roe, D. C.; Tulip, T. H. *J. Am. Chem. Soc.* **1985**, *107*, 251.
(20) Williams, D. S.; Anhaus, J. T.; Schofield, M. H.; Schrock, R. R.; Davis, W. M. *J. Am. Chem. Soc.* **1991**, *113*, 5480.
(21) Williams, D. S.; Schofield, M. H.; Anhaus, J. T.; Schrock, R. R. *J. Am. Chem. Soc.* **1990**, *112*, 6728.
(22) Williams, D. S.; Schrock, R. R. *Organometallics* **1993**, *12*, 1148.
(23) Schofield, M. H.; Kee, T. P.; Anhaus, J. T.; Schrock, R. R.; Johnson, K. H.; Davis, W. M. *Inorg. Chem.* **1991**, *30*, 3595.
(24) Chong, A. O.; Oshima, K.; Sharpless, K. B. *J. Am. Chem. Soc.* **1977**, *99*, 3420.
(25) Schaller, C. P.; Wolczanski, P. T. *Inorg. Chem.* **1993**, *32*, 131.
(26) DeWith, J.; Horton, A. D. *Angew. Chem. Int. Edit.* **1993**, *32*, 903.
(27) Kennedy-Smith, J. J.; Nolin, K. A.; Gunterman, H. P.; Toste, F. D. *J. Am. Chem. Soc.* **2003**; *125*, 4056.
(28) Nolin, K. A.; Ahn, R. W.; Toste, F. D. *J. Am. Chem. Soc.* **2005**, *127*, 12462.
(29) Nolin, K. A.; Krumper, J. R.; Pluth, M. D.; Bergman, R. G.; Toste, F. D. *J. Am. Chem. Soc.* **2007**, *129*, 14684.
(30) Toste, F. D.; Nolin, K. A.; Ahn, R. W.; Kobayashi, Y.; Kennedy-Smith, J. J. *Chem. Eur. J.* **2010**, *16*, 9555.

(31) Walsh, P. J.; Hollander, F. J.; Bergman, R. G. *J. Am. Chem. Soc.* **1988**, *110*, 8729.
(32) Sweeney, Z. K.; Salsman, J. L.; Andersen, R. A.; Bergman, R. G. *J. Am. Chem. Soc.* **2000**, *39*, 2339.
(33) Sweeney, Z. K.; Polse, J. L.; Bergman, R. G.; Andersen, R. A. *J. Am. Chem. Soc.* **1999**, *18*, 5502.
(34) Polse, J. L.; Andersen, R. A.; Bergman, R. G. *J. Am. Chem. Soc.* **1998**, *120*, 13405.
(35) Parkin, G.; Bercaw, J. E. *J. Am. Chem. Soc.* **1989**, *111*, 391.
(36) Blake, R. E.; Antonelli, D. M.; Henling, L. M.; Schaefer, W. P.; Hardcastle, K. I.; Bercaw, J. E. *Organometallics* **1998**, *17*, 718.
(37) Cummins, C. C.; Baxter, S. M.; Wolczanski, P. T. *J. Am. Chem. Soc* **1988**, *110*, 8731.
(38) Cummins, C. C.; Schaller, C. P.; Vanduyne, G. D.; Wolczanski, P. T.; Chan, A. W. E.; Hoffmann, R. *J. Am. Chem. Soc.* **1991**, *113*, 2985.
(39) Schafer, D. F.; Wolczanski, P. T. *J. Am. Chem. Soc.* **1998**, *120*, 4881.
(40) Ignatov, S. K.; Rees, N. H.; Dubberley, S. R.; Razuvaev, A. G.; Mountford, P.; Nikonov, G. I. *Chem. Comm.* **2004**, 952.
(41) Khalimon, A. Y.; Simionescu, R.; Kuzmina, L. G.; Howard, J. A. K.; Nikonov, G. I. *Angew. Chem., Int. Edit.* **2008**, *47*, 7701.
(42) Mountford, P.; Ignatov, S. K.; Khalimon, A. Y.; Rees, N. H.; Razuvaev, A. G.; Nikonov, G. I. *Inorg. Chem.* **2009**, *48*, 9605.
(43) Nikonov, G. I.; Khalimon, A. Y.; Simionescu, R. *J. Am. Chem. Soc.* **2011**, *133*, 7033.
(44) Mountford, P.; Ignatov, S. K.; Rees, N. H.; Merkoulov, A. A.; Dubberley, S. R.; Razuvaev, A. G.; Nikonov, G. I. *Chem. Eur. J.* **2008**, *14*, 296.
(45) DeWith, J.; Horton, A. D.; Orpen, A. G. *Organometallics* **1990**, *9*, 2207.
(46) DeWith, J.; Horton, A. D.; Orpen, A. G. *Organometallics* **1993**, *12*, 1493.
(47) Preuss, F.; Becker, H.; Wieland, T. *Naturforsch. B.* **1990**, 191.
(48) Kilgore, U. J.; Karty, J. A.; Pink, M.; Gao, X.; Mindiola, D. J. *Angew. Chem., Int. Edit.* **2009**, *48*, 2394.
(49) Tsai, Y.; Wang, P.; Lin, K.; Chen, S.; Chen, J. *Chem. Commun.* **2008**, 205.
(50) Chao, Y. W.; Wexler, P. A.; Wigley, D. E. *Inorg. Chem.* **1990**, *29*, 4592.
(51) Tomson, N. C.; Arnold, J.; Bergman, R. G. *Organometallics* **2010**, *29*, 2926.
(52) Rehder, D.; Polenova, T.; Buhl, M. *Ann. Rep. NMR Spectrosc.* **2007**, *62*, 49.
(53) Cummins, C. C.; Schrock, R. R.; Davis, W. M. *Inorg. Chem.* **1994**, *33*, 1448.
(54) Gerlach, C. P.; Arnold, J. *Inorg. Chem.* **1996**, *35*, 5770.
(55) Preuss, F.; Towae, W. *Z. Natforsch. B: Anorg. Allg. Chem.* **1981**, *36*, 1130.
(56) Devore, D. D.; Lichtenhan, J. D.; Takusagawa, F.; Maatta, E. A. *J. Am. Chem. Soc.* **1987**, *109*, 7408.
(57) Landis, C. R.; Uddin, J.; Morales, C. M.; Maynard, J. H. *Organometallics* **2006**, *25*, 5566.
(58) Hawkeswood, S. B.; Stephan, D. W. *Inorg. Chem.* **2003**, *42*, 5429.
(59) Degroot, F. M. F. *Coord. Chem. Rev.* **1994**, *67*, 529.
(60) Sawatzky, G. A.; Post, D. *Phys. Rev. B.* **1979**, *20*, 1546.
(61) Collison, D.; Gahan, B.; Garner, C. D.; Mabbs, F. E. *Dalton Trans*. **1980**, 667.
(62) Abbate, M.; Degroot, F. M. F.; Fuggle, J. C.; Ma, Y. J.; Chen, C. T.; Sette, F.; Fujimori, A.; Ueda, Y.; Kosuge, K. *Phys. Rev. B* **1991**, *43*, 7263.

(63) Pen, H. F.; Tjeng, L. H.; Pellegrin, E.; deGroot, F. M. F.; Sawatzky, G. A.; vanVeenendaal, M. A.; Chen, C. T. *Phys. Rev. B* **1997**, *55*, 15500.
(64) Havecker, M.; Knop-Gericke, A.; Mayer, R. W.; Fait, M.; Bluhm, H.; Schlogl, R. *J. Electron. Spectrosc. Relat. Phenom.* **2002**, *125*, 79.
(65) Zhang, G. P.; Callcott, T. A.; Woods, G. T.; Lini, L.; Sales, B.; Mandrus, D.; He, J. *Phys. Rev. Lett*. **2002**, *88*.
(66) Zhang, G. P.; Woods, G. T.; Shirley, E. L.; Callcott, T. A.; Lin, L.; Chang, G. S.; Sales, B. C.; Mandrus, D.; He, J. *Phys. Rev. B* **2002**, *65*.
(67) Liu, X.; Taschner, C.; Leonhardt, A.; Rummeli, M. H.; Pichler, T.; Gemming, T.; Buchner, B.; Knupfer, M. *Phys. Rev. B* **2005**, *72*.
(68) Zhang, G. P.; Callcott, T. A. *Phys. Rev. B* **2006**, *73*.
(69) Hellmann, I.; Taeschner, C.; Klingeler, R.; Leonhardt, A.; Buechner, B.; Knupfer, M. *J. Chem. Phys*. **2008**, *128*.
(70) Fronzoni, G.; Stener, M.; Decleva, P.; de Simone, M.; Coreno, M.; Franceschi, P.; Furlani, C.; Prince, K. C. *J. Phys. Chem. A* **2009**, *113*, 2914.
(71) Abbate, M.; Pen, H.; Czyzyk, M. T.; Degroot, F. M. F.; Fuggle, J. C.; Ma, Y. J.; Chen, C. T.; Sette, F.; Fujimori, A.; Ueda, Y.; Kosuge, K. *J. Electron. Spectrosc. Relat. Phenom.***1993**, *62*, 185.
(72) Chen, J. G.; Kim, C. M.; Fruhberger, B.; Devries, B. D.; Touvelle, M. S. *Surf. Sci.* **1994**, *321*, 145.
(73) Goering, E.; Muller, O.; Klemm, M.; denBoer, M. L.; Horn, S. *Philos. Mag. B* **1997**, *75*, 229.
(74) Su, D. S.; Zandbergen, H. W.; Tiemeijer, P. C.; Kothleitner, G.; Havecker, M.; Hebert, C.; Knop-Gericke, A.; Freitag, B. H.; Hofer, F.; Schlogl, R. *Micron* **2003**, *34*, 235.
(75) Woll, C.; Khyzhun, O. Y.; Strunskus, T.; Grunert, W. *J. Electron. Spectrosc. Relat. Phenom.* **2005**, *149*.
(76) Brik, M. G.; Ogasawara, K.; Ikeno, H.; Tanaka, I. *European Physical Journal B* **2006**, *51*, 345.
(77) De Francesco, R.; Stener, M.; Causa, M.; Toffoli, D.; Fronzoni, G. *PCCP* **2006**, *8*, 4300.
(78) Ma, C.; Yang, H. X.; Li, Z. A.; Ueda, Y.; Li, J. Q. *Solid State Commun.* **2008**, *146*, 30.
(79) Patridge, C. J.; Jaye, C.; Abtew, T. A.; Ravel, B.; Fischer, D. A.; Marschilok, A. C.; Zhang, P.; Takeuchi, K. J.; Takeuchi, E. S.; Banerjee, S. *J. Phys. Chem. C* **2011**, *115*, 14437.
(80) Grigg, J.; Collison, D.; Garner, C. D.; Helliwell, M.; Tasker, P. A.; Thorpe, J. M. *Chem. Comm.* **1993**, 1807.
(81) Collison, D.; Garner, C. D.; Grigg, J.; McGrath, C. M.; Mosselmans, J. F. W.; Pidcock, E.; Roper, M. D.; Seddon, J. M. W.; Sinn, E.; Tasker, P. A.; Thornton, G.; Walsh, J. F.; Young, N. A. *Dalton Trans*. **1998**, 2199.
(82) George, S. D.; Brant, P.; Solomon, E. I. *J. Am. Chem. Soc.* **2005**, *127*, 667.
(83) Solomon, E. I.; Lever, A. B. P. *Inorganic Electronic Structure and Spectroscopy*; John Wiley & Sons: Hoboken, New Jersey, 2006; Vol. 2.
(84) de Groot, F. *Coord. Chem. Rev.* **2005**, *249*, 31.
(85) Zaanen, J.; Sawatzky, G. A. *Phys. Rev. B* **1986**, *33*, 8074.

(86) Vanderlaan, G.; Kirkman, I. W. *J. Phys.: Condens. Matter* **1992**, *4*, 4189.
(87) Solomon, E. I.; Hedman, B.; Hodgson, K. O.; Dey, A.; Szilagyi, R. K. *Coord. Chem. Rev.* **2005**, *249*, 97.
(88) Kozimor, S. A.; Yang, P.; Batista, E. R.; Boland, K. S.; Burns, C. J.; Clark, D. L.; Conradson, S. D.; Martin, R. L.; Wilkerson, M. P.; Wolfsberg, L. E. *J. Am. Chem. Soc.* **2009**, *131*, 12125.
(89) Kozimor, S. A.; Yang, P.; Batista, E. R.; Boland, K. S.; Burns, C. J.; Christensen, C. N.; Clark, D. L.; Conradson, S. D.; Hay, P. J.; Lezama, J. S.; Martin, R. L.; Schwarz, D. E.; Wilkerson, M. P.; Wolfsberg, L. E. *Inorg. Chem.* **2008**, *47*, 5365.
(90) Tolman, C. A. *Chem. Rev.* **1977**, *77*, 313.
(91) Immirzi, A.; Musco, A. *Inorg. Chim. Acta* **1977**, *25*, L41.
(92) Nugent, W. A.; Mckinney, R. J.; Kasowski, R. V.; Vancatledge, F. A. *Inorganica Chimica Acta* **1982**, *65*, L91.
(93) Rehder, D. *Coord. Chem. Rev.* **2008**, *252*, 2209.
(94) Luetkens, M. L.; Sattelberger, A. P.; Murray, H. H.; Basil, J. D.; Fackler, J. P.; Jones, R. A.; Heaton, D. E. In *Inorganic Syntheses* 1990; Vol. 28, p 305-310.
(95) Krossing, I. *Chem: Eur. J.* **2001**, *7*, 490.
(96) Andersen, R. A.; Wilkinson, G. *J. Chem. Soc. Dalton Trans.* **1977**, 809.
(97) Preuss, F.; Fuchslocher, E.; Leber, E.; Towae, W. *Z. Naturforsch. B* **1989**, *44*, 271.
(98) Shadle, S. E. Ph.D., Stanford University, 1994.
(99) Bradley, J. A.; Yang, P.; Batista, E. R.; Boland, K. S.; Burns, C. J.; Clark, D. L.; Conradson, S. D.; Kozimor, S. A.; Martin, R. L.; Seidler, G. T.; Scott, B. L.; Shuh, D. K.; Tyliszczak, T.; Wilkerson, M. P.; Wolfsberg, L. E. *J. Am. Chem. Soc.* **2010**, *132*, 13914.
(100) Minasian, S. G.; Krinsky, J. L.; Rinehart, J. D.; Copping, R.; Tyliszczak, T.; Janousch, M.; Shuh, D. K.; Arnold, J. *J. Am. Chem. Soc.* **2009**, *131*, 13767.
(101) aXis Version 17-Sep-08 Hitchcock, A. P. McMaster University, McMaster University: Hamilton, Ontario, Canada, 2008.
(102) Tyliszczak, T.; Warwick, T.; Kilcoyne, A. L. D.; Fakra, S.; Shuh, D. K.; Yoon, T. H.; Brown, G. E.; Andrews, S.; Chembrolu, V.; Strachan, J.; Acremann, Y. In *Synchrotron Radiation Instrumentation 2003, AIP Conference Proceedings* 2004; Vol. 705, 1356.
(103) SMART: Area-Detector Software package Bruker Analytical X-ray Systems, Inc, Madison, WI, 2001-2003.
(104) SAINT: SAX Area-Detector Integration Program, V6.40 Bruker Analytical X-ray Systems, Inc, Madison, WI, 2003.
(105) XPREP Bruker Analytical X-ray Systems, Inc, Madison, WI, 2003.
(106) SADABS: Bruker-Nonius Area Detector Scaling and Absorption V2.05 Bruker Analytical X-ray Systems, Inc, Madison, WI, 2003.
(107) A. L. Spek, *PLATON—A Multipurpose Crystallographic Tool*, Utrecht University, Utrecht, The Netherlands, 2007.
(108) Helm, L.; Bodizs, G.; Raabe, I.; Scopelliti, R.; Krossing, I. *Dalton Trans.* **2009**, 5137, and references therein.

Chapter 2:

(*Z*)-Selective, Semihydrogenation of Alkynes Catalyzed by the Cationic, Vanadium Bisimido Complex, $[V(N\textit{t}Bu)_2(PMe_3)_3][Al(PFTB)_4]$

Introduction:

Early metal hydrogenation catalysts have received less attention than comparable late-metal systems – particularly since the discovery of Wilkinson's catalyst.[1] This emphasis on late-metal systems has been largely driven by practical concerns including functional group tolerance and ease-of-handling. Further examination of early metal systems is particularly attractive from two viewpoints: the identification and elucidation of unusual mechanisms of dihydrogen activation and the application of the intrinsic properties of early-metals, in particular high-valent complexes, to the selective hydrogenation of alkynes to (*Z*)-alkenes. This transformation is typically accomplished by Lindlar's catalyst which is practically difficult to employ and suffers, particularly in the case of conjugated, aromatic systems, from *E*/*Z* isomerization and over hydrogenation.[2] The development of effective molecular catalysts for this transformation remains an area of intense research with recent notable success.[3-6]

We previously reported the intermediacy of a [1,2]-addition of a Si-H σ bond to an oxo ligand of $ReIO_2(PPh_3)_2$ in the catalytic hydrosilylation of ketones.[7-11] We hypothesized that a properly ligated Group V analog of $ReIO_2(PPh_3)_2$ could afford the activation of dihydrogen and discriminate between alkenes and alkynes, as alkenes are particularly poor ligands for d^0 complexes. The [1,2]-addition of H_2 to metal-ligand multiple bonds (*e.g.* $L_nM{=}X$; X=O,[12-17] S,[18] NR[19-23]) is a relatively rare transformation and its potential in catalysis has not been rigorously pursued. To combine the previously established early metal activation of H_2 by polarized metal-ligand multiple bonds with catalytic reduction of organic substrates, we sought a vanadium bisimide supported by labile ligands. Herein we report the application of the cationic, vanadium bisimido complex $[V(N\textit{t}Bu)_2(PMe_3)_3][Al(PFTB)_4]$ (**1.10**, PFTB = perfluoro-*tert*-butoxide, Scheme 1) to the selective, catalytic hydrogenation of alkynes to (*Z*)-alkenes.

Results and Discussion:

Treatment of a solution of **1.10** in $PhCF_3$ with 1 atm of H_2 resulted in recovery of only starting material after workup. Conversely, **1.10** rapidly decomposed under an atmosphere of H_2 in PhCl. These contrasting results suggests that **1.10** reversibly activates H_2. A ^1H VT NMR of complex **1.10** under N_2 in $PhCF_3$ revealed that the equatorial PMe_3 readily disassociates at 40°C. Free PMe_3 is not observed due to fast exchange. The remaining axial PMe_3 ligands significantly broadened at 70°C. Under H_2 in $PhCF_3$, **1.10** is in equilibrium with at least one other species even at room temperature. At 60°C the loss of symmetry equivalence of the imido *tert*-butyl resonances (from 1.09 ppm to 1.12 ppm (imide) and 1.19 ppm (amide)) in this new complex, as seen in the $^1H\{^{31}P\}$ spectrum, suggests that reaction with H_2 proceeds via [1,2]-, rather than [3+2]-addition, and generates a vanadium hydrido amido complex (**A**).[24] A trace amount of free PMe_3 is also observed at 0.86 ppm. However, the isolation of **A** either by the direct reaction of **1.10** with H_2 or by indirect synthetic methods has not been successful to date. Attempts to observe the hydride, **A**, by *in situ* IR were complicated by the inability to generate a sufficient concentration of the intermediate, as were attempts to observe it by ^1H NMR (presumably further complicated by coupling to ^{51}V (I=7/2) and ^{31}P).

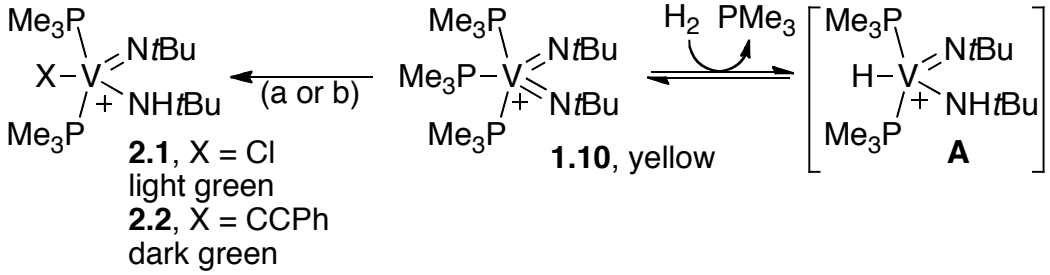

Scheme 2.1: In complexes **1.10**, **2.1**, **2.2** and **A** the counteranion, $[Al(PFTB)_4]^-$, is not depicted for clarity. Conditions: (a) 1.05 equiv. 2.0 M HCl in Et_2O, RT, ovn. 46%; (b) 1.05 equiv. phenylacetylene in Et_2O, RT, 71%; (c) 1 atm H_2, $PhCF_3$.

We sought further synthetic evidence for the generation of a vanadium hydride *via* the [1,2]-addition of H_2 to an imido ligand of **1.10**. To this end, we found complex **1.10** to be a competent catalyst for the hydrogenation of alkynes. Under standard conditions,[25] methylphenylacetylene was readily and selectively reduced to *cis*-*β*-methylstyrene in quantitative yield in 24 h. Further reduction to *n*-propylbenzene and isomerization to *trans*-*β*-methylstyrene or allylbenzene was not observed. The addition of a fresh atmosphere of H_2 and resubmission of the reaction mixture containing the product alkene to reaction conditions also resulted in no further reduction or isomerization. Internal alkyl, aryl, and silyl alkynes were similarly hydrogenated, all yielding the *cis*-alkenes (44-100% yield, eq. 1). Terminal alkynes (alkyl and aryl) are hydrogenated to the corresponding alkenes, albeit in significantly lower yields (10-52%) due to competitive addition of the terminal C-H bond.[26]

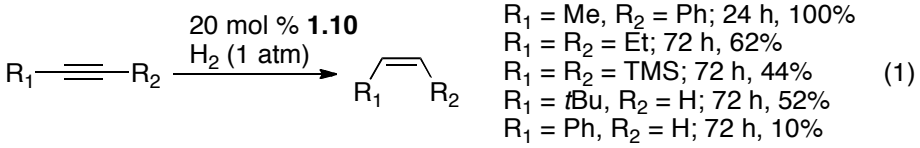

(1)

In order to gain further spectroscopic and analytical insight to **A**, **1.10** was treated with HCl, in order to shift the equilibrium towards the [1,2]-addition product. Adding a slight excess of 2.0 M HCl in diethyl ether solution to **1.10** afforded **2.1** in 46% yield after workup as light green blocks. The solid-state structure depicted in Figure 2.1 clearly shows it to be related to the proposed intermediate **A**. The V-N bond lengths are inequivalent; V(1)-N(1), 1.635(6) Å and V(1)-N(2), 1.807(8) Å. This data, inconjunction with the V-N-C angles of 166.9(7)° and 132.8(7)°, clearly demonstrates the protonation of an imide of **1.10** to form an amide. In solution, **2.1** is a mixture of rotamers about the V-N amide bond and has similar symmetry inequivalence of imido and amide *tert*-butyl groups as in the mixture of **1.10** and **A**. Furthermore, the ^{27}Al NMR of **2.1** exhibits a single sharp resonance at 36.01 ppm ($\Delta\nu_{1/2}$ = 2.54 Hz, compared to 34.70 ppm and $\Delta\nu_{1/2}$ = 2.99 Hz for **1.10**). This narrow $\Delta\nu_{1/2}$ indicates that there is no loss of symmetry at $[Al(PFTB)_4]^-$ and that the proton is associated with the vanadium center in solution. While this synthetic work cannot rule out a [3+2]-addition followed by a subsequent

[1,2]-shift in the activation of H_2, it does further corroborate DFT studies (*see below*), observed VT NMR

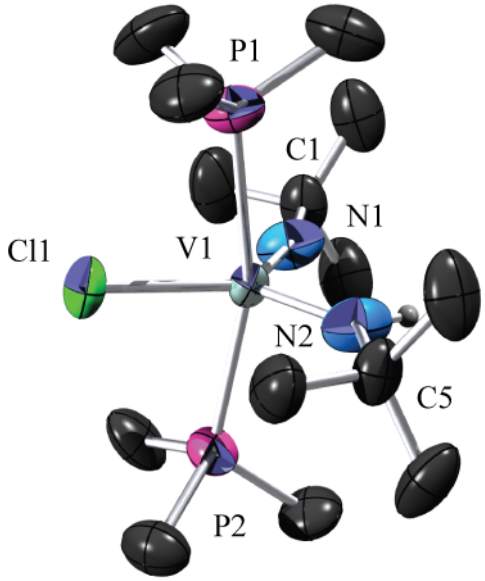

Figure 1.1: Molecular structures of **2.1**. Thermal ellipsoids are drawn at 50% probability level. Hydrogen atoms and counteranions ($[Al(PFTB)_4]^-$) have been removed for clarity. Selected bond lengths (Å) and angles (deg): V(1)-N(1), 1.640(6); V(1)-N(2), 1.774(6); V(1)-Cl(1), 2.3165(15); V(1)-P(2), 2.5004(16); V(1)-P(1), 2.4959(15); N(1)-V(1)-N(2), 105.2(4); P(1)-V(1)-P(2), 162.88(7); C(1)-N(1)-V(1), 168.4(6); C(5)-N(2)-V(1), 137.6(6).

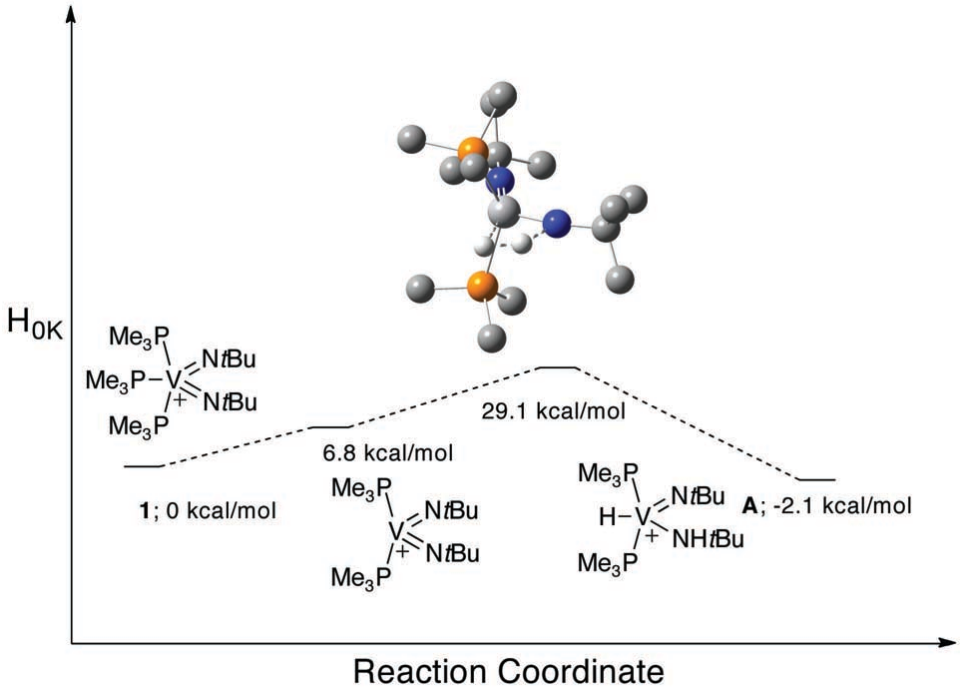

Scheme 2.2: Free enthalpy of H_2-addition to complex **1.10**.

behavior, and catalytic reactivity of **1.10**, as well previous experimental and DFT studies of σ bond addition to early metal imido complexes.[22,27]

The addition of terminal alkynes in a [1,2] fashion was confirmed by the preparative scale synthesis of [V(CCPh)(PMe_3)$_2$(N*t*Bu)(NH(*t*Bu))][Al(PFTB)], **2.2**, by the addition of 1.05 equivalents of phenylacetylene to **1.10** in diethyl ether. Compound **2.2** was isolated in 71% yield after crystallization from dichloroethane. In solution, **2.2**, like **2.1**, is a mixture of rotamers about the V-N amide bond. Similarly to **1.10** and **2.1**, **2.2** has single sharp resonance in ^{27}Al NMR at 34.68 ppm ($\Delta\nu_{1/2}$ = 3.81 Hz).

B3LYP/6-31G(d,p) (LANL2DZ for V) calculations were performed in order to probe the mechanism of H_2 activation by **1.10** (Scheme 2).[24] The reaction proceeds *via* a [1,2]-addition of H_2 to an imido ligand of the four coordinate complex [(PMe_3)$_2$V(N*t*Bu)$_2$]$^+$ generated by the elimination of the equatorial PMe_3. The four-membered, kite-like transition state is similar to those calculated by Cundari for C-H bond addition to (RO)$_2$Ti(NSi(*t*Bu)$_3$),[28] and Chirik for H_2 addition to Cp*$_2$Zr(NtBu).[22] Dihydrogen addition to a three coordinate complex resulting from the loss of two PMe_3 ligands was also considered, but found to be considerably higher in energy. No transition states corresponding to a [3+2]-addition could be located: all attempts collapsed to [1,2]-addition transition states, and, furthermore, IRC calculations for these transition states failed to link to the corresponding, hypothetical product [(PMe_3)$_2$V(NH(*t*Bu))$_2$]$^+$.

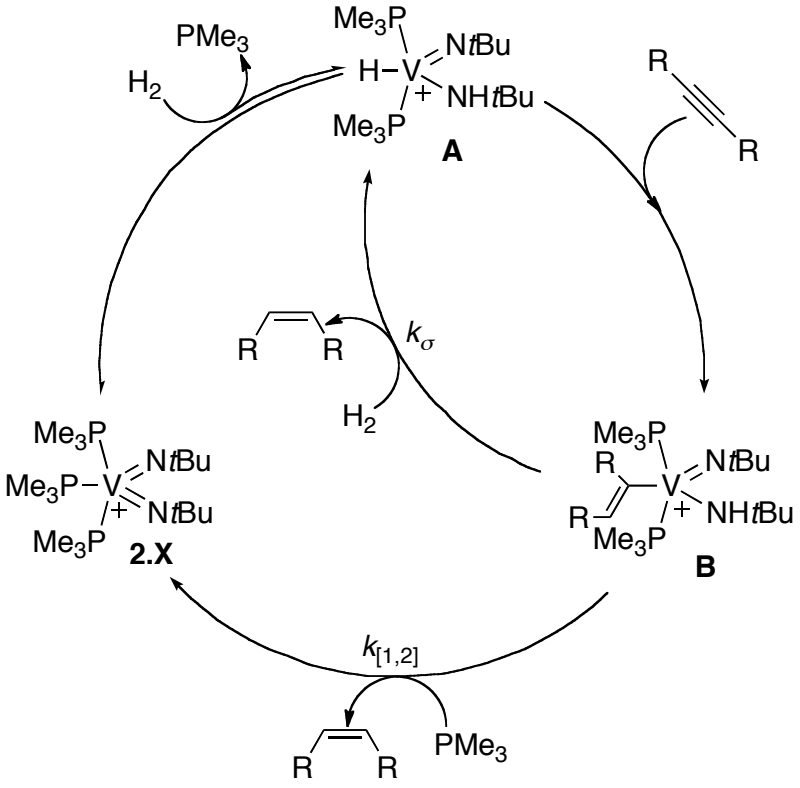

Scheme 2.3: Mechanistic Hypotheses.

With these synthetic and DFT results, two reasonable mechanisms may be proposed for the hydrogenation of alkynes by **1** (Scheme 3). Upon insertion of an alkyne into the hydride of **A**, the alkenyl amide, **B**, may undergo σ-bond metathesis with a second equivalent of H_2 (k_σ). Alternatively, intermediate **B** may yield the product and **1.10** *via* [1,2]-α-NH-elimination ($k_{[1,2]}$).[27] These two mechanistic possibilities were distinguished by a series of H_2/D_2 crossover experiments in the reduction of methylphenylacetylene (ratio of H_2/D_2, 1:1 and 1:9; ratio of alkyne to **1.10**, 1:1, 5:1, and 25:1). If $k_\sigma \geq k_{[1,2]}$, then a mixture of d_0-, d_1,-, d_2-*cis*-β-methylstyrene should be observed. However, exclusively d_0- and d_2-*cis*-β-methylstyrene are observed by ^{1}H and ^{2}H{^{1}H} NMR when there is large excess of alkyne and early in the course of the reaction (eq. 2). This result implies that $k_{[1,2]} >> k_\sigma$, and that, at high concentration, alkyne insertion is faster than the background formation of HD by σ bond metathesis with **A**. At longer reaction times (12-24 h) and low concentration of alkyne, d_1-isotopomers appear in small amounts concomitantly with observation of HD. In sum, these crossover experiments imply that both the [1,2]-addition of H_2 to an imido ligand and the [1,2]-α-NH-elimination of alkene lie on the dominant catalytic cycle.

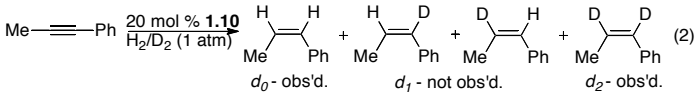

(2)

Complementary PHIP-NMR experiments were also performed.[29-31] Hydrogenation of methylphenylacetylene (25:1, alkyne:**1.10**) by 90% *p*-H_2 at 60 °C in *protio*-$PhCF_3$ afforded two antiphase singlets in the proton spectrum at 6.33 and 5.64 ppm. The transfer of polarization to the product alkene confirms the results of the H_2/D_2 crossover experiments demonstrating that a single molecule of H_2 is involved in the reduction of the alkyne. This result further indicates that possible mechanisms that involve splitting H_2 into two distinct molecules, as in hydrogenation by frustrated Lewis pairs, are *not* operative in this system as the H atoms remain *J* coupled throughout the course of the hydrogenation. Similarly, the transfer of polarization to the product suggests that paramagnetic intermediates or impurities are *not* involved in the hydrogenation or in solution, as such species would rapidly catalyze the conversion of *p*-H_2 to *o*-H_2 and prevent the observation of PHIP phenomena.

Conclusion:

In summary, we have demonstrated that the cationic, group 5 bisimido complex, **1.10**, reacts with H_2 and is a competent catalyst for the *Z*-selective hydrogenation of alkynes. We also present evidence for an unusual [1,2]-α-NH-elimination of an alkene to regenerate the active catalyst, **1.10**. Further methodology development should be directed to the use of other main group hydrides for use in organic and materials synthesis. Preliminary efforts on these systems are presented in Appendix C. Further Mechanistic work on this system is presented in the following chapter and and Appendix A.

Experimental Section:

General Considerations. Unless otherwise noted, all reactions were performed using standard Schlenk line techniques or in an MBraun inert atmosphere box under an atmosphere of argon or dinitrogen (<1 ppm O_2/H_2O), respectively. All glassware and cannulae were stored in an oven at ca. 425 K. Pentane, diethyl ether, and toluene were purified by passage through a column of activated alumina and degassed prior to use. C_6D_6 was vacuum-transferred from sodium/benzophenone and degassed with three freeze-pump-thaw cycles. 1,2-$C_2D_4Cl_2$ was vacuum transferred from CaH_2 and degassed with three freeze-pump-thaw cycles. NMR spectra were recorded on Bruker AV-300, AVB-400, AVQ-400, AV-500, and AV-600 spectrometers. ^1H and $^{13}C\{^1H\}$ chemical shifts are given relative to residual solvent peaks. ^{31}P, ^{51}V, ^{19}F, and ^{27}Al chemical shifts were referenced to external standards ($P(OMe)_3$ at 1.67 ppm, $VOCl_3$ at 0.00 ppm, $CFCl_3$ at 0.00 ppm, and 1M $Al(NO_3)_3$ in H_2O/D_2O at 0 ppm, respectively). Proton and carbon NMR assignments were routinely confirmed by ^1H-^1H (COSY) or ^1H-^{13}C (HSQC and HMBC) experiments as necessary. Infrared (IR) samples were prepared as Nujol mulls and were taken between KBr disks. The following chemicals were purified prior to use: α, α', α''-trifluorotoluene ($PhCF_3$), was distilled from P_2O_5 and degassed by bubbling argon through the liquid for 15 minutes, and liquid alkynes were stored over 4 Å seives and degassed by three freeze-pump-thaw cycles. All other reagents were acquired from commercial sources and used as received. Elemental analyses were determined at the College of Chemistry, University of California, Berkeley. The X-ray structural determination was performed at CHEXRAY, University of California, Berkeley, on a MicroSTAR-H X8 APEXII diffractometer.

$[VCl(PMe_3)(N^tBu)(NHtBu)][Al(PFTB)_4]$ (2.1). To a solution of **1.10** (300 mg, .22 mmol) in 10 mL of diethyl ether, chilled to -78 °C was added 2.0 M HCl in diethyl ether (1.05 equiv., 115 μL, .23 mmol) *via* syringe. After this addition, the reaction mixture was allowed to warm to room temperature and was stirred for 12 h. The reaction mixture was reduced to a residue *in vacuo* and triturated with 10 mL of pentane. The residue was extracted with 1,2-dichloroethane, filtered *via* cannula, and reduced until the product began to crystallize and then chilled at -15 °C for two days. After decantation, the title compound was afforded in 46% yield in two crops (113 mg and 20 mg) as small, light green blocks. X-ray quality crystals were grown from a concentrated 1,2-dichloroethane solution at -15 °C over two weeks. At room temperature in 1,2-$C_2D_4Cl_2$ $[VCl(PMe_3)(N^tBu)(NHtBu)][Al(pftb)_4]$ is a mixture of two isomers about the V-N amide bond (isomer A:B, as determined by ^{51}V NMR integration). NMR data is reported at room temperature. Low temperature NMR is insufficient to resolve the two rotamers. ^1H NMR (d_4-DCE, 600 MHz) δ 14.16 (br s, N-*H*, rel. int. .08), 1.55 (br s, P*Me*$_3$ and underlying *t*Bu, rel. int. 3.25), 1.45 (br s, N*t*Bu, rel. int. 1.1), 1.43 (br s, N*t*Bu, rel. int. 1.12), 1.30 (br s, N*t*Bu, rel. int. 1). ^{13}C NMR (d_4-DCE, 150.9 MHz) δ 121.53 (q, C(*C*F_3)$_3$, $^1J_{CF}$ = 29.42 Hz), 32.44 (br s), 31.66 (br s), 31.27 (br s), 15.35 (m, coincident triplets, P*Me*$_3$) . The imide and amide α-*t*Bu carbon and the α-C(CF_3)$_3$ resonances could not be observed. $^{31}P\{^1H\}$ NMR (d_4-DCE, 242.9 MHz) δ –0.58 (br s, $\Delta\nu_{1/2}$ = 211.33 Hz). $^{51}V\{^1H\}$ NMR (d_4-DCE, 157.7 MHz) δ –347.17 (unresolved triplet, $\Delta\nu_{1/2}$ = 316.40 Hz, rel. int. 1.4), –367.17 (unresolved triplet, $\Delta\nu_{1/2}$ = 414.01 Hz, rel. int. 1). ^{19}F NMR (d_4-

DCE, 376.5 MHz) δ –73.19 (s, $\Delta\nu_{1/2}$ = 5.50 Hz). ^{27}Al NMR (d_4-DCE, 104.3 MHz) δ 36.01 (s, $\Delta\nu_{1/2}$ = 2.54 Hz). Anal. Calcd (%) for $C_{30}H_{37}AlClF_{36}N_2O_4P_2V$: C, 26.71; H, 2.76; N, 2.08. Found: C, 26.66; H, 2.72; N, 2.06. IR (KBr, nujol, cm^{-1}): 3322 (w), 1086 (w), 973 (s), 560 (s), 536 (s), 447 (s). Mp = 217-219 °C.

[V(CCPh)(PMe$_3$)(N^{t}Bu)(NH*t*Bu)][Al(PFTB)$_4$] (2.2). To a solution of **1.10** (400 mg, .29 mmol) in 15 mL of diethyl ether was added phenylacetylene (1.05 equiv., 33 µL, .30 mmol) *via* syringe. After this addition, the reaction mixture was stirred for 12 h. The reaction mixture was then reduced to a residue *in vacuo* and extracted with 1,2-dichloroethane, filtered *via* cannula, and reduced until the product began to crystallize. After cooling the solution to -15 °C for four days, the title compound was afforded in 71% yield (290 mg) after decantation, as small, very dark green blocks. At room temperature in $PhCF_3$ with a d_8-toluene locking insert, [VCl(PMe$_3$)(N^{t}Bu)(NH*t*Bu)][Al(pftb)$_4$] is a mixture of two isomers about the V-N amide bond (isomer A:B, 1.8:1 ,as determined by ^{1}H NMR integration). NMR data is reported at room temperature. ^{1}H NMR ($PhCF_3$ (C_7D_8 insert), 500 MHz) δ 12.48 (s, N-*H*, rel. int. .086), 10.40 (s, N-*H*, rel. int. .09), 1.432 (pseudo-d, P*Me*$_3$, rel. int. 1.23, $^1J_{CP}$ = 9 Hz), 1.40 (pseudo-d, P*Me*$_3$, rel. int. 1.728, , $^1J_{CP}$ = 9.5 Hz), 1.260 (s, N*t*Bu, rel. int. 1), 1.16 (s, N*t*Bu, rel. int. .59), 1.13 (s, N*t*Bu, rel. int. .90), 1.02 (s, N*t*Bu, rel. int. .56). ^{13}C NMR ($PhCF_3$ (C_7D_8 insert), 125.8 MHz) δ 137.49 (br s), 132.09 (br s) 130.69 (q, C(*C*F$_3$)$_3$, $^1J_{CF}$ = 32.08 Hz), 129.09 (vbr s), 128.9 (brs), 128.16 (br s), 127.97 (br s), 127.85 (br s), 127.78 (br s), 125.33 (br s), 124.27 (br s), 32.35 (br s, β-N*tBu*), 31.94 (br s, β-N*tBu*), 31.26 (br s, β-N*tBu*), 30.86 (br s, β-N*tBu*), 16.30 (t, P*Me*$_3$, $^1J_{CP}$ = 15.6 Hz), 16.00 (t, P*Me*$_3$, $^1J_{CP}$ = 9.8 Hz) . The imide and amide α-*t*Bu carbon and the α-C(CF$_3$)$_3$ resonances could not be observed. Assignment of phenyl and alkyne carbons complicated by unresolved coupling and overlapping solvent resonances, 10 of 12 expected located. ^{31}P{^{1}H} NMR ($PhCF_3$ (C_7D_8 insert), 242.9 MHz) δ 3.28 (br s, $\Delta\nu_{1/2}$ = 498.58 Hz). ^{51}V{^{1}H} NMR ($PhCF_3$ (C_7D_8 insert), 157.7 MHz) δ –460.67 (s, $\Delta\nu_{1/2}$ = 674.86 Hz), –488.62 (s, $\Delta\nu_{1/2}$ = 1013.14 Hz,). ^{19}F NMR ($PhCF_3$ (C_7D_8 insert), 376.5 MHz) δ –76.09 (s). ^{27}Al NMR ($PhCF_3$ (C_7D_8 insert), 104.3 MHz) δ 34.68 (s, $\Delta\nu_{1/2}$ = 3.81 Hz). Anal. Calcd (%) for $C_{38}H_{41}AlF_{36}N_2O_4P_2V$: C, 32.39; H, 2.92; N, 1.98. Found: C, 32.60; H, 3.04; N, 2.04. IR (KBr, nujol, cm^{-1}): 3319 (s), 3160 (w), 2726 (w), 2573 (w), 2191 (w), 2073 (s), 2026 (w), 1947 (w), 1877 (w), 1800 (w), 1724 (w), 1668 (w), 1594 (m), 1571(w), 1512 (m), 1069 (w), 1024 (w), 1013 (w), 831 (s), 800 (m), 786 (m), 755 (s), 727 (s), 713 (m), 702 (m), 689 (s), 672 (w), 560 (s), 536 (s), 444 (s). Mp = 114-115 °C (dec.).

General Procedure for Catalytic Hydrogenation. Inside a glovebox a solution of **1.10** (10 mg, .007 mmol) and 1,3,5-trimethoxybenzene (TMB, 5.2-5.6 mg) in 700 µL of $PhCF_3$ was added to a J. Young tube fitted with C_6D_6 locking standard, sealed capillary insert. To this mixture was further added alkyne substrate (5 equiv., .035 mmol). The tube was sealed, removed from the box, and a baseline spectrum was acquired. The tube was then attached to a Schlenk line, degassed by three freeze-pump-thaw cycles, and filled with 1 atm of H_2. The reaction was monitored by ^{1}H NMR spectroscopy and yield determined by integration versus the internal standard (TMB).

H_2/D_2 Crossover Experiments. Inside a glovebox a solution of **1.10** (10 mg, .007 mmol) and trimethoxybenzene (TMB, 2-5 mg) in 600 μL of $PhCF_3$ was added to a J. Young tube fitted with C_6D_6 locking standard, sealed capillary insert. To this mixture was further added methylphenylacetylene (25, 5, or 1 equiv.). The tube was sealed, removed from the box, and a baseline spectrum was acquired. The tube was then attached to a Schlenk line, degassed by three freeze-pump-thaw cycles, and filled with 1 atm of H_2/D_2 (ratio 1:1 or 1:9). The reactions were monitored by ^1H and $^2H\{^1H\}$ NMR spectroscopy. The mixtures of H_2 and D_2 were prepared by filling the sealed, evacuated vacuum tube of the Schlenk line sequentially with H_2 and D_2 from the opposite ends of a 4-tap line. The partial pressure of the gases was measured *via* a mercury manometer attached directly to the vacuum tube. The mixture of gases was allowed to equilibrate for 10 minutes prior to its introduction to the evacuated and frozen J. Young tube. The reactions were monitored by ^1H and $^2H\{^1H\}$ NMR spectroscopy.

VT NMR

Figure 2.1: VT ^{1}H NMR spectra of 1.10 in $PhCF_3$ under N_2**.**

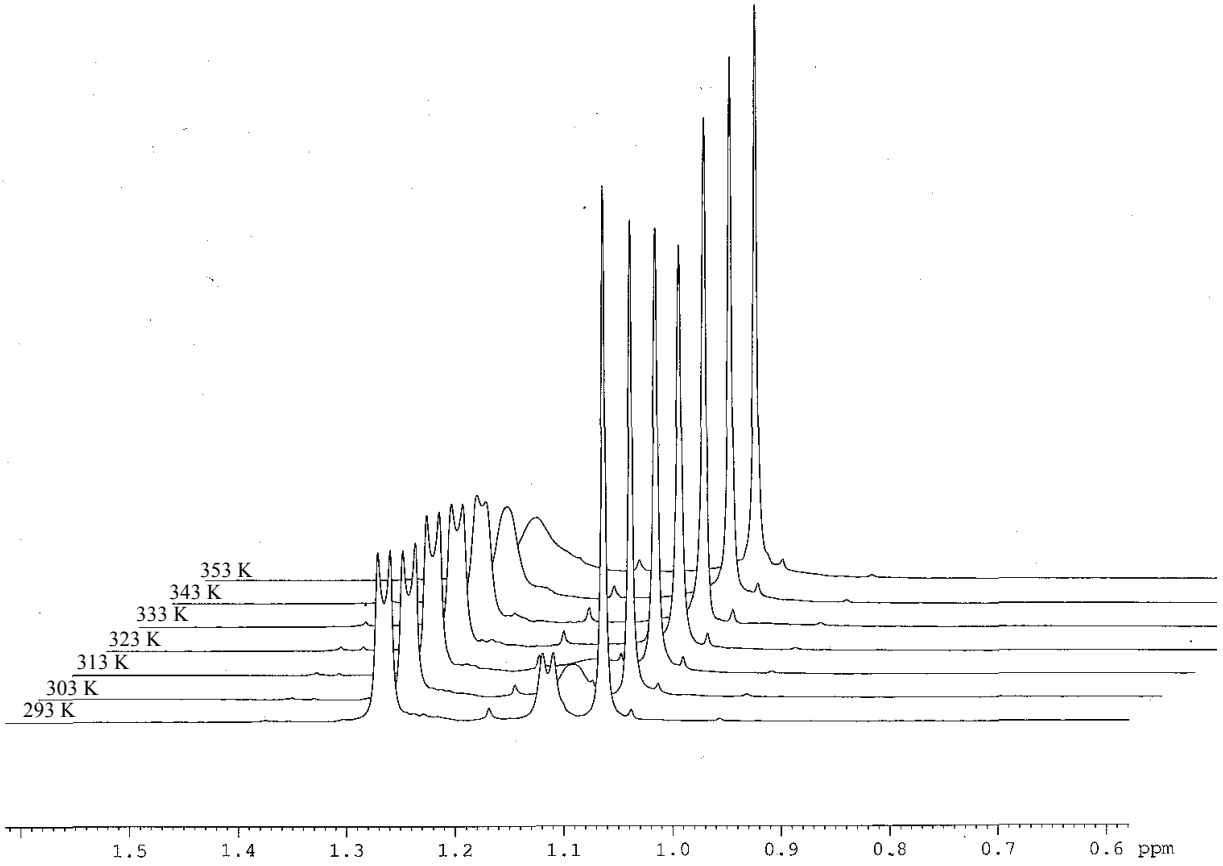

Figure 2.3: VT NMR spectra of 1.10 under 1 atm H_2.

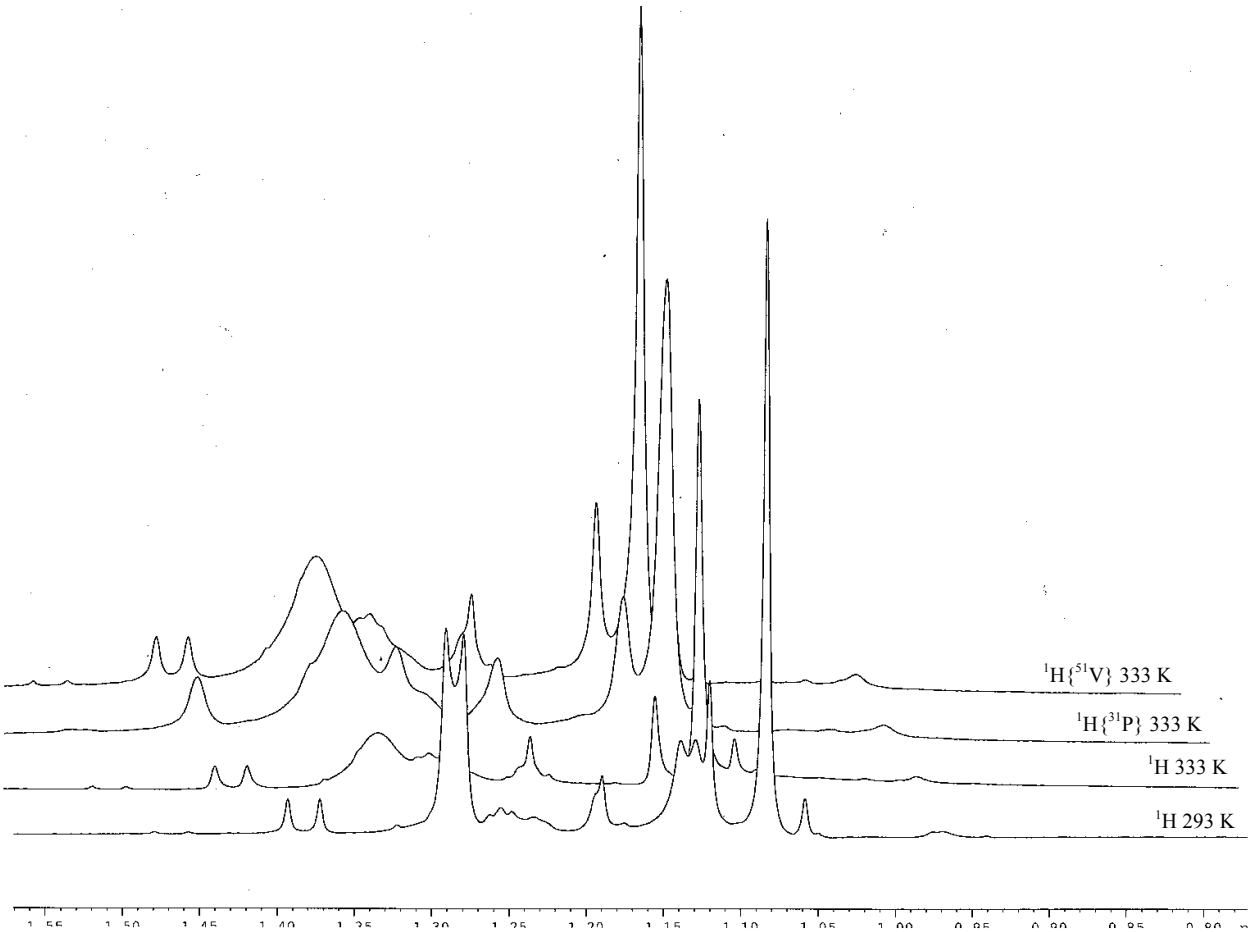

PHIP-PASADENA NMR Experiments:

Parahydrogen Production: A hydrogen mixture enriched in the para spin state (60% *p*-H_2) was donated by the Pines laboratory in an aluminum cylinder filled with the para-enriched H_2 to 40 psig. The ortho:para ratio was verified by measuring the NMR signal intensities of H_2 in a cell packed with porous alumina (Al_2O_3).[32,33]

NMR Experiments: To a J. Young tube was filled with 10 mg of **1.10** (.0072 mmol) in 600 μL of $C_6H_5CF_3$ with a C_6D_6 locking standard inside of a glass capillary tube was added methylphenylacetylene (25 equiv., 22 μL). The lock and pulse calibration were determined for a Bruker AV-600 probe at 60 °C (Typical excitation pulses (π/4) were 6.55 μs in duration). The tube was then removed from the probe and fitted to a Schlenk line and freeze-pumped-thawed three times and filled with 1 atm of parahydrogen-enriched H_2. While keeping the tube chilled at -196 °C in liquid N_2, the NMR tube was carried to the spectrometer and then quickly transferred to the previously warmed probe. After allowing the tube to thermally equilibrate (5 min), single scan ^{1}H NMR experiments were acquired after 20 min. Examination of spectra revealed antiphase singlets at 6.33 and 5.64 ppm, indicating transfer of polarization to the product alkene *cis*-β-methylstyrene.

Figure 2.4: PHIP signals from *p*-H_2 hydrogenation of methylphenylacetylene.

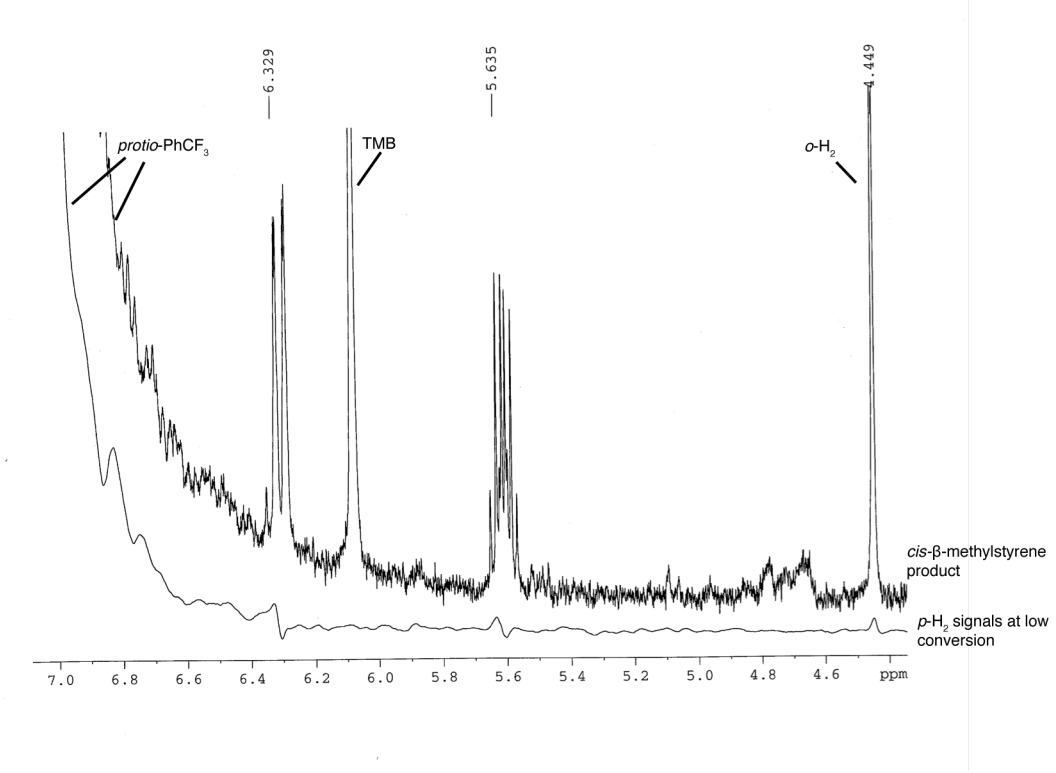

Computational Methods

All structures and energies were calculated using the Gaussian03[34] suite of programs. Geometry optimizations were converged to at least the default geometric convergence criteria. The use of symmetry was explicitly turned off for all computations. Frequencies were calculated analytically at 298.15 K and 1 atm, and structures were considered true minima if they did not exhibit imaginary modes. Calculated transition state structures exhibited only a single imaginary mode. IRC calculations were performed to ensure the transition state geometries connected the reactant and the product. The hybrid functional used was B3LYP.[35-37] A LANL2DZ small core ECP and its appropriate valence basis set was used for V.[38] The remaining atoms were treated with Pople's 6-31G(d,p) double-ζ split-valence basis using the 5 spherical d orbital functions instead of the default.[39,40]

Figure 2.5: Free enthalpy of H_2-addition to complex **1.10**.

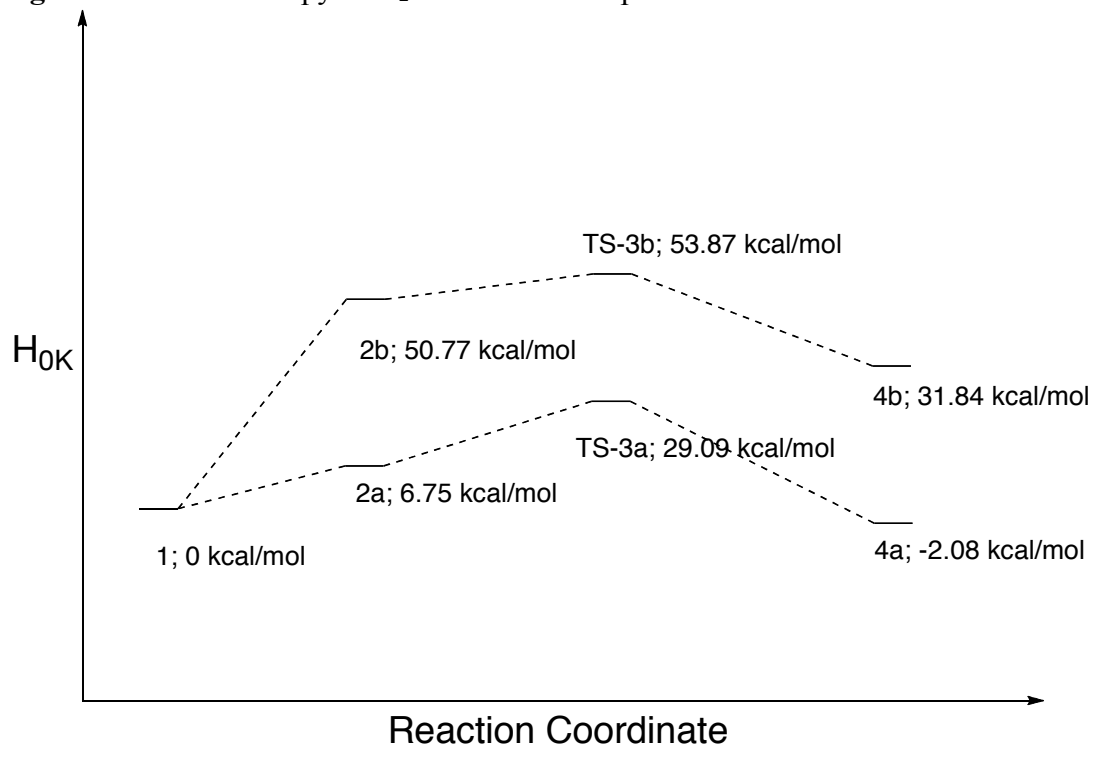

Figure 2.6: Calculated Structures (hydrogen atoms (except for H_2, V-H, and N-H) removed for clarity).

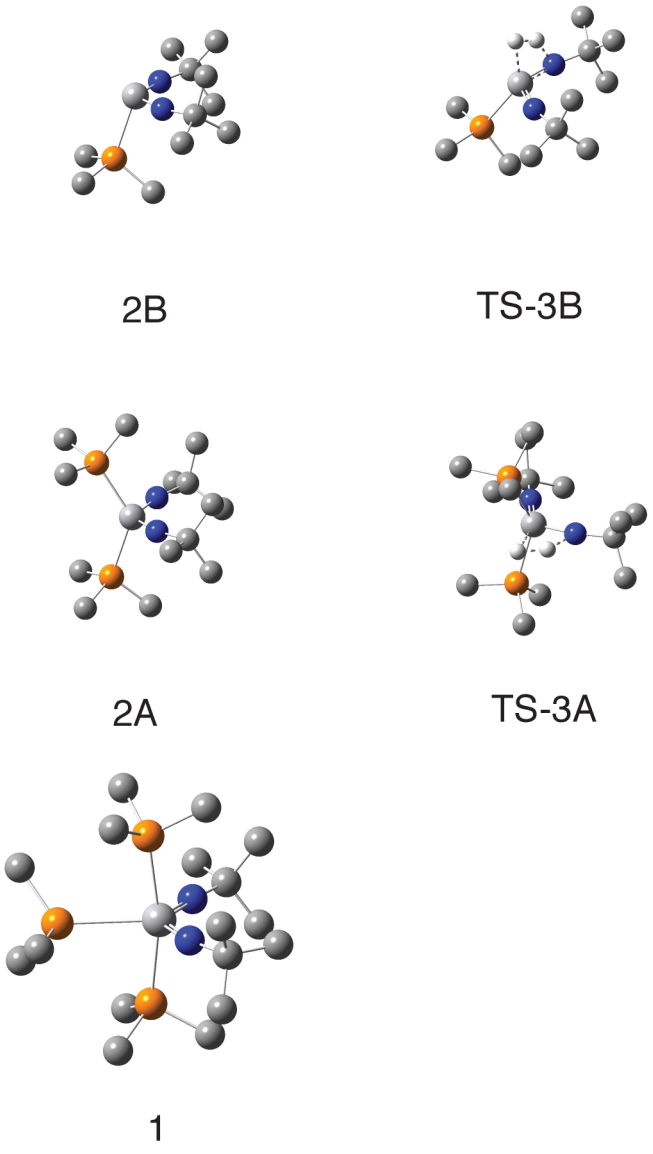

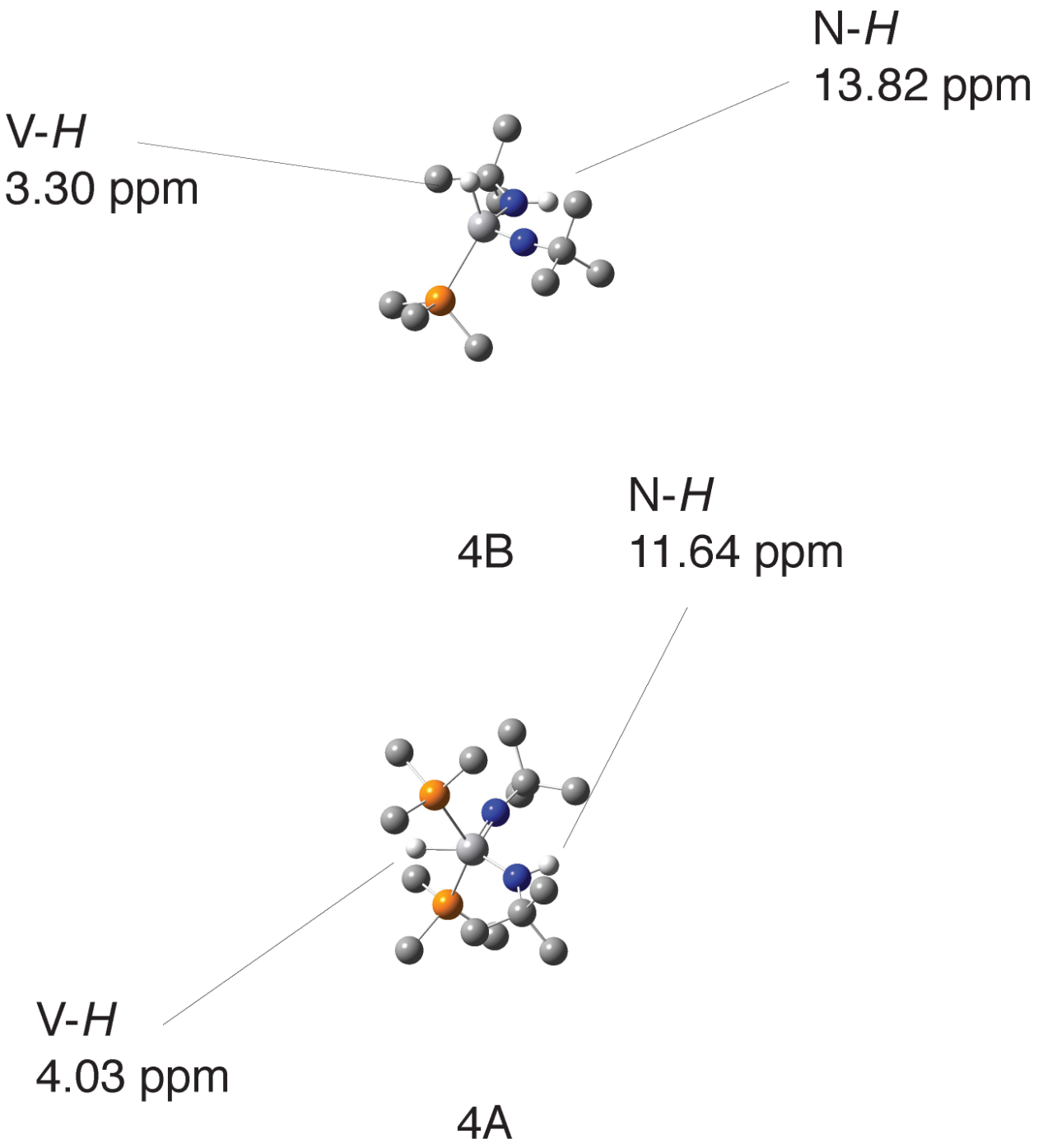
N-*H*
13.82 ppm
V-*H*
3.30 ppm
4B
N-*H*
11.64 ppm
V-*H*
4.03 ppm
4A

General Considerations for Compound 2.1.

A single crystal of appropriate size was coated in Paratone-N oil and mounted on a Cryo loop. The loop was transferred to a MicroSTAR-H X8 diffractometer equipped with a CCD area detector,[41] centered in the beam, and cooled by an Oxford Cryostream 700 LT device. Preliminary orientation matrices and cell constants were determined by collection of three sets of 40, 5 s frames, followed by spot integration and least-squares refinement. COSMO was used to determine an appropriate data collection strategy, and the raw data were integrated using SAINT.[42] Cell dimensions reported were calculated from all reflections with $I > 10\ \sigma$. The data were corrected for Lorentz and polarization effects; no correction for crystal decay was applied. Data were analyzed for agreement and possible absorption using XPREP.[43] An absorption correction based on comparison of redundant and equivalent reflections was applied using SADABS.[44] Structures were solved by direct methods with the aid of successive difference Fourier maps and were refined on F^2 using the SHELXTL 5.0 software package. Thermal parameters for all non-hydrogen atoms on the vanadium cation were refined anisotropically. The disorder model for the anion is described below. ORTEP diagrams were created using the ORTEP-3 software package.[45]

Disorder Modeling of Compound 2.1:

The poor quality of the data for **2.1** is due to the spherical (S_4 symmetric) $[Al(PFTB)_4]^-$ anion, which is often heavily disordered in the solid state even at 100 K.[47] Two solutions are presented to resolve the disorder in the anion. In the full structure solution, SADI and ISOR restraints are employed to restrict the $-C(CF_3)_3$ groups to reasonable bond lengths, angles and thermal parameters. In the second solution, the $[Al(PFTB)_4]^-$ anion is reduced to the AlO_4 tetrahedral core and treated with the SQUEEZE routine included in PLATON.[48] The final refinement by this approach provides better residuals and, as the two cation models are very nearly super imposable, implies that poor residuals for the full structure determination are due solely to unresolved disorder in the anion and that the X-ray structure connectivity agrees with the spectroscopic and analytical data. Attempts to remove restraints in the full structure determination resulted only in the collapse of the model or in the generation of unrealistic bond parameters in the anion.

Table 2.1: X-Ray Diffraction Data for Compound 3.X: $[VCl(PMe_3)(N^tBu)(NH^tBu)][Al(PFTB)_4]$.

	2.1-Full	**2.1 - Partial**
empirical formula	$C_{30}H_{37}AlClF_{36}N_2O_4P_2V$	$C_{17}H_{37}AlClN_2O_4P_2V$
formula weight	1348.93	472.77
temp., K	100(2)	100(2)
λ	1.54178	1.54178
crystal system	monoclinic	monoclinic
space group	$P2_1/c$	$P2_1/c$
a, Å	10.7422(9)	10.7422(9)
b, Å	27.581(3)	27.581(3)
c, Å	17.1914(15)	17.1914(15)
α, deg	90	90
β, deg	93.283(4)	93.283(4)°
γ, deg	90	90
volume, $Å^3$	5085.1(8)	2739.2
Z	4	4
d_{calc}, mg/m^3	1.762	0.618
F_{000}	2680	1000
μ, mm^{-1}	4.478	2.955
no. rflns measd	48134	48134
no. indep reflns	9208	9208
R_{int}	0.0274	0.0274
Restr/param	42/774	0/226
R_1, wR_2 $[I > 2\sigma(I)]$	0.1575, 0.4546	0.1499, 0.4546
R_1 (all data)	0.1615	0.1582
GOF	2.413	1.938
Resid peak, hole ($e^-/Å^3$)	2.966, -1.169	3.069, -0.592

Figure 2.7: ORTEP representation of Complex 2.1 – Full structure determination: Thermal ellipsoids are drawn at 50% probability level. Hydrogen atoms are omitted for clarity. Selected bond lengths (Å) and angles (deg): V(1)-N(1), 1.635(6); V(1)-N(2), 1.807(8); V(1)-Cl(1), 2.3182(18); V(1)-P(2), 2.5031; V(1)-P(1), 2.4923(19); N(1)-V(1)-N(2), 102.9(4); P(1)-V(1)-P(2), 163.05(8); C(1)-N(1)-V(1), 166.9(7); C(5)-N(2)-V(1), 132.8(7).

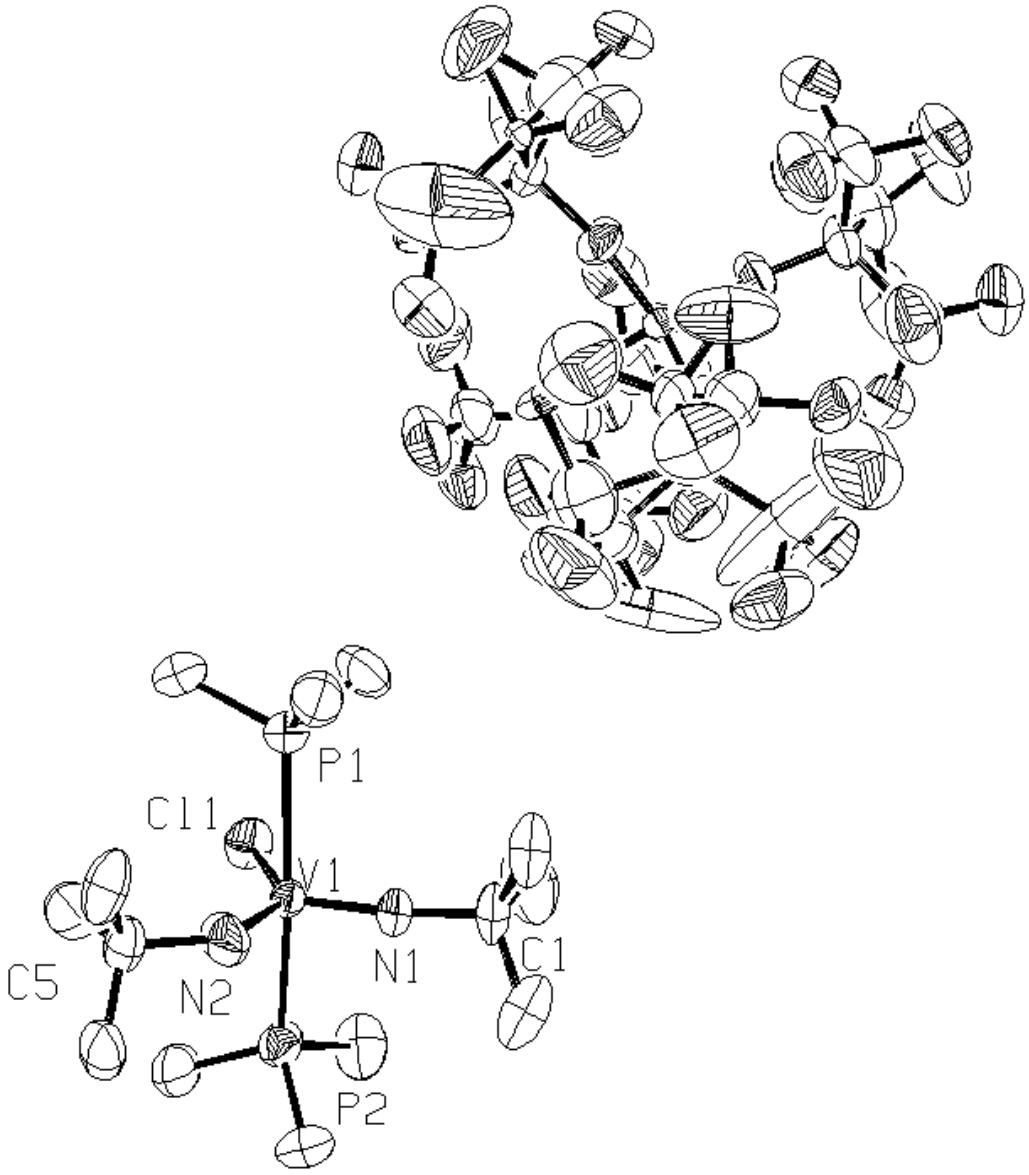

Figure 2.8: ORTEP representation of Complex 2.1 – Partial structure determination. Thermal ellipsoids are drawn at 50% probability level. Hydrogen atoms are omitted for clarity. Selected bond lengths (Å) and angles (deg): V(1)-N(1), 1.640(6); V(1)-N(2), 1.774(6); V(1)-Cl(1), 2.3165(15); V(1)-P(2), 2.5004(16); V(1)-P(1), 2.4959(15); N(1)-V(1)-N(2), 105.2(4); P(1)-V(1)-P(2), 162.88(7); C(1)-N(1)-V(1), 168.4(6); C(5)-N(2)-V(1), 137.6(6).

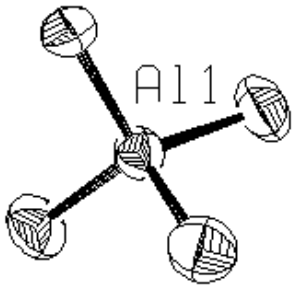

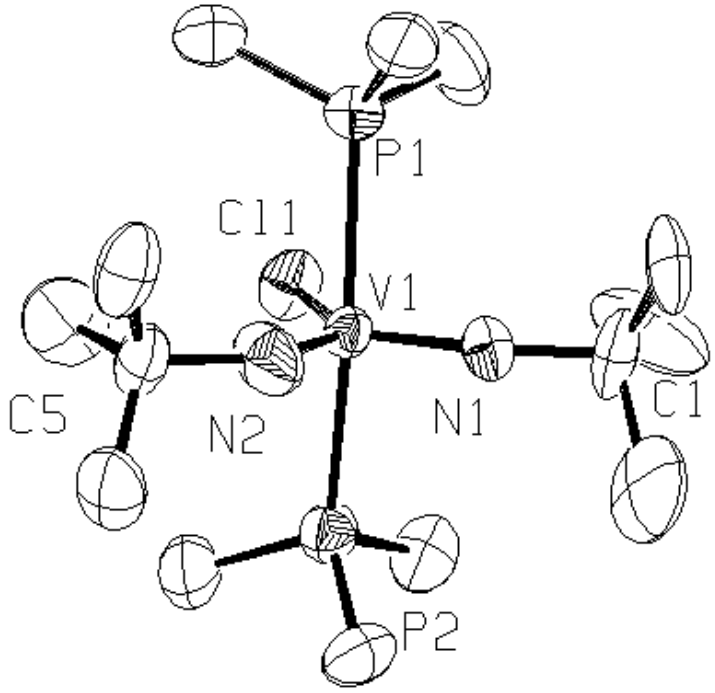

Notes and References:

(1) Young, J. F.; Osborn, J. A.; Jardine, F. H.; Wilkinson, G. *J. Chem. Soc., Chem. Comm.* **1965**, 131.
(2) H. Lindlar, *Helv. Chim. Acta* **1952**, *35*, 446.
(3) A. Molnár, A. Sárkány, M. Varga, *J. Mol. Catal. A* **2001**, *173*, 185.
(4) Kluwer, A. M.; Elsevier, C. J. in *Handbook for Homogeneous Hydrogenation*, Vol. 1, 1st ed. (Eds. : J. G. de Vries, C. J. Elsevier), Wiley-VCH, Weinheim, **2007**, p. 375.
(5) Warsink, S.; Chang, I. H.; Weigand, J. J.; Hauwert, P.; Chen, J. T.; Elsevier, C. J. *Organometallics* **2010**, *29*, 4555.
(6) Hauwert, P.; Maestri, G.; Sprengers, J. W.; Catellani, M.; Elsevier, C. J. *Angew. Chem. Int. Ed. Engl.* **2008**, *47*, 3223.
(7) Kennedy-Smith, J. J.; Nolin, K. A.; Gunterman, H. P.; Toste, F. D. *J. Am. Chem. Soc.* **2003**, *125*, 4056.
(8) Nolin, K. A.; Krumper, J. R.; Pluth, M. D.; Bergman, R. G.; Toste, F. D. *J. Am. Chem. Soc.* **2007**, *129*, 14684.
(9) Nolin, K. A.; Ahn, R. W.; Toste, F. D. *J. Am. Chem. Soc.* **2005**, *127*, 12462.
(10) Khalimon, A. Y.; Simionescu, R.; Kuzimina, L. G.; Howard, J. A. K.; Nikonov, G. I. *Angew. Chem., Int. Ed.* **2008**, *47*, 7701.
(11) Gountchev, T. I.; Tilley, T. D. *J. Am. Chem. Soc.* **1997**, *117*, 12831.
(12) Parkin, G.; Bercaw, J. E. *J. Am. Chem. Soc.* **1989**, *111*, 391.
(13) Hanna, T. E.; Lobkovsky, E.; Chirik, P. J. *Inorg. Chem.* **2007**, *46*, 2359.
(14) Reis, P. M.; Costa, P. J.; Romao, C. C.; Fernandes, J. A.; Calhorda, M. J.; Royo, B. *Dalton Trans.* **2008**, 1727.
(15) Howard, W. A.; Waters, M.; Parkin, G. *J. Am. Chem. Soc.* **1993**, *115*, 4917.
(16) For conceptually related [3+2]-additions of H2 to late metal cis-dioxo compounds see Collman, J.P.; Slaugher, L. M.; Eberspacher, T. A.; Strassner, T; Brauman, J. I. *Inorg. Chem.* **2001**, *40*, 6272.
(17) Dehastani, A.; Lam, W. H.; Hrovat, D. A.; Davidson, E. R.; Borden, W. T.; Mayer, J. M. *J. Am. Chem. Soc.* **2005**, *127*, 3423 and references therein.
(18) Sweeney, Z. K.; Polse, J. L.; Bergman, R. G.; Andersen, R. A. *Organometallics* **1999**, *18*, 5502.
(19) Blake, R. E.; Antonelli, D. M.; Henling, L. M.; Schaefer, W. P.; Hardcastle, K. I.; Bercaw, J. E. *Organometallics* **1998**, *17*, 718.
(20) Polse, J. L.; Andersen, R. A.; Bergman, R. G. *J. Am. Chem. Soc.* **1998**, *120*, 13405.
(21) Hanna, T. E.; Keresztes, I.; Lobkovsky, E.; Bernskoetter, W. H.; Chirik, P. J. *Organometallics* **2004**, *23*, 3448.
(22) Toomey, H. E.; Pun, D.; Veiros, L. F.; Chirik, P. J. *Organometallics* **2008**, *27*, 872.
(23) Cummins, C. C.; Baxter, S. M.; Wolczanski, P. T. *J. Am. Chem. Soc.* **1988**, *110*, 8731.
(24) See Experimental section for details.
(25) 1 atm H_2, 700 μL $PhCF_3$, 20 mol% **1.10**, C_6D_6 insert, TMB internal standard.
(26) Alkynes are selectively hydrogenated, among other functional groups tolerated by the catalyst. Substrates that are substantially stronger ligands for **1.10** than PMe_3, such as acetonitrile, undergo exclusive ligand exchange at the equatorial position and are not

reduced. Weaker ligands, such as olefins, are also not reduced. Aldehydes and ketones lead to the degraditive consumption of catalyst.
(27) Holmes, S. A.; Schafer, D. F.; Wolczanski, P. T.; Lobkovsky, E. B. *J. Am. Chem. Soc.* **2001**, *123*, 10571.
(28) Cundari, T. R.; Klinckman, T. R.; Wolczanski, P. T. *J. Am. Chem. Soc.* **2002**, *124*, 1481.
(29) Blazina, D.; Duckett, S. B.; Dunne, J. P.; Godard, C. *Dalton Trans.* **2004**, 2601.
(30) Millar, S. P.; Zubris, D. L.; Bercaw, J. E.; Eisenberg, R. *J. Am. Chem. Soc.* **1998**, *120*, 5329.
(31) Carson, P. J.; Bowers, C. R.; Weitekamp, D. P. *J. Am. Chem. Soc.* **2001**, *123*, 11821.
(32) Koptyug, I. V.; Kovtunov, K. V.; Burt, S. R.; Anwar, M. S.; Hilty, C.; Han, S. I.; Pines, A.; Sagdeev, R. Z. *J. Am. Chem. Soc.* **2007**, *129*, 5580.
(33) Bouchard, L. S.; Kovtunov, K. V.; Burt, S. R.; Anwar, M. S.; Koptyug, I. V.; Sagdeev, R. Z.; Pines, A. *Ang. Chem. Int. Ed.* **2007**, *46*, 4064.
(34) Gaussian 03 Frisch, M. J.; Trucks, G. W.; Schlegel, H. B.; Scuseria, G. E.; Robb, M. A.; Cheeseman, J. R.; Scalmani, G.; Barone, V.; Mennucci, B.; Petersson, G. A.; Nakatsuji, H.; Caricato, M.; Li, X.; Hratchian, H. P.; Izmaylov, A. F.; Bloino, J.; Zheng, G.; Sonnenberg, J. L.; Hada, M.; Ehara, M.; Toyota, K.; Fukuda, R.; Hasegawa, J.; Ishida, M.; Nakajima, T.; Honda, Y.; Kitao, O.; Nakai, H.; Vreven, T.; Montgomery, J., J. A.; Peralta, J. E.; Ogliaro, F.; Bearpark, M.; Heyd, J. J.; Brothers, E.; Kudin, K. N.; Staroverov, V. N.; Kobayashi, R.; Normand, J.; Raghavachari, K.; Rendell, A.; Burant, J. C.; Iyengar, S. S.; Tomasi, J.; Cossi, M. R.; Millam, N. J.; Klene, M.; E., K. J.; Cross, J. B.; Bakken, V.; Adamo, C.; Jaramillo, J.; Gomperts, R. E.; Stratmann, O.; Yazyev, A. J.; Austin, R.; Cammi, C.; Pomelli, J. W.; Ochterski, R.; Martin, R. L.; Morokuma, K.; Zakrzewski, V. G.; Voth, G. A.; Salvador, P.; Dannenberg, J. J.; Dapprich, S.; Daniels, A. D.; Farkas, O.; Foresman, J. B.; Ortiz, J. V., Cioslowski, J., and Fox, D. J. Gaussian, Inc., Wallingford CT, 2009.
(35) Becke, A. D. *Phys. Rev. A* **1988**, *38*, 3098.
(36) Lee, C. T.; Yang, W. T.; Parr, R. G. *Phys. Rev. B* **1988**, *37*, 785.
(37) Stephens, P. J.; Devlin, F. J.; Chabalowski, C. F.; Frisch, M. J. *J. Phys. Chem.* **1994**, *98*, 11623.
(38) Dunning Jr., T. H.; Hay, P. J. In *Modern Theoretical Chemistry*; Schaefer III, H. F., Ed.; Plenum: New York, 1976; Vol. 3, p 1-28.
(39) Hehre, W. J.; Ditchfie.R; Pople, J. A. *J. Chem. Phys.* **1972**, *56*, 2257.
(40) Harihara, P. C.; Pople, J. A. *Theo. Chem. Acta* **1973**, *28*, 213.
(41) SMART: Area-Detector Software package Bruker Analytical X-ray Systems, Inc, Madison, WI, 2001-2003.
(42) SAINT: SAX Area-Detector Integration Program, V6.40 Bruker Analytical X-ray Systems, Inc, Madison, WI, 2003.
(43) XPREP Bruker Analytical X-ray Systems, Inc, Madison, WI, 2003.
(44) SADABS: Bruker-Nonius Area Detector Scaling and Absorption V2.05 Bruker Analytical X-ray Systems, Inc, Madison, WI, 2003.
(46) Farrugia, L. J. *J. Appl. Crystallogr.* **1997**, *30*, 565.
(47) Bodizs, G.; Raabe, I.; Scopelliti, R.; Krossing, I.; Helm, L. *Dalton Trans.* **2009**, 5137 and references therein.

(48) A. L. Spek, *PLATON—A Multipurpose Crystallographic Tool*, Utrecht University, Utrecht, The Netherlands, 2007.

Chapter 3:

Carbon Monoxide, Isocyanide, and Nitrile Complexes of a Cationic, d^0 Vanadium Bisimide: Pi-Back Bonding Derived from the Pi Symmetry Metal Bisimido

Introduction:

There has been renewed interest in transition metal and actinide carbonyl complexes based both on fundamental coordination chemistry and their application in developing homogeneous alternatives to non-selective Fischer-Tropsch chemistry.[1-14] In particular, d^0 transition metal carbonyl complexes have recently been shown to be important intermediates in two potentially industrially relevant transformations. Chirik and co-workers have characterized the complex $((Me_2Si(\eta^5\text{-}C_5Me_4)(\eta^5\text{-}C_5H_3\text{-}3\text{-}^t\!Bu)Hf)_2(\mu\text{-}NCO)(CO)(NCO)$ and have shown that the carbonyl ligand controls the regioselectivity in the products formed during the CO-induced cleavage of dinitrogen promoted by the *ansa*-hafnocene $((Me_2Si(\eta^5\text{-}C_5Me_4)(\eta^5\text{-}C_5H_3\text{-}3\text{-}t\!Bu)Hf)_2(\mu^2,\eta^2,\eta^2\text{-}N_2)$.[15,16] Arnold and Bergman have also recently shown that the d^0 carbonyl, (BDI)Nb(N*t*Bu)(η^2-MeC≡CPh)(CO), is a key intermediate in the (*z*)-selective hydrogenation of alkynes to alkenes by (BDI)Nb(N^{t}Bu)$(CO)_2$ under an atmosphere of H_2/CO.[17,18] Remarkably this system yields exclusively products of hydrogenation and not hydroformylation.

Table 1: d^0 Group 4 and 5 Carbonyl Complexes.

Compound	C-O stretch in cm^{-1}	Ref.
$((Me_2Si(\eta^5\text{-}C_5Me_4)(\eta^5\text{-}C_5H_3\text{-}3\text{-}^t\!Bu)Hf)_2(\mu\text{-}NCO)(CO)(NCO)$	1959	15, 16
(BDI)Nb(N*t*Bu)(η^2-RC≡CPh)(CO)	2052, R = Ph; 2039 R = Me	17, 18
$(Cp_2Ti(CO))_2(\mu\text{-}\eta^1\text{-}C_2(CN)_4)$	2055	19
$[TiCp_2(CO)_2][BPh_4]_2$	2119, 2099	20
$Cp^*_2ZrH_2CO$	2044	21,22
$Cp^*_2HfH_2CO$	2036	23
$Cp_2Zr(\eta^2\text{-}Me_2Si{=}N'Bu)(CO)$	1797	24
$Cp^*_2Zr(\eta^2\text{-}E)(CO)$	E=S, 2057; Se, 2037; Te, 2006	25
$Cp^*_2Zr(Se)(CO)$	2037	26
$[Cp_3Zr(CO)][B(Ph_4)]$	2150	27
$[Cp^*_2Zr(\eta^3\text{-}C_3H_5)(CO)][B(Ph)_4]$	2079	28
$[Cp_2Zr(CH(Me)(6\text{-ethylpyrid-2-yl})(CO)][B(Ph)_4]$	2095	29
$[(C_5Me_5)_2Zr(\eta^2\text{-}COCH_3)(CO)][CH_3B(C_6F_5)_3]$	2105, 2152 (isomers)	30
$[Cp_2Ta(CO)H_2][PF_6]$	2112	31
Cp*(ArN=)Ta(CO)[Si(SiMe$_3$)$_3$]H	1986	32
[V(PEt)$_2$(N^{t}Bu)$_2$(CO)][Al(PFTB)$_4$]	2015	this work

Since the initial report of a Ti(IV) carbon monoxide complex in 1976 by Bigorne and co-workers,[19] a small group of formally d^0 transition metal[20-32] (Table 3.1) and actinide carbonyl complexes[33-35] have been described. These complexes, both neutral and cationic, are intriguing from a coordination chemistry perspective because the nature of the bonding of the carbonyl ligand is not readily described by a simple model. Some of these complexes possess C-O stretching frequencies greater than free CO (υ = 2143 cm^{-1}), which implies that σ bonding is the dominant interaction between the metal fragment and the carbonyl. This property has also been demonstrated for main group[36-42] and closed shell, d^8 and d^{10} transition metal compounds.[43-48] Compounds possessing this property have been deemed 'non-classical' because, in contrast to the large number of $d^n \geq 0$ transition metal carbonyls, the stretching frequency of the carbonyl ligand is not reduced *via* π to π^* back-bonding from the metal atomic orbitals to the carbonyl ligand LUMOs.

In this context, the formally d^0 complexes that possess significantly reduced C-O stretching frequencies are of particular interest. These complexes do not possess electron density in a metal atomic orbital with which to back-bond with the carbonyl as would fit a classic Dewar-Chatt-Duncanson analysis of π backbonding.[49,50] However, donation of electron density from σ M-E bonds (M = Ti, Zr, Hf, Nb, Ta; E = H, C, Si, O, S, Se, Te; Table 3.1) has been proposed as the primary means by which the metal fragment molecular orbitals (MO) participate electron donation to the π^* orbitals of the carbonyl ligand (Figure 3.1).[22,24,28]

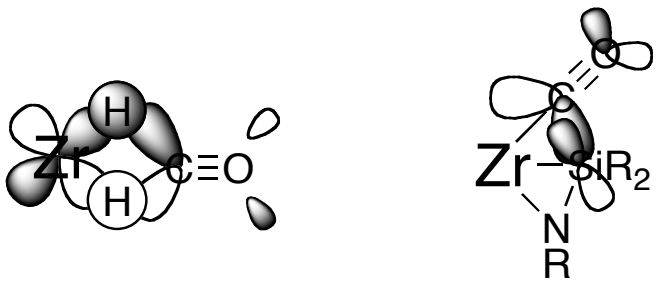

Figure 3.1: Two modes of σ to π^* donation in d^0 carbonyls described previously. Zr = Cp_2Zr or Cp^*_2Zr; Orbital interaction shown in the *xy* plane; see refs. 22 and 24 for complete descriptions.

In contrast to this analysis, a recent theoretical study demonstrates that the bond between CO and $(Cp')_3U$ (Cp' = C_5H_5, C_5H_4TMS, C_5Me_4H, C_5Me_5) in $(Cp')_3U(CO)$ complexes involves back-bonding from the Cp'_3U ligand-based orbitals of π symmetry.[9] In other words, the partially filled, non-bonding *f*-orbitals do not significantly contribute to the reduction in the C-O stretching frequency. The extension of this model to d^0 transition metal complexes does not necessarily hold. The complex $[Cp_3Zr(CO)][B(Ph)_4]$ possesses a C-O stretching frequency of 2150 cm^{-1}.[27] Even when compared to the stretching frequency for CO^+ (υ = 2184 cm^{-1}),[36,37] there appears to be little to no back-bonding from the ligand-based orbitals of π symmetry. However, this theoretical analysis of the C-O stretching frequencies in $(Cp')_3U$ clearly demonstrates the possibility of a similar interaction in transition metal complexes.[32]

In chapter 2, we reported the (*z*)-selective hydrogenation of alkynes to alkenes by $[V(PMe_3)_3(N^tBu)_2][Al(PFTB)_4]$, **1.10**, (PFTB = perfluoro-*tert*-butoxide).[51] This complex is notable for several reasons including its 'bent-metallocene like' electronic structure. This similarity derives from the nature of the donor orbitals of cyclopentadienes and imides – *i.e.* both are 1σ, 2π ligands.[52-55] This analogy between bent-metallocenes and bisimides has been noted previously.[56-60] Given the central role metallocenes have played in the development of organometallic chemistry,[61-64] some efforts have been made to access the frontier orbitals of bisimide systems in order to explore reactivity that is similar but not identical to that of the bent metallocenes.[65]

This previous work, however, has primarily focused on the heavier group 6 and 7 bisimides[56,57] and the activation of small molecule substrates by employing the d^0/d^2 redox couple.[66-71] The $M(NR)_2$ fragment in these complexes is isolobal and isoelectronic to the d^2 Cp_2Hf molecular fragment (Figure 3.2, Left), and suggests that the d^2, 16 e^-, $Cp_2Ti(PMe_3)_2$ is an apt model for their behavior. Two seminal works have explored the reactivity of neutral d^0 bisimides (V and Ta).[72,73] Both of these systems demonstrate remarkable σ C-H bond activation chemistry. However, these systems do not afford access to frontier MOs of the $M(NR)_2$ fragment as the covalently bonded, bulky silyl amide/imide ligands direct reactivity to the π orbitals of the individual imides.

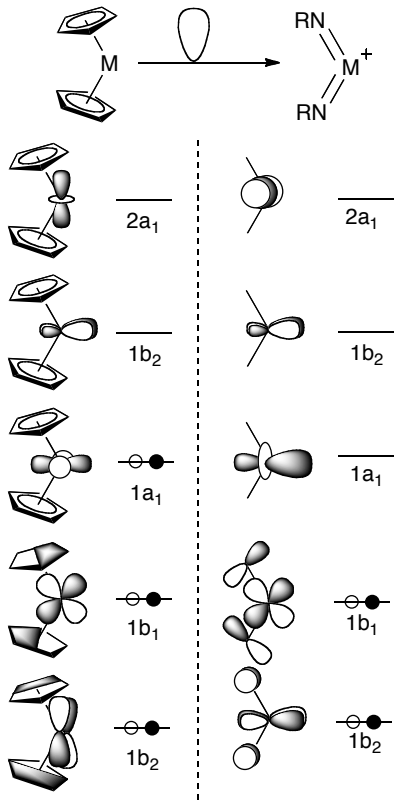

Figure 3.2: Illustration of the isolobal relationship between the frontier orbitals of Cp_2M and $(RN)_2M^+$ complexes. The given orbital occupation corresponds to a d^2 electron configuration for the Group 4 metallocene and d^0 for the cationic, group 5 bisimide, as Cp's are monovalent and imides are divalent ligands.

We hypothesized that the use of labile supporting ligands and less sterically demanding imides as part of a cationic, group 5 complex would afford access to the frontier orbitals of the bent metallocene analog and to the σ bond reactivity of these d^0 bisimides.[74-80] A simple analysis of the bonding in the 16 e^-, $[V(PR_3)_2(N^tBu)_2][Al(PFTB)_4]$, (R = Me, Et) suggests that these compounds would be isolobal with $Cp_2Ti(PMe_3)_2$, but have a HOMO/LUMO gap shifted one set down (Figure 3.2, right). Given the remarkable hydrogenation chemistry observed for **1.10,** the nature of the bonding interactions of the complexes $[V(PR_3)_2(N^tBu)_2][Al(PFTB)_4]$ (R = Me, Et) with alkynes and dihydrogen were of particular importance. Our interest in the bonding of d^0 transition metal carbonyl complexes stems from the ability to use carbon monoxide as a spectroscopic probe to determine the nature of the frontier molecular orbitals in these bisimide complexes. Quantitative analysis of the molecular structure is not possible using substrates involved in the catalytic reaction due to several factors, including the complex spin system (ABC_2; *i.e.* X (C or H), V, and P) in complexes of the type $[VL(PR_3)_2(N^tBu)_2][Al(PFTB)_4]$, (R = Me, Et, L = H_2, internal alkyne), high anisotropy of vanadium (I = 7/2), weak bonding of the substrates of interest, the fluxional nature of the complexes, a narrow range of thermal stability, and a limited number of compatible solvents. Carbon monoxide, on the other hand, is the ideal π accepting ligand with which to study the electronic structure of these complexes because of its strong infrared signal and the ease of isotopic labeling.

In this chapter we report the synthesis and characterization of a series of nitrile, isocyanide, and carbon monoxide complexes of $[V(PR_3)_2(N^tBu)_2][Al(PFTB)_4]$ (R = Me, Et). Structural, spectroscopic, and DFT analyses demonstrate that the bond between $[V(PEt_3)_2(N^tBu)_2][Al(PFTB)_4]$ and CO involves back-bonding from the $[V(PEt_3)_2(N^tBu)_2]$ ligand-based orbitals of π symmetry. Furthermore, $[V(PR_3)_2(N^tBu)_2]^+$, (R = Me, Et) can act as both a σ acceptor and π donor in its binding of small molecule substrates.

Results and Discussion

Synthesis of Isocyanide and Nitrile Complexes of $[V(PMe_3)_2(N^tBu)_2][Al(PFTB)_4]$, 1.10. In the course of exploring the scope of the catalytic hydrogenation by **1**, isocyanides and nitriles were found to undergo exclusive ligand exchange with the equatorial PMe_3. Even in the presence of a 5-fold excess of substrate, no further exchange with the axial PMe_3 ligands in **1.10** was observed (Scheme 3.1). While the equatorial phosphine readily disassociates at 30 °C, the site selectivity of this exchange process suggests that there is a significant electronic contribution to the bonding in the newly formed complexes.

In order to explore the nature of bonding in these complexes, an isocyanide complex was synthesized on a preparative scale. The addition of a solution of one equivalent of 2,6-xylylisocyanide (CNXyl) in diethyl ether to a solution of **1.10** resulted in a rapid color change from yellow to orange. After workup, $[V(PMe)_2(N^tBu)_2(CNXyl)][Al(PFTB)_4]$, **3.1**, was isolated in 58% yield *via* crystallization from 1,2-dichloroethane (DCE) (Scheme 1). The NMR characterization of this isolated complex matched that of the *in situ* prepared complex. In solution ($PhCF_3$, C_6D_6 insert)

3.1 presents both equivalent imido *tert*-butyl groups at 1.13 ppm and axial PMe_3 ligands at 1.28 ppm ($^2J_{PH}$ = 3.6 Hz). The xylyl methyl groups are also equivalent with a single sharp singlet at 2.22 ppm. Most interestingly, the ^{51}V NMR presents as a singlet at -930.21 ppm ($\Delta\nu_{1/2}$ = 159.88 Hz), 138 ppm upfield from that of the starting complex, **1**, at -792.29 ppm, implying that the vanadium nucleus is significantly more shielded. This upfield shift suggests that the isocyanide ligand is not acting solely as a σ donor, like PMe_3 or MeCN (^{51}V NMR δ -810.15, $\Delta\nu_{1/2}$ = 939.0 Hz).

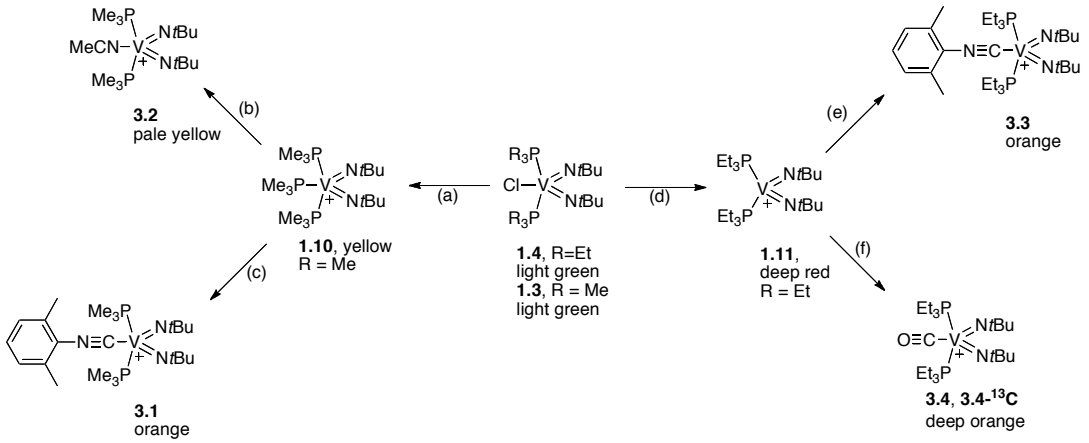

Scheme 3.1: For cationic vanadium complexes, the counteranion, $[Al(PFTB)_4]^-$, is not depicted for clarity. Conditions: (a) 3 equiv. PMe_3; 1 equiv. $Li[Al(PFTB)_4]$, PhCl, 75%; see Chapter 1; (b) 5 equiv. MeCN in $PhCF_3$; *in situ* characterization; (c) 1 equiv. CNXyl, diethyl ether, 58%; (d) 1 equiv. $Li[Al(PFTB)_4]$, DCE, 47%; (e) 1 equiv. CNXyl, DCE, 58%; (g) 1 atm CO, excess.

An X-ray crystallographic study confirmed the solution structural assignment. Complex **3.1** presents as distorted square base pyramid (τ = 0.46, Figure 3.3, Table 3.2 contains relevant crystallographic data) with C_{2v} symmetry. This distortion from ideal sp geometry (τ = 0.0)[81,82] reflects the still significant steric demands of the *tert*-butyl imido ligands on the relatively small vanadium nucleus (in comparison to Nb and Ta with either 2,6-diisopropylarylimido or *tris*-*tert*-butylsilylimido ligands).[73,82] As a result, the axial phosphines are displaced away from the imides as indicated by the N(1)-V(1)-P(2) and N(2)-V(1)-P(1) angles of 93.71(10)° and 97.96(11)°. The angle between the axial phosphines, 155.93(4)°, is about 5° greater than the corresponding angle in $(py)_2MeTa(NSi(tBu)_3)_2$, and about 5° smaller than that in $(py)_2MeTa(NAr)_2$ (Ar = 2,6-diisopropyl),[73,82] which suggests that the combination of *tert*-butyl imides and vanadium is intermediate in terms of steric constraint in comparison to the much larger imides employed in the analogous V,[72,83,84] Nb,[82] and Ta[73] systems. However, such a comparison is purely qualitative because of the significantly greater $V\text{-}P_{phospine}$ bond lengths (2.4526(10) and 2.4463(11) Å) in comparison to the $Ta\text{-}N_{pyridine}$ lengths (2.316(14) Å**)**.
As high quality X-ray data sets for this series of cationic, vanadium bisimides are difficult to acquire on a routine basis due to the potential for extensive disorder in the S_4 symmetric anion, $[Al(PFTB)_4]^-$,[85,86] it is revealing to compare the metrical parameters of the bisimide core with the neutral precursor to **3.1**, $VCl(PMe_3)_2(N^tBu)_2$, **1.3**, and

appropriate monoimido vanadium complexes (see the Experimental Section for a full ORTEP representation of the salt pair). As has been noted previously for other group 5 bisimides,[73] the angle N_{imide}-V-N_{imide} is less than the ideal of 120°. However, in contrast to its neutral precursor, $VCl(PMe_3)_2(N^tBu)_2$, (115.88(10)°) and the few other known neutral group 5 bisimides (115.3(7)° and 113.2 (3)°),[73,82] it is expanded by about 5° to 118.35(15)°. This contraction of the angle between the imides in the neutral compounds, which is counter to the increased steric repulsion between the imide R groups, has been rationalized on the basis of electronic arguments. This rationalization of the observed

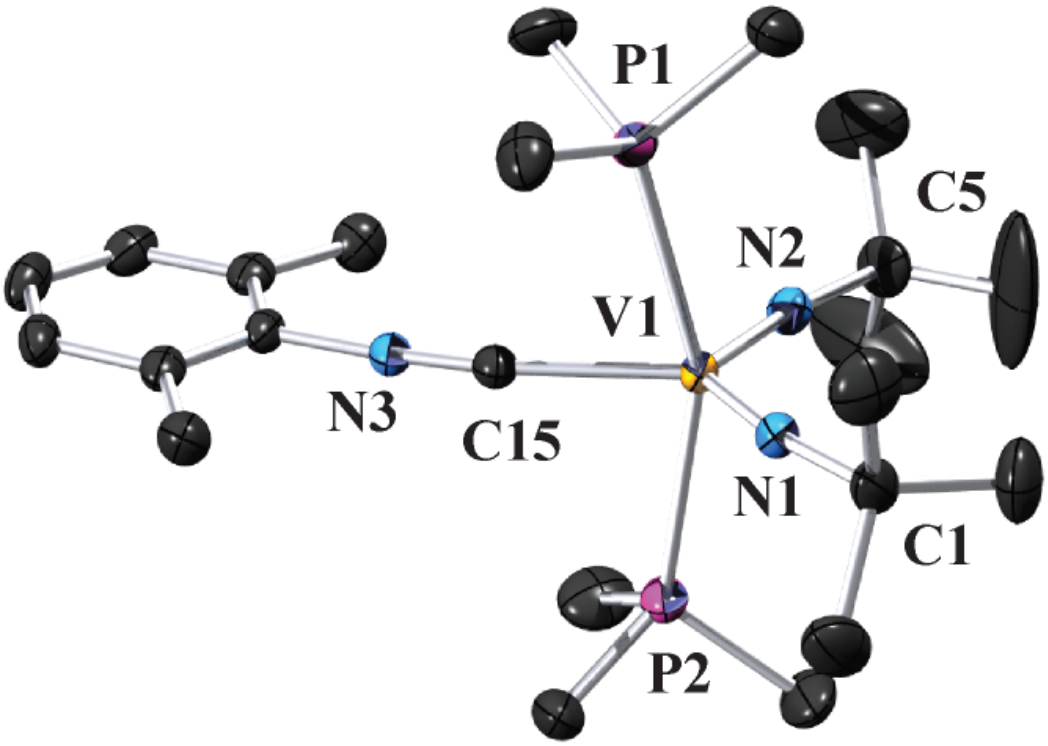

Figure 3. Molecular structure of **3.1**. Thermal ellipsoids are drawn at 50% probability level. Hydrogen atoms and counteranions ($[Al(PFTB)_4]^-$) have been removed for clarity. Selected bond lengths (Å) and angles (deg): N(1)-V(1), 1.690(3); N(2)-V(1), 1.679(3); P(1)-V(1), 2.4526(10); P(2)-V(1), 2.4463(11); C(15)-V(1), 2.152(4); C(15)-N(3), 1.152(4); N(2)-V(1)-N(1), 118.35(15); C(1)-N(1)-V(1), 167.6(3); C(5)-N(2)-V(1), 168.7(3); N(2)-V(1)-C(15), 114.24(14); N(1)-V(1)-C(15), 127.41(14); N(2)-V(1)-P(2), 97.75(11); N(1)-V(1)-P(2), 93.71(10); N(2)-V(1)-P(1), 97.96(11); N(1)-V(1)-P(1), 94.75(10); P(2)-V(1)-P(1), 155.93(4); C(15)-V(1)-P(1), 78.15(9); C(15)-V(1)-P(2), 78.81(10); N(3)-C(15)-V(1), 173.9(3).

Table 3.2: Crystal and Refinement Data for Complexes **3.1**.

	3.1
empirical formula	$C_{39}H_{45}AlF_{36}N_3O_4P_2V$
formula weight	1443.64
temp., K	100(2)
λ	0.71073
crystal system	monoclinic
space group	$P2_1/c$
a, Å	10.040
b, Å	17.360
c, Å	33.167
α, deg	90
β, deg	91.26
γ, deg	90
volume, $Å^3$	5779.4
Z	4
d_{calc}, mg/m^3	1.659
F_{000}	2888
μ, mm^{-1}	0.399
no. rflns measd	156432
no. indep reflns	10613
R_{int}	0.0498
Restr/param	0/775
R_1, wR_2	0.0572, 0.1200
[$I > 2\sigma(I)$]	
R_1 (all data)	0.0735
GOF	1.020
Resid peak, hole (e-/$Å^3$)	2.012, -2.237

trend in the neutral group 5 bisimides implies that the bisimides contribute less than 8e- to the metal (neutral ligand method). The expansion of the bisimide angle in the cation **3.1** could be driven by more effective donation of electron density to the metal center in order to compensate for the increased charge separation in the cation.

The imide bond lengths are nearly equivalent (1.690(3) and 1.679(3) Å). Surprisingly, they are about the same length as the imides on the neutral precursor $VCl(PMe_3)_2(N^tBu)_2$ (1.6888(19) and 1.6839(19) Å). These bond lengths in themselves are notable in that they are somewhat long in comparison to those of neutral vanadium monoimides such as $VCl_3(N\textit{t}Bu)$,[87,88] (1.616(9) Å), where bond lengths are consistent with triple bonding. The V=N-C angles in **3.1** and $VCl(PMe_3)_2(N^tBu)_2$ are nearly equivalent and lie in the range of 167-169°. While these angles lie at the lower end of the range generally accepted to indicate linearity at an imide, they are smaller than their equivalent angles on group 5 aryl and silyl bisimides (*c.f.* 176.3(10) and 168.1(8)°; $TaNSiR_3$[73] and 170.9(5) and 165.4(5)°; TaNAr).[82] These silyl and aryl bisimides can participate in either N(pπ)⇒Si(dπ) or N(pπ)⇒Ar(pπ*) interactions that lead to linearization of the M=N-X angle (X = C or Si). This geometric difference suggests that

3.1 and $VCl(PMe_3)_2(N^tBu)_2$, with alkyl imides, have greater electron density localized at nitrogen and a larger contribution of sp^2 hybridization. The main difference between **3.1** and its neutral precursor is the slight contraction of the V-P bond lengths from 2.4507(7) and 2.4546(7) Å to 2.4526(10) and 2.4463(11) Å.

In the context of defining the bonding of π accepting ligands to $[V(PR_3)_2(N^tBu)_2]^+$, the geometric parameters of the isocyanide ligand, like the NMR data for **3.1**, indicate some degree of π back-bonding from the complex. The isocyanide ligand is essentially coplanar with the N_{imide}-V-N_{imide} plane, and it is centrally located in the bisimide wedge, equidistant from the imides and phosphines. The V-C-N angle is near linear, 173.9(3)°. The V-C bond length is 2.152(4) Å and the C-N bond length is 1.152(4) Å. Crystallographically characterized vanadium CNXyl complexes are rare. The nearest point of comparison is the V(III) $(PNP^{ipr})VTe(CNXyl)_2$ (PNP^{ipr} = N(2-$PiPr_2$-4-methylphenyl)$_2$), which possess two crystallographically equivalent isocyanides with a V-C bond of 2.050 Å and a C-N bond of 1.155 Å.[89] As **3.1** exhibits a C-N stretching frequency of 2164 cm^{-1}, and $(PNP^{ipr})VTe(CNXyl)_2$ has stretching frequencies of 2022 and 2002 cm^{-1} (Free CNXyl = 2116 cm^{-1}, Table 3),[90] it is clear that the C-N bond length is not always an accurate measure of back-bonding. In comparing these two complexes, the V-C bond length correlates best with the observed IR stretching frequencies, and, as the absorption for **3.1** is slightly blue shifted from that of free CNXyl, might initially suggest an absence of π back-bonding.

However, a clear trend can be delineated by examining the d^0 and d^1 Group 4, CNXyl complexes. Two factors make analysis of π back-bonding *via* isocyanide C-N bond lengths and stretching frequencies complex. (1) In isocyanides, the HOMOs are the degenerate π orbitals and the HOMO-1 is the σ donor orbital, the inverse pattern of CO. Therefore isocyanides are better σ donors, and as this interaction plays a greater role in bonding to metal centers in comparison to carbon monoxide it leads to shortened C-N bond lengths in the solid state. (2) As with carbon monoxide, the stretching C-N stretching frequency is higher in cationic complexes. With these constraints in mind, it is of interest to compare free CNXyl with a C-N bond length of 1.160(3) Å and a C-N stretching frequency of 2116 cm^{-1} with the d^0, Ti(IV) complex, $[Ti(CNXyl)Cl_4]_2$, which has a C–N distance of 1.147(8) Å and an IR absorption at 2210 cm^{-1} (Table 3.3).[91] This pair of data implies that in the complex $[Ti(CNXyl)Cl_4]_2$, CNXyl can be thought of as very nearly a solely σ donor. Therefore the bonding in **3.1** must be considered to contain some component of π back-bonding from $[V(PR_3)_2(N^tBu)_2]^+$. The d^1 Ti(III) complex, $CpTiI_2(CNXyl)_2$, possesses similar metrics to **3.1** (1.154(4) Å and C-N absorption at 2156 cm^{-1}).[92] The authors propose that this complex, in comparison to $[Ti(CNXyl)Cl_4]_2$, possesses π back-bonding along the classical Dewar-Chatt-Duncanson model. The sole other reported cationic, d^0 CNXyl complex, $[Cp_2Hf(CNXyl)(\eta^2\text{-RCNXyl})][B(Ph)_4]$ (R = CCMe), has an isocyanide C-N absorption at 2189 cm^{-1}.[93] As the C-N absorption of complex **3.1** lies 25 cm^{-1} lower than $[Cp_2Hf(CNXyl)(\eta^2\text{-RCNR'})][B(Ph)_4]$, the V-C bond in **3.1** must contain some component of π back-bonding.

Table 3.3: Reference CNXyl stretching frequencies and C-N bond lengths.

Compound	C-N Bond Length, Å	C-N Stretching frequency, cm^{-1}	ref.
CNXyl	1.160(3)	2116	90
$[V(PMe_3)_2(N^tBu)_2(CNXyl)]^+$	1.152(4)	2164	this work
$[V(PEt_3)_2(N^tBu)_2(CNXyl)]^+$	N/A	2156	this work
$(PNP^{ipr})VTe(CNXyl)_2$	1.155	2022, 2002	89
$[Ti(CNXyl)Cl_4]_2$	1.147(8)	2210	91
$CpTiI_2(CNXyl)_2$	1.154(4)	2156	92
$[Cp_2Hf(CNXyl)(\eta^2\text{-}RCNR')]^+$	N/A	2189	93

Isocyanide and Carbon Monoxide Complexes of $[V(PEt_3)_2(N^tBu)_2][Al(PFTB)_4]$. With access to a four-coordinate bisimide complex, the isocyanide complex to analogous to **3.1** was pursued. Treatment of a DCE solution of freshly prepared **1.11** with a solution of CNXyl in DCE resulted in a rapid color change from deep red to orange. Stirring the reaction mixture overnight resulted in no further observable reactivity and it afforded, after appropriate workup, complex **3.3** in 60% yield as orange blades (Scheme 3.1). Several attempts to obtain an XRD structure failed to yield resolution sufficient to obtain connectivity, but solution NMR studies confirmed a structure analogous to **3.1** with equivalent *tert*-butyl imido groups and PEt_3 ligands. Most notably, the vanadium NMR shift is essentially unchanged from that of the PMe_3 analog **3.1** at δ -903.43 ppm (compared with -930.21 ppm). This similarity in bonding structure is mirrored in the IR spectrum of **3.3** in which the C-N stretch is located at 2156 cm^{-1} (Table 3), very nearly identical to that of **3.1** at 2164 cm^{-1}. This pattern suggests that bonding of the isocyanide is unperturbed by the nature of the phosphine and that any π back-bonding is independent of the V-P σ bonds, as the C-N stretching frequency is largely independent of the identity of the supporting phosphine ligand.

The carbonyl complex was most readily prepared by the addition of 1 atm of CO to a degassed solution of **1.11** in $PhCF_3$ or d_4-DCE in a J. Young NMR tube. Within 5 minutes the color shifted from deep red to deep orange and examination by NMR revealed complete conversion to the desired product **3.4** (Scheme 3.1). While **3.4** can be isolated on a preparative scale, it decomposed before satisfactory elemental analysis could be obtained. Likewise, crystallographic analysis proved troublesome: when single crystals were placed on a slide in Paratone-N oil under a lamp they rapidly evolved a gas, presumably CO, and immediate interrogation via X-ray led to sudden crystal decay.

The *tert*-butyl imido groups of **3.4** are equivalent in solution as are the supporting triethyl phosphine ligands, similar to its isocyanide congener **3.3**. The ^{51}V NMR presents as a pseudo doublet at δ -843.71 ppm ($^1J_{VP}$ = 225.13 Hz), which is significantly shielded in comparison to the four coordinate presursor **5**, although not quite as shielded as the two isocyanide complexes (Figure 3.4). This upfield shift suggests that carbon monoxide, like isocyanide, is not acting solely as a σ donor. The pseudo doublet of **3.3** in the ^{51}V NMR spectrum is unusual. Since **3.4-^{13}C** presents as a broad singlet at -845.06 ppm ($\Delta\nu_{1/2}$ = 531.05 Hz), the observed coupling constant is not due to V-C coupling. Rather it is the result of V-P coupling. This phenomenon is similar to that observed for metal complexes containing two equivalent PMe_3 ligands. The proton resonance for the PMe_3

ligands in these systems shows a pseudo triplet in the extreme where J_{PP} is greater than J_{HP}. The equivalent scenario for ^{51}V NMR was reported by us for the *bis*-PMe_3 complex, $[VCl(PMe_3)_2(N^tBu)(NHtBu)][Al(PFTB)_4]$, which presents unresolved pseudo triplets in its ^{51}V spectra: *i.e.* J_{PP} is larger than J_{VP}.[51] In the case of **3.4**, the opposite is true J_{VP} is larger than J_{PP}, leading to the observed 'Batman,' pseudo doublet. It is tempting in the context of the larger argument – that CO binds *via* π back-bonding with filled vanadium bisimido orbitals of π symmetry – to ascribe the observation of this coupling constant to the decreased local anisotropy at vanadium due to increased local symmetry via the formation of the π bonds. It should be noted that among the five coordinate bisphosphine, bisimido complexes presented here and previously, those containing a π accepting axial ligand generally present ^{51}V resonances with a smaller $\Delta\nu_{1/2}$.

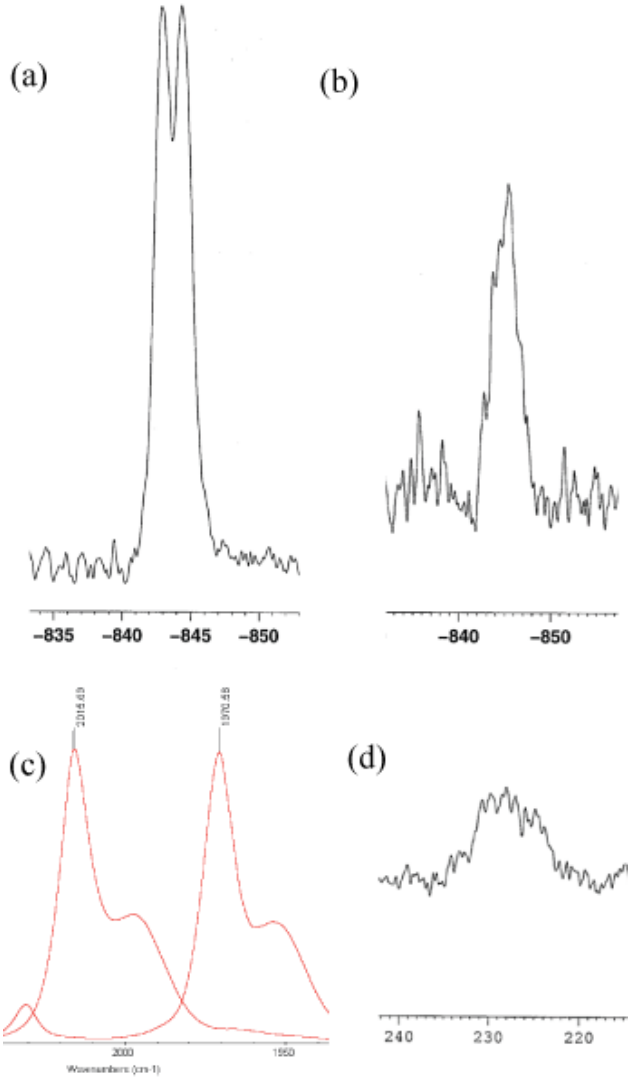

Figure 3.4: (a) ^{51}V NMR of **3.4**. (b) ^{51}V NMR of **3.4-^{13}C**. (c) Solution IR of **3.4** and **3.4-^{13}C**. (d) $^{13}C\{^{31}P\}\{^{1}H\}$ NMR spectrum of **3.4-^{13}C**.

These NMR data, which imply a π interaction, are supported by examining the solution infrared spectrum of **3.4** which shows a strong C-O absorption at 2015 cm^{-1}. Upon labeling with ^{13}CO this absorption shifts to 1970 cm^{-1}, as is expected by the simple harmonic oscillator model and confirms the species as a terminal, (i.e η^1) CO complex (Figure 4). The $^{13}C\{^{31}P\}\{^{1}H\}$ NMR spectrum of **3.4-^{13}C** gives a very broad resonance due to unresolved V-C coupling at 228.36 ppm (Figure 3.4). This resonance is shifted downfield of that of free CO (181.83 ppm in $PhCF_3$) by 46.56 ppm, which demonstrates donation of electron density into the π* orbitals of the CO ligand (Figure 3.4). Sigma only complexes present ^{13}C shifts upfield of free CO. Taken together, this experimental data strongly supports the hypothesis that the carbonyl and isocyanide ligands participate in π back-bonding with $[V(PR_3)_2(N^tBu)_2]^+$ and that reduction in C-O stretching frequency is *not* due solely to a σ to π* interaction, as has been proposed to be the dominant electronic interaction in other d^0 carbonyl complexes.

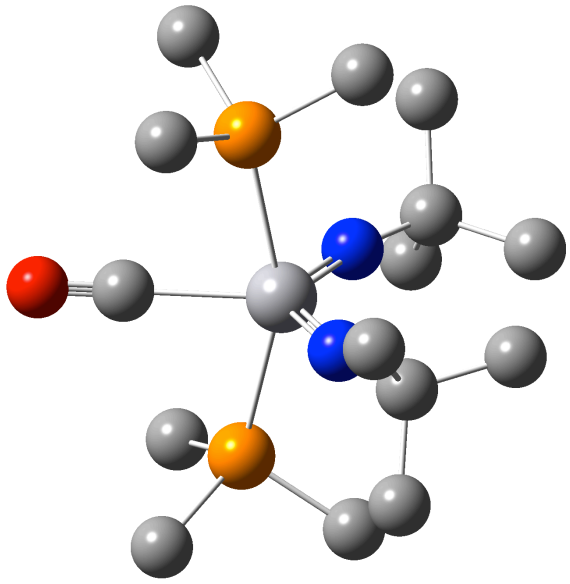

Figure 5. Geometry-optimized (B3LYP) coordinates of **3.5**. The hydrogen atoms were omitted for clarity.

Computational Studies and the Electronic Structure of $[V(\eta^1\text{-}CO)(PR_3)_2(N^tBu)_2]^+$. In order to gain further understanding of the bonding in the carbonyl complex and to confirm the hypothesis that the V-C bond involves π back-bonding from the $[V(PEt_3)_2(N^tBu)_2]^+$ ligand-based orbitals of π symmetry, DFT calculations were performed on the model complex $[V(\eta^1\text{-}CO)(PMe_3)_2(N^tBu)_2]^+$, **3.5**, (B3LYP, see experimental section and supplementary information). The geometry optimized structure of **3.5** reveals overall C_{2v} symmetry in accord with the solution-state symmetry observed by NMR for complex **3.4** and the solution and solid-state symmetry observed for **3.1** (Figure 3.5). The geometry of **3.5** is best approximated as a distorted trigonal bipyramid with τ = .60 (Figure 3.5). The N_{imide}-V-N_{imide} bond angle is 118.4°; the

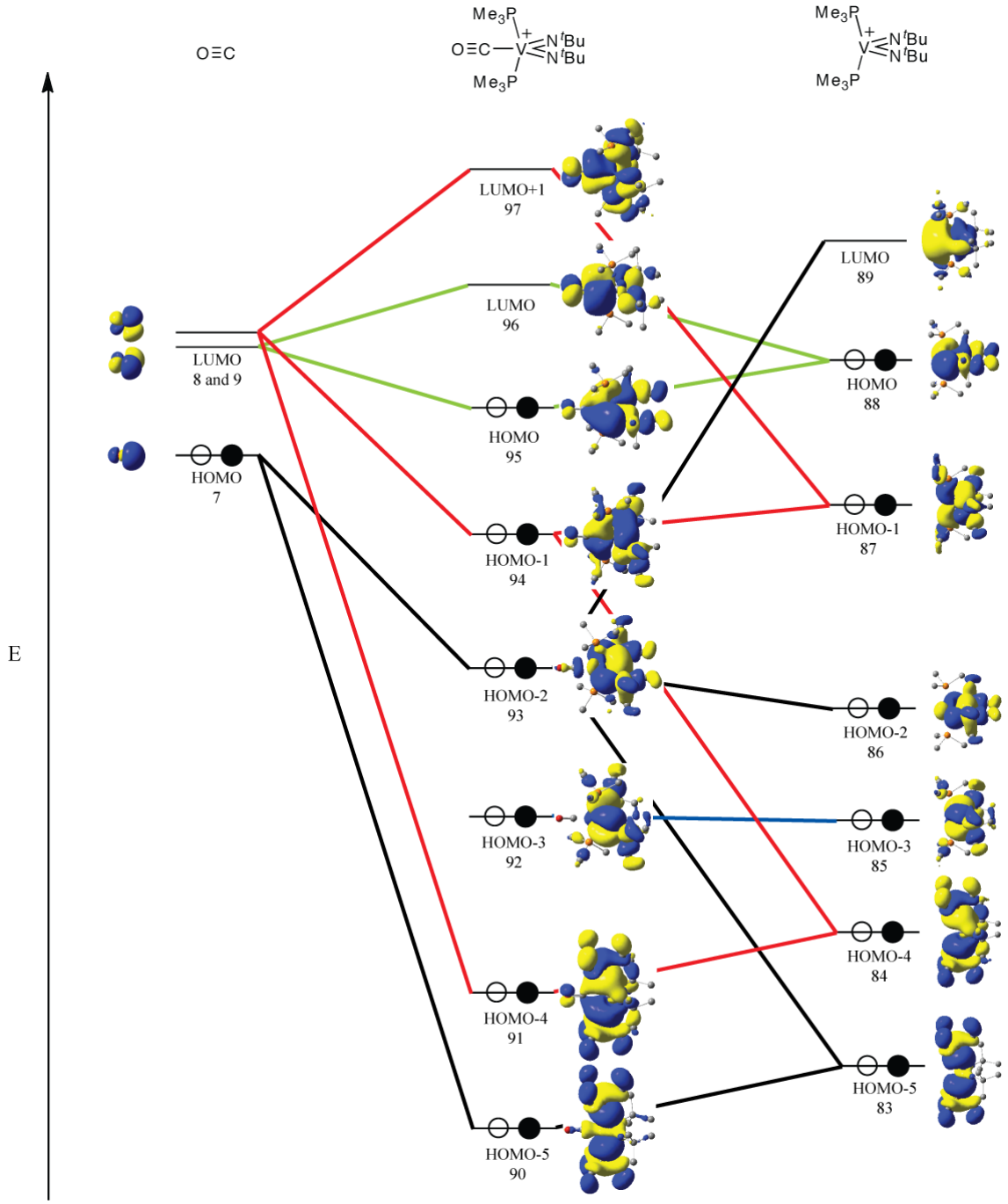

Figure 5. DFT MO correlation diagram of $[V(PMe_3)_2(N^tBu)_2]^+$ and CO in the bonding of **3.5**. Relative energies and overlap are not to scale. Green lines show in-plane π interactions, red lines show out of plane interactions, black lines show σ interactions, and blue non-bonding. Two σ orbitals (one filled, one empty) are not shown for clarity.

$V\text{-}N_{imide}$ distances are both 1.67 Å; and the $V\text{-}N_{imide}\text{-}C$ angles are both 168° in good agreement with the parameters observed for the isocyanide complex **3.1**.

The frontier orbitals of **3.5** were then compared with fragment orbitals of $[V(PMe_3)_2(N^tBu)_2]^+$ and CO. The fragment analysis was performed using the coordinates generated by the geometry optimization on **3.5**. This analysis is the basis of molecular orbital correlation diagram presented in Figure 3.5. The key features of this diagram and the molecular orbital plots are the interactions of the $1b_1$, $2b_1$, and $1b_2$ orbitals of the $[V(PMe_3)_2(N^tBu)_2]^+$ with the π* of CO. This is clearly seen in the interaction of in plane π* orbital of CO (plane as defined by $N_{imide}\text{-}V\text{-}N_{imide}$) with $1b_2$ orbital of $[V(PMe_3)_2(N^tBu)_2]^+$ (HOMO (88)), which gives rise to HOMO (95) and LUMO (96) of the complex (Green lines, Figure 3.5). The out of plane π* orbital of CO interacts with the linear combination of the $1b_1$ and $2b_1$ (HOMO-4 (84) and HOMO-1 (87)) orbitals of the $[V(PMe_3)_2(N^tBu)_2]^+$, which gives rise to three molecular orbitals LUMO+1 (97), HOMO-1 (94), and HOMO-4 (91) (Red lines, Figure 3.5). This interaction is more complex and implicates the previously proposed σ to π* interaction is a component of the π back-bonding. There is also a slight σ interaction contributing to the bonding between vanadium and carbon, as seen in HOMO-5 (90) *via* donation to the equatorial lobe of the $1a_1$ orbital (HOMO-5 (83)) of $[V(PMe_3)_2(N^tBu)_2]^+$, which is predominantly vanadium d_{z2} based. However, it should be noted that the filled orbital HOMO-3 (93) is slightly σ anti-bonding with respect to the V-C bond. The frontier orbital diagram is completed by the non-bonding orbital HOMO-4 (92) which is primarily vanadium $d_{x2\text{-}y2}$ in character.

In comparison to the typical axis choice for the depiction of bent-metallocenes in which the Cp centroids and the metal lie on the *xz* or *yz* plane, the vanadium bisimide MO diagram is best based with the imido nitrogens and the vanadium center on the *xy* plane. This change in the parentage of the metal atomic orbital for $1A_1$ participating SALC molecular orbital is most likely due to the difference in the radial extent of the N 2*p* orbitals in comparison to the π orbitals of Cp and their more effective overlap with the vanadium 4*p* rather than 3*d* orbitals. While this phenomenon is evident in the molecular orbital correlation diagram, it most clearly illustrated in the ChemDraw depicted in Figure 3.2 (right column).

Conclusion

A series of carbon monoxide, isocyanide, and nitrile complexes of cationic, vanadium bisimides were prepared. In the case of the more strongly σ donating isocyanide or nitrile ligands, this synthesis was most conveniently achieved by the displacement of PMe_3 from $[V(PMe_3)_3(N^tBu)_2][Al(PFTB)_4]$. However, in the case of carbon monoxide the use of a four coordinate precursor, $[V(PEt_3)_2(N^tBu)_2][Al(PFTB)_4]$, was necessary to isolate the desired complex. The formation of the requisite $[V(PEt_3)_2(N^tBu)_2][Al(PFTB)_4]$ was confirmed *via* derivitization with DMAP and CNXyl. The examination of these complexes implicates the role of π back-bonding from the formally d^0 vanadium complex in binding π accepting ligands.

The bonding model developed here for the lowered C-O stretching frequency in **3.4** is distinctly different from that used to account for the lowered C-O stretching frequency in most *d*-transition metal complexes. In this case, the electron density

originates from the *d* π symmetry orbitals that are RN-V bonding. This mode of weak bonding of π accepting ligands provides the basis to understand the bonding and hence activation barriers of small molecules to d^0 transition metal complexes. Wolczanski, Chirik, and Andersen have indirectly implicated similar d^0 imide/Cp and bisimide complexes in the formation of intermediate σ H_2 and C-H complexes via KIE and EXSY experiments, as well as DFT calculations.[95,96,97] The results presented here suggest that these reaction intermediates may be formed not just on the basis of a simple Lewis acid/base pair, but may also involve π back-bonding. Ongoing work focuses on applying the understanding of the molecular orbital structure of these unusual complexes to the design of other novel catalytic reactions and the direct observation of reaction intermediates.

Experimental

General Details. Unless otherwise noted, all reactions were performed using standard Schlenk line techniques or in an MBraun inert atmosphere box under an atmosphere of argon or dinitrogen (<1 ppm O_2/H_2O), respectively. All glassware and cannulae were stored in an oven at ca. 425 K. Pentane, diethyl ether, tetrahydrofuran, 1,2-dimethoxyethane, dichloromethane and toluene were purified by passage through a column of activated alumina and degassed prior to use. HMDSO was distilled from sodium/benzophenone, degassed by bubbling argon through the liquid for 15 minutes, and stored over 4 Å sieves. Acetonitrile was distilled from P_2O_5 and degassed by bubbling argon through the liquid for 15 minutes. C_6D_6 was vacuum-transferred from sodium/benzophenone and degassed with three freeze-pump-thaw cycles. 1,2-$C_2D_4Cl_2$ was vacuum transferred from CaH_2 and degassed with three freeze-pump-thaw cycles. NMR spectra were recorded on Bruker AV-300, AVB-400, AVQ-400, AV-500, and AV-600 spectrometers. ^1H and $^{13}C\{^1H\}$ chemical shifts are given relative to residual solvent peaks. ^{31}P, ^{51}V, ^{19}F, and ^{27}Al chemical shifts were referenced to external standards ($P(OMe)_3$ at 1.67 ppm, $VOCl_3$ at 0.00 ppm, $CFCl_3$ at 0.00 ppm, and 1M $Al(NO_3)_3$ in H_2O/D_2O at 0 ppm, respectively). Proton and carbon NMR assignments were routinely confirmed by ^1H-^1H (COSY) or ^1H-^{13}C (HSQC and HMBC) experiments as necessary: ^{13}C resonances marked with * are observed only by HMBC. Infrared (IR) samples were prepared as Nujol mulls and were taken between KBr disks on a Thermo Scientific iS10 FT-IR spectrometer except where noted in text. The following chemicals were purified prior to use: 1,2-dichloroethane was distilled from CaH_2 and was degassed by bubbling argon through the liquids for 15 minutes and α, α', α''-trifluorotoluene ($PhCF_3$), was distilled from P_2O_5 and degassed by bubbling argon through the liquid for 15 minutes. $Li[Al(PFTB)_4]$,[85] was prepared using standard literature procedures. All other reagents were acquired from commercial sources and used as received. Elemental analyses were determined at the College of Chemistry, University of California, Berkeley. The X-ray structural determination was performed at CHEXRAY, University of California, Berkeley, on aMicroSTAR-H X8 APEXII diffractometer.

Preparation of $[V(PMe_3)_2(N^tBu)_2(CNXyl)][Al(PFTB)_4]$ (2). To a solution of **1.10** (777 mg, 0.56 mmol) in 15 mL of diethyl ether was added 2,6-xylylisocyanide (1 equiv., 75 mg, 0.56 mmol) in 10 mL of diethyl ether *via* cannula. After this addition, the

reaction mixture was stirred for 12 h. The reaction mixture was then reduced to a residue *in vacuo* and extracted with 1,2-dichloroethane, filtered *via* cannula, and reduced until the product began to crystallize. After cooling the solution to -15 °C overnight, the product was obtained in 58% yield (467 mg) after decantation, as yellow-orange blocks. Subsequent recrystallization from DCE at -15 °C afforded X-ray quality crystals. ^{1}H NMR ($PhCF_3$ (C_6D_6 insert), 600.1 MHz) δ 2.22 (s, *ortho*-ArMe, 6H), 1.28 (pseudo t, axial P*Me*$_3$, 18H, $^{2}J_{PH}$ = 3.6 Hz), 1.13 (s, N*tBu,* 18H). Aryl proton resonances could not be observed due to overlapping *protio*-solvent resonances. ^{13}C NMR ($PhCF_3$ (C_6D_6 insert), 150.9 MHz) δ 135.09 (s, *Ar*), 131.12 (q, C(*C*F_3)$_3$, $^{1}J_{CF}$ = 41.35 Hz), 69.5* (α-N*t*Bu), 33.17 (t, β-N*t*Bu , $^{3}J_{PC}$ = 3.32 Hz), 18.01 (s, Ar-*ortho-Me*), 17.40 (d, P*Me*$_3$, $^{1}J_{PC}$ = 14.34 Hz), 17.33 (d, P*Me*$_3$, $^{1}J_{PC}$ = 14.34 Hz). The α-C$(CF_3)_3$ resonance and three Ar carbons could not be observed. ^{31}P{^{1}H} NMR ($PhCF_3$ (C_6D_6 insert), 242.9 MHz) δ 2.61 (vbr s, $\Delta\nu_{1/2}$ = 2056.60 Hz). ^{51}V{^{1}H} NMR ($PhCF_3$ (C_6D_6 insert), 157.7 MHz) δ -930.21 (br s, $\Delta\nu_{1/2}$ = 159.88 Hz). ^{19}F NMR ($PhCF_3$ (C_6D_6 insert), 376.5 MHz). -74.55 (s). ^{27}Al NMR ($PhCF_3$ (C_6D_6 insert), 104.3 MHz) δ 34.74 (s, $\Delta\nu_{1/2}$ = 3.18 Hz). Anal. Calcd (%) for $C_{40}H_{49}AlF_{36}N_3O_4P_2V$: C, 32.91; H, 3.38; N, 2.88. Found: C, 32.67; H, 3.10; N, 2.84. IR (KBr, cm^{-1}): 2164 (s), 1352 (s), 1172 (s), 1110 (w), 945 (s), 831 (m), 755 (w), 601 (w), 560 (w), 537 (w), 446 (s). Mp = 185-187 °C (dec.).

Observation of [V(PMe$_3$)$_2$(N^{t}Bu)$_2$(MeCN)][Al(PFTB)$_4$] (3.2). A J. Young NMR tube was charged with [V(PMe$_3$)$_3$(N^{t}Bu)$_2$][Al(PFTB)$_4$] (34.7 mg, 0.025 mmol), ~ 0.7 mL of $PhCF_3$, MeCN (5 equiv., 7 μL, 0.13 mmol) and a sealed capillary filled with C_6D_6. On mixing, the solution shifted from yellow to pale yellow – nearly colorless. ^{1}H NMR ($PhCF_3$ (C_6D_6 insert), 600.1 MHz) δ 1.50 (br s, free MeCN), 1.28 (br s, equatorial *Me*CN, 1.5H), 1.25 (d, axial P*Me*$_3$, 18H, $^{2}J_{PH}$ = 7.8 Hz), 1.12 (s, N*tBu,* 18H), 0.78 (br s, free P*Me*$_3$, 9H). ^{13}C NMR ($PhCF_3$ (C_6D_6 insert), 150.9 MHz) δ 131.11 (q, C(*C*F_3)$_3$, $^{1}J_{CF}$ = 32.14 Hz), 32.38 (s, β-N*t*Bu), 14.92 (d, P*Me*$_3$, $^{1}J_{PC}$ = 22.63 Hz). The α-N*t*Bu and α-C$(CF_3)_3$ resonances could not be observed. ^{31}P{^{1}H} NMR ($PhCF_3$ (C_6D_6 insert), 242.9 MHz) δ -1.43 (vbr s, , $\Delta\nu_{1/2}$ = 2236.40 Hz). ^{51}V{^{1}H} NMR ($PhCF_3$ (C_6D_6 insert), 157.7 MHz) δ -810.15 (br s, $\Delta\nu_{1/2}$ = 939.0 Hz). IR (CaF_2, solution cell, $PhCF_3$ subtracted, cm^{-1}): Insufficient intensity above $PhCF_3$ in nitrile absorption region.

Preparation of [V(PEt)$_2$(N^{t}Bu)$_2$(CNXyl)][Al(PFTB)$_4$] (3.3). To a solution of [V(PEt)$_3$(N^{t}Bu)$_2$][Al(PFTB)$_4$] (184 mg, 0.13 mmol) in 5 mL of 1,2-dichlorethane was added 2,6-xylylisocyanide (1 equiv., 17 mg, 0.13 mmol) in 5 mL of DCE *via* cannula. After this addition, the reaction mixture was stirred for 12 h. The reaction mixture was then filtered *via* cannula and reduced until the product began to crystallize. After cooling the solution to -15 °C overnight, the title compound was afforded in 60% yield (120 mg) after decantation, as yellow-orange blades. ^{1}H NMR ($PhCF_3$ (C_6D_6 insert), 600.1 MHz) δ 2.23 (s, *Me*, 6H), 1.68 (pseudo quintet (doublet of quartets), 12H, P(*C*H_2CH$_3$)$_3$), 1.19 (s, N*tBu*, 18H), .99 (pseudo quintet (doublet of triplets, P(CH$_2$*C*H_3)$_3$, 18H). Aryl proton resonances could not be observed due to overlapping *protio*-solvent resonances. ^{13}C NMR ($PhCF_3$ (C_6D_6 insert), 150.9 MHz) δ 159.67 (s, *Ar*), 134.30 (s, *Ar*), 130.38 (q, C(*C*F_3)$_3$, $^{1}J_{CF}$ = 32.14 Hz), 118.81 (s, *Ar*), 96.57 (s, *Ar*), 70.5* (α-N*t*Bu), 32.91 (unresolved t, β-N*t*Bu), 18.46 (dd, P(*C*H_2CH$_3$)$_3$), $^{1}J_{PC}$ = 11.92 Hz, $^{3}J_{PC}$ = 9.20 Hz), 17.24 (s, Ar-*ortho-Me*), 7.57 (s, P(CH$_2$*C*H_3)$_3$). The α-C$(CF_3)_3$ resonance could not be observed.

$^{31}P\{^{1}H\}$ NMR ($PhCF_3$ (C_6D_6 insert), 242.9 MHz) δ 32.26 (vbr s, $\Delta\nu_{1/2}$ = 1803.50 Hz). $^{51}V\{^{1}H\}$ NMR ($PhCF_3$ (C_6D_6 insert), 157.7 MHz) δ -903.43 (br s, $\Delta\nu_{1/2}$ = 109.39 Hz). Anal. Calcd (%) for $C_{45}H_{57}AlF_{36}N_3O_4P_2V$: C, 35.38; H, 3.76; N, 2.75. Found: C, 35.27; H, 3.61; N, 2.70. IR (KBr, cm^{-1}): 2156 (m), 1353 (s), 1277 (s), 1220 (s), 1163 (m), 1034 (w), 832 (w), 770 (w), 754 (w), 560 (w), 537 (w), 445 (m). Mp = 110 °C (dec.).

Observation of $[V(PEt)_2(N^tBu)_2(CO)][Al(PFTB)_4]$ (3.4). A scintillation vial was charged with $Li[Al(PFTB)_4]$ (21 mg, 0.02 mmol) and ~300 μL of $PhCF_3$. To this slurry was added a solution of **3** (10 mg, 0.02 mmol) in ~150 μL in $PhCF_3$. On mixing, the solution color shifted from green to deep red. The reaction mixture was agitated *via* pipette for 5 min and transferred *via* pipette to a J. Young NMR tube charged with a sealed capillary filled with C_6D_6. The scintillation vials and pipettes were washed with a further ~150 μL of solvent and then the combined solution was transferred to the J. Young NMR tube. This NMR tube was removed from the box, attached to a line, and degassed by 3 freeze-pump-thaw cycles. Carbon monoxide (1 atm, excess) was added to the thawed solution *via* the vacuum manifold. ^{1}H NMR ($PhCF_3$ (C_6D_6 insert), 600.1 MHz) δ 1.52 (unresolved m, 12H, $P(CH_2CH_3)_3$), 1.24 (s, N*tBu*, 18H), 1.01 (unresolved m, $P(CH_2CH_3)_3$, 18H). ^{13}C NMR ($PhCF_3$ (C_6D_6 insert), 150.9 MHz) δ 131.18 (q, $C(CF_3)_3$, $^{1}J_{CF}$ = 32.29 Hz), 32.07 (s, β-N*t*Bu), 16.51 (unresolved m, $P(CH_2CH_3)_3$), 7.89 (s, $P(CH_2CH_3)_3$). The α-$C(CF_3)_3$ resonance could not be observed. $^{31}P\{^{1}H\}$ NMR ($PhCF_3$ (C_6D_6 insert), 242.9 MHz) δ 25.39 (vbr s, $\Delta\nu_{1/2}$ = 2533.94 Hz). $^{51}V\{^{1}H\}$ NMR ($PhCF_3$ (C_6D_6 insert), 157.7 MHz) δ -843.71 (pseudo d, $^{1}J_{VP}$ = 225.13 Hz, $\Delta\nu_{1/2}$ = 233.93 Hz). IR (CaF_2, solution cell, $PhCF_3$ subtracted, cm^{-1}): 2015 (s). **(8-^{13}C).** was prepared similarly. ^{13}C NMR ($PhCF_3$ (C_6D_6 insert), 150.9 MHz) δ 228.36 (br s, ^{13}CO). $^{51}V\{^{1}H\}$ NMR ($PhCF_3$ (C_6D_6 insert), 157.7 MHz) δ -845.06 (br s, $\Delta\nu_{1/2}$ = 531.05 Hz). IR (CaF_2, solution cell, $PhCF_3$ subtracted, cm^{-1}): 1970 (s).

General Remarks on the Determination of Molecular Structure by X-ray Diffraction. X-ray diffraction data were collected using either Bruker AXS three-circle or Bruker AXS Microstar kappa-geometry diffractometers with either graphite-monochromated Mo-Kα radiation (λ = 0.71073 Å) or HELIOS-monochromated Cu-Kα radiation (λ = 1.54178 Å). A single crystal of appropriate size was coated in Paratone-N oil and mounted on a Cryo loop. The loop was transferred to a diffractometer equipped with a CCD area detector,[98] centered in the beam, and cooled by an Oxford Cryostream 700 LT device. Preliminary orientation matrices and cell constants were determined by collection of three sets of 40, 5 s frames or three sets of 30, 10 s frames, followed by spot integration and least-squares refinement. COSMO was used to determine an appropriate data collection strategy, and the raw data were integrated using SAINT.[99] Cell dimensions reported were calculated from all reflections with $I > 10\ \sigma$. The data were corrected for Lorentz and polarization effects; no correction for crystal decay was applied. Data were analyzed for agreement and possible absorption using XPREP.[100] An absorption correction based on comparison of redundant and equivalent reflections was applied using SADABS.[101] Structures were solved by direct methods with the aid of successive difference Fourier maps and were refined on F^2 using the SHELXTL 5.0 software package. All non-hydrogen atoms were refined anistropically; all hydrogen

atoms were included into the model at their calculated positions and refined using a riding model. For all structures, $R_1 = \Sigma(|Fo| - |Fc|)/\Sigma(|Fo|)$; $wR_2 = [\Sigma]^{1/2}$.

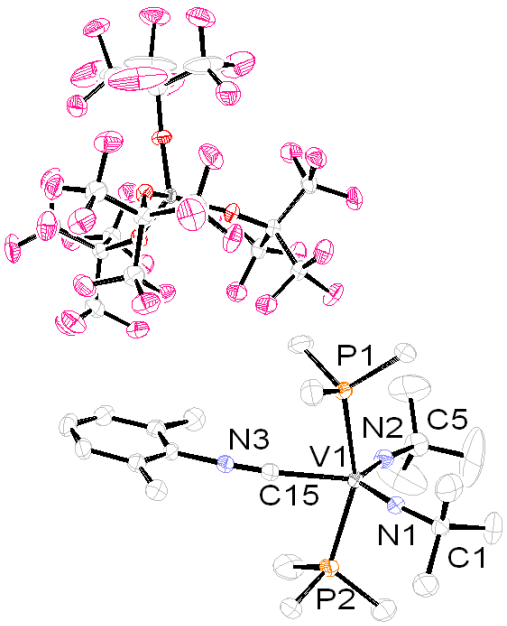

Figure 3.6: Full ORTEP representation of Complex 3.1.

Computational Methods. Density functional theory (DFT) calculations were performed using the Gaussian09 software package.[102] Geometries were fully optimized and converged to at least the default geometric convergence criteria. The use of symmetry was explicitly turned off for all computations. Frequencies were calculated analytically at 298.15 K and 1 atm in the gas phase, and structures were considered true minima if they did not exhibit imaginary modes. The hybrid functional used was B3LYP.[103-105] A LANL2DZ small core ECP and its appropriate valence basis set was used for V.[106,107] The remaining atoms were treated with Pople's 6-31G(d,p) double-ζ split-valence basis using the 5 spherical d orbital functions instead of the default.[108] Optimized structures were subjected to vibrational frequency analysis and visualized using the Gaussian09 software package. Orbital contributions were determined with pop=orbitals. Atom Cartesian coordinates are listed in Appendix E Table E.2.

Notes and References

(1) Chirik, P. J.; Knobloch, D. J.; Lobkovsky, E. *J. Am. Chem. Soc.* **2010**, *132*, 10553.
(2) Cloke, F. G. N.; Frey, A. S.; Hitchcock, P. B.; Day, I. J.; Green, J. C.; Aitken, G. *J. Am. Chem. Soc.* **2008**, *130*, 13816.
(3) Cloke, F. G. N.; Summerscales, O. T.; Hitchcock, P. B.; Green, J. C.; Hazari, N. *J. Am. Chem. Soc.* **2006**, *128*, 9602.
(4) Summerscales, O. T.; Cloke, F. G. N.; Hitchcock, P. B.; Green, J. C.; Hazari, N. *Science* **2006**, *311*, 829.
(5) Frey, A. S. P.; Cloke, F. G. N.; Coles, M. P.; Maron, L.; Davin, T. *Angew. Chem., Int. Ed.* **2011**, *50*, 6881.
(6) Martínez-Salvador, S.; Forniés, J.; Martín, A.; Menjón, B. *Chem. Eur. J.* **2011**, *17*, 8085.
(7) Maron, L.; Perrin, L.; Eisenstein, O.; Andersen, R. A. *J. Am. Chem. Soc.* **2002**, *124*, 5614.
(8) Werkema, E. L.; Maron, L.; Eisenstein, O.; Andersen, R. A. *J. Am. Chem. Soc.* **2007**, *129*, 6662.
(9) Eisenstein, O.; Maron, L.; Andersen, R. A. *Organometallics* **2009**, *28*, 3629.
(10) Williams, V. A.; Manke, D. R.; Cundari, T. R.; Wolczanski, P. T. *Inorg. Chim. Acta* **2011**, *369*, 203.
(11) Labinger, J. A.; West, N. M.; Miller, A. J. M.; Bercaw, J. E. *Coord. Chem. Rev.* **2011**, *255*, 881.
(12) Labinger, J. A.; Miller, A. J. M.; Bercaw, J. E. *J. Am. Chem. Soc.* **2010**, *132*, 3301.
(13) Labinger, J. A.; Miller, A. J. M.; Bercaw, J. E. *Organometallics* **2010**, *29*, 4499.
(14) Labinger, J. A.; Miller, A. J. M.; Bercaw, J. E. *J. Am. Chem. Soc.* **2008**, *130*, 11874.
(15) Chirik, P. J.; Knobloch, D. J.; Lobkovsky, E. *Nature Chemistry* **2010**, *2*, 30.
(16) Knobloch, D. J.,Ph.D. Thesis, Cornell University, **2011**.
(17) Arnold, J.; Tomson, N. C.; Bergman, R. G. *Organometallics* **2010**, *29*, 5010.
(18) Gianetti, T. L.; Tomson, N. C.; Arnold, J.; Bergman, R. G. *J. Am. Chem. Soc.* **2011**, *Accepted*.
(19) Demerseman, B.; Pankowski, M.; Bouquet, G.; Bigorgne, M. *J. Organometal. Chem.* **1976**, *117*, C10.
(20) Calderazzo, F.; Pampaloni, G.; Tripepi, G. *Organometallics* **1997**, *16*, 4943.
(21) Manriquez, J. M.; Mcalister, D. R.; Sanner, R. D.; Bercaw, J. E. *J. Am. Chem. Soc.* **1978**, *100*, 2716.
(22) Manriquez, J. M.; Mcalister, D. R.; Sanner, R. D.; Bercaw, J. E. *J. Am. Chem. Soc.* **1976**, *98*, 6733.
(23) Roddick, D. M.; Fryzuk, M. D.; Seidler, P. F.; Hillhouse, G. L.; Bercaw, J. E. *Organometallics* **1985**, *4*, 97.
(24) Procopio, L. J.; Carroll, P. J.; Berry, D. H. *Polyhedron* **1995**, *14*, 45.
(25) Howard, W. A.; Parkin, G.; Rheingold, A. L. *Polyhedron* **1995**, *14*, 25.
(26) Howard, W. A.; Trnka, T. M.; Parkin, G. *Organometallics* **1995**, *14*, 4037.
(27) Brackemeyer, T.; Erker, G.; Frohlich, R. *Organometallics* **1997**, *16*, 531.
(28) Antonelli, D. M.; Tjaden, E. B.; Stryker, J. M. *Organometallics* **1994**, *13*, 763.
(29) Guram, A. S.; Swenson, D. C.; Jordan, R. F. *J. Am. Chem. Soc.* **1992**, *114*, 8991.

(30) Guo, Z. Y.; Swenson, D. C.; Guram, A. S.; Jordan, R. F. *Organometallics* **1994**, *13*, 766.
(31) Reynoud, J. F.; Leboeuf, J. F.; Leblanc, J. C.; Moise, C. *Organometallics* **1986**, *5*, 1863.
(32) Burckhardt, U.; Tilley, T. D. *J. Am. Chem. Soc.* **1999**, *121*, 6328. Tilley has proposed π back-bonding from the filled π symmetry metal-Cp orbitals to CO , but argues convincingly in favor of Ta-Si σ to π* interaction in the complex presented in this communication.
(33) Brennan, J. G.; Andersen, R. A.; Robbins, J. L. *J. Am. Chem. Soc.* **1986**, *108*, 335.
(34) Parry, J.; Carmona, E.; Coles, S.; Hursthouse, M. *J. Am. Chem. Soc.* **1995**, *117*, 2649.
(35) Conejo, M. D.; Parry, J. S.; Carmona, E.; Schultz, M.; Brennann, J. G.; Beshouri, S. M.; Andersen, R. A.; Rogers, R. D.; Coles, S.; Hursthouse, M. *Chem. Eur. J.* **1999**, *5*, 3000.
(36) Foster, S. C.; Mckellar, A. R. W.; Sears, T. J. *J. Chem. Phys.* **1984**, *81*, 578.
(37) Davies, P. B.; Hamilton, P. A.; Rothwell, W. J. *J. Chem. Phys.* **1984**, *81*, 1598.
(38) Strandberg, M. W. P.; Pearsall, C. S.; Weiss, M. T. *J. Chem. Phys.* **1949**, *17*, 429.
(39) Sanchez, R.; Arrington, C.; Arrington, C. A. *J. Am. Chem. Soc.* **1989**, *111*, 9110.
(40) Selg, P.; Brintzinger, H. H.; Andersen, R. A.; Horvath, I. T. *Angew. Chem., Int. Ed.* **1995**, *34*, 791.
(41) Selg, P.; Brintzinger, H. H.; Schultz, M.; Andersen, R. A. *Organometallics* **2002**, *21*, 3100.
(42) Bodenbinder, M.; BalzerJollenbeck, G.; Willner, H.; Batchelor, R. J.; Einstein, F. W. B.; Wang, C.; Aubke, F. *Inorg. Chem.* **1996**, *35*, 82.
(43) Willner, H.; Bodenbinder, M.; Brochler, R.; Hwang, G.; Rettig, S. J.; Trotter, J.; von Ahsen, B.; Westphal, U.; Jonas, V.; Thiel, W.; Aubke, F. *J. Am. Chem. Soc.* **2001**, *123*, 588.
(44) Willner, H.; Aubke, F. *Inorg. Chem.* **1990**, *29*, 2195.
(45) Hurlburt, P. K.; Rack, J. J.; Luck, J. S.; Dec, S. F.; Webb, J. D.; Anderson, O. P.; Strauss, S. H. *J. Am. Chem. Soc.* **1994**, *116*, 10003.
(46) Hurlburt, P. K.; Rack, J. J.; Dec, S. F.; Anderson, O. P.; Strauss, S. H. *Inorg. Chem.* **1993**, *32*, 373.
(47) Hurlburt, P. K.; Anderson, O. P.; Strauss, S. H. *J. Am. Chem. Soc.* **1991**, *113*, 6277.
(48) Hakansson, M.; Jagner, S. *Inorg. Chem.* **1990**, *29*, 5241.
(49) Dewar, J. S. *Bull. Chem. Soc. Fr.* **1951**, *18*, C71.
(50) Chatt, J.; Duncanson, L. A. *J. Chem. Soc.* **1953**, 2939.
(51) La Pierre, H. S.; Arnold, J.; Toste, F. D. *Angew. Chem., Int. Ed.* **2011**, *50*, 3900.
(52) Nugent, W. A.; Mayer, J. M. *Metal-Ligand Multiple Bonds*; Wiley: New York, NY, 1988.
(53) Cockcroft, J. K.; Gibson, V. C.; Howard, J. A. K.; Poole, A. D.; Siemeling, U.; Wilson, C. *J. Chem. Soc. Chem. Comm.* **1992**, 1668.
(54) Poole, A. D.; Gibson, V. C.; Clegg, W. *J. Chem. Soc. Chem. Comm.* **1992**, 237.
(55) Glueck, D. S.; Green, J. C.; Michelman, R. I.; Wright, I. N. *Organometallics* **1992**, *11*, 4221.
(56) Williams, D. S.; Schofield, M. H.; Anhaus, J. T.; Schrock, R. R. *J. Am. Chem. Soc.* **1990**, *112*, 6728.

(57) Williams, D. S.; Schofield, M. H.; Schrock, R. R. *Organometallics* **1993**, *12*, 4560.
(58) Albright, T. A.; Burdett, J. K.; Whangbo, M. H. *Orbital Interactions in Chemistry*; John Wiley & Sons: New York, 1985.
(59) Lauher, J. W.; Hoffmann, R. *J. Am. Chem. Soc.* **1976**, *98*, 1729.
(60) Brintzinger, H. H.; Lohr, L. L.; Wong, K. L. T. *J. Am. Chem. Soc.* **1975**, *97*, 5146.
(61) Chirik, P. J. *Organometallics* **2010**, *29*, 1500.
(62) Antonio Togni; Halterman, R. L. *Metallocenes: Synthesis - Reactivity - Application*; Wiley-VCH: New York, 1998.
(63) Kealy, T. J.; Pauson, P. L. *Nature* **1951**, *168*, 1039.
(64) Wilkinson, G.; Rosenblum, M.; Whiting, M. C.; Woodward, R. B. *J. Am. Chem. Soc.* **1952**, *74*, 2125.
(65) Wigley, D. E. *Prog. Inorg. Chem.* **1994**, 239.
(66) Dyer, P. W.; Gibson, V. C.; Howard, J. A. K.; Whittle, B.; Wilson, C. *J. Chem. Soc. Chem. Comm.* **1992**, 1666.
(67) Khalimon, A. Y.; Simionescu, R.; Kuzmina, L. G.; Howard, J. A. K.; Nikonov, G. I. *Angew. Chem., Int. Edit.* **2008**, *47*, 7701.
(68) Nikonov, G. I.; Khalimon, A. Y.; Simionescu, R. *J. Am. Chem. Soc.* **2011**, *133*, 7033.
(69) Mountford, P.; Ignatov, S. K.; Khalimon, A. Y.; Rees, N. H.; Razuvaev, A. G.; Nikonov, G. I. *Inorg. Chem.* **2009**, *48*, 9605.
(70) Green, J. C.; Khalimon, A. Y.; Holland, J. P.; Kowalczyk, R. M.; McInnes, E. J. L.; Mountford, P.; Nikonov, G. I. *Inorg. Chem.* **2008**, *47*, 999.
(71) Ignatov, S. K.; Rees, N. H.; Dubberley, S. R.; Razuvaev, A. G.; Mountford, P.; Nikonov, G. I. *Chem. Comm.* **2004**, 952.
(72) DeWith, J.; Horton, A. D. *Angew Chem Int Edit* **1993**, *32*, 903.
(73) Schaller, C. P.; Wolczanski, P. T. *Inorg. Chem.* **1993**, *32*, 131.
(74) Toste, F. D.; Nolin, K. A.; Ahn, R. W.; Kobayashi, Y.; Kennedy-Smith, J. J. *Chem. Eur. J.* **2010**, *16*, 9555.
(75) Nolin, K. A.; Krumper, J. R.; Pluth, M. D.; Bergman, R. G.; Toste, F. D. *J. Am. Chem. Soc.* **2007**, *129*, 14684.
(76) Nolin, K. A.; Ahn, R. W.; Toste, F. D. *J. Am. Chem. Soc.* **2005**, *127*, 12462.
(77) Kennedy-Smith, J. J.; Nolin, K. A.; Gunterman, H. P.; Toste, F. D. *J. Am. Chem. Soc.* **2003**, *125*, 4056.
(78) Hoyt, H. M.; Michael, F. E.; Bergman, R. G. *J. Am. Chem. Soc.* **2004**, *126*, 1018.
(79) Tomson, N. C.; Arnold, J.; Bergman, R. G. *Organometallics* **2010**, *29*, 2926.
(80) Walsh, P. J.; Hollander, F. J.; Bergman, R. G. *J. Am. Chem. Soc.* **1988**, *110*, 8729.
(81) Addison, A. W.; Rao, T. N.; Reedijk, J.; Vanrijn, J.; Verschoor, G. C. *J. Chem. Soc. Dalton Trans.* **1984**, 1349.
(82) Chao, Y. W.; Wexler, P. A.; Wigley, D. E. *Inorg. Chem.* **1990**, *29*, 4592.
(83) DeWith, J.; Horton, A. D.; Orpen, A. G. *Organometallics* **1990**, *9*, 2207.
(84) DeWith, J.; Horton, A. D.; Orpen, A. G. *Organometallics* **1993**, *12*, 1493.
(85) Krossing, I. *Chem: Eur. J.* **2001**, *7*, 490.
(86) Helm, L.; Bodizs, G.; Raabe, I.; Scopelliti, R.; Krossing, I. *Dalton Trans.* **2009**, 5137, and references therein.
(87) Preuss, F.; Towae, W. *Z. Natforsch. B: Anorg. Allg. Chem.* **1981**, *36*, 1130.

(88) Massa, W.; Wocadlo, S.; Lotz, S.; Dehnicke, K. *Z. Anorg. Allg. Chem.* **1990**, *589*, 79.
(89) Kilgore, U. J.; Karty, J. A.; Pink, M.; Gao, X.; Mindiola, D. J. *Angew. Chem. Int. Edit.* **2009**, *48*, 2394.
(90) Mathieson, T.; Schier, A.; Schmidbaur, H. *J. Chem. Soc. Dalton Trans.* **2001**, 1196.
(91) Carofiglio, T.; Floriani, C.; Chiesivilla, A.; Guastini, C. *Inorg. Chem.* **1989**, *28*, 4417.
(92) Ellis, J. E.; Allen, J. M. *J. Organometal. Chem.* **2008**, *693*, 1536.
(93) Ahlers, W.; Erker, G.; Frohlich, R. *J. Organometal. Chem.* **1998**, *571*, 83.
(94) Tolman, C. A. *Chem. Rev.* **1977**, *77*, 313.
(95) Schafer, D. F.; Wolczanski, P. T. *J. Am. Chem. Soc.* **1998**, *120*, 4881.
(96) Toomey, H. E.; Pun, D.; Veiros, L. F.; Chirik, P. J. *Organometallics* **2008**, *27*, 872.
(97) Andersen, R. A. *Personal Communication.* H_2 addition to $Cp^*_2Ti(N^tBu)$
(98) SMART: Area-Detector Software package Bruker Analytical X-ray Systems, Inc, Madison, WI, 2001-2003.
(99) SAINT: SAX Area-Detector Integration Program, V6.40 Bruker Analytical X-ray Systems, Inc, Madison, WI, 2003.
(100) XPREP Bruker Analytical X-ray Systems, Inc, Madison, WI, 2003.
(101) SADABS: Bruker-Nonius Area Detector Scaling and Absorption V2.05 Bruker Analytical X-ray Systems, Inc, Madison, WI, 2003.
(102) Gaussian 09, Revision **A.1**, Frisch, M. J.; Trucks, G. W.; Schlegel, H. B.; Scuseria, G. E.; Robb, M. A.; Cheeseman, J. R.; Scalmani, G.; Barone, V.; Mennucci, B.; Petersson, G. A.; Nakatsuji, H.; Caricato, M.; Li, X.; Hratchian, H. P.; Izmaylov, A. F.; Bloino, J.; Zheng, G.; Sonnenberg, J. L.; Hada, M.; Ehara, M.; Toyota, K.; Fukuda, R.; Hasegawa, J.; Ishida, M.; Nakajima, T.; Honda, Y.; Kitao, O.; Nakai, H.; Vreven, T.; Montgomery, Jr., J. A.; Peralta, J. E.; Ogliaro, F.; Bearpark, M.; Heyd, J. J.; Brothers, E.; Kudin, K. N.; Staroverov, V. N.; Kobayashi, R.; Normand, J.; Raghavachari, K.; Rendell, A.; Burant, J. C.; Iyengar, S. S.; Tomasi, J.; Cossi, M.; Rega, N.; Millam, N. J.; Klene, M.; Knox, J. E.; Cross, J. B.; Bakken, V.; Adamo, C.; Jaramillo, J.; Gomperts, R.; Stratmann, R. E.; Yazyev, O.; Austin, A. J.; Cammi, R.; Pomelli, C.; Ochterski, J. W.; Martin, R. L.; Morokuma, K.; Zakrzewski, V. G.; Voth, G. A.; Salvador, P.; Dannenberg, J. J.; Dapprich, S.; Daniels, A. D.; Farkas, Ö.; Foresman, J. B.; Ortiz, J. V.; Cioslowski, J.; Fox, D. J. Gaussian, Inc., Wallingford CT, 2009.
(103) Becke, A. D. *Phys. Rev. A* **1988**, *38*, 3098.
(104) Lee, C. T.; Yang, W. T.; Parr, R. G. *Phys. Rev. B* **1988**, *37*, 785.
(105) Stephens, P. J.; Devlin, F. J.; Chabalowski, C. F.; Frisch, M. J. *J. Phys. Chem.* **1994**, *98*, 11623.
(106) Dunning Jr., T. H.; Hay, P. J. In *Modern Theoretical Chemistry*; Schaefer III, H. F., Ed.; Plenum: New York, 1976; Vol. 3, p 1-28.
(107) Hehre, W. J.; Ditchfie.R; Pople, J. A. *J. Chem. Phys.* **1972**, *56*, 2257.
(108) Harihara, P. C.; Pople, J. A. *Theo. Chem. Acta* **1973**, *28*, 213.

Appendix A:

PHIP NMR Identification of the Product of [1,2]-Addition of *para*-Dihydrogen to $[V(PMe_3)_3(N\textit{t}Bu)_2]^+$

Introduction

PHIP NMR is useful mechanistic tool that provides definitive evidence for pairwise addition of dihydrogen to unsaturated organic substrates and inorganic complexes.[1,2] In order to observe PHIP phenomena several chemical constraints must be observed: (1) dihydrogen must be enriched in the para spin state, (2) it must add in a pairwise fashion such that spin correlation is maintained between the transferred protons, and (3) the resultant protons in the substrate or complex must be magnetically distinct and remain *J* coupled.[2,3] If these requirements are met and transfer of dihydrogen occurs faster than proton relaxation, then non-Boltzman population of spin states will result and enhanced absorption and emission lines in the NMR spectra will be observed. This technique has so far primarily been used to interrogate late metal complexes that add dihydrogen *via* a three centered, oxidative addition mechanism (*e.g.* Rh,[4-7] Ir,[8-10] Ru,[11] and Pt[12]). A single example of the addition of PHIP experiment with a low-valent early metal (Ta) has been published.[3] Observation of dihydrogen activation via addition to metal-ligand multiple bonds with *para*-dihydrogen has been limited to a solid state NMR study of ZnO.[13] The reactivity of **1.10** with dihydrogen presents an opportunity to employ PHIP NMR spectroscopy to study dihydrogen activation by an early metal, metal-ligand multiple bond complex and gather further insight into the mechanism of dihydrogen activation by **1.10**.

Results and Discussion

As described in Chapter 2, treatment of a solution of **1.10** in $PhCF_3$ with 1 atm of H_2 resulted in recovery of only starting material after workup. However, comparison ^1H VT NMRs (20 °C to 80 °C, in 10° intervals) of complex **1.10** under N_2 and H_2 atmospheres revealed that, under H_2, **1.10** is in equilibrium with at least one other species even at room temperature.[6] The loss of symmetry equivalence of the imido *tert*-butyl resonances (from 1.09 ppm to 1.12 ppm (imide) and 1.19 ppm (amide)) in this new complex suggests that reaction with H_2 proceeds via [1,2]-, rather than [3+2]-addition, and generates a vanadium hydrido amido complex (**A**) (Scheme A.1).

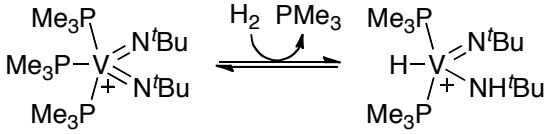

1.10 **A**

Scheme A.1: [1,2]-addition of dihydrogen by **1.10**.

This hypothesis was confirmed by PHIP-NMR. Initial attempts to observe the hydride, **A**, by *in situ* IR were complicated by the inability to generate a sufficient concentration of the intermediate, as were attempts to observe it by ^1H NMR (presumably further complicated by coupling to ^{51}V (I =7/2)). However, amplification of the V-*H* and N-*H* resonances is observed under PASADENA conditions. Warming a frozen solution of **1** under *p*-H_2 (90% *p*-H_2 est.) to 60°C inside a 600 MHz spectrometer and allowing the

spectrometer to cool to room temperature (22°C) over 20 minutes revealed two amplified signals in the ^{1}H NMR spectra (centered at 3.65 ppm (V-*H*) and 10.79 ppm (N-*H*))

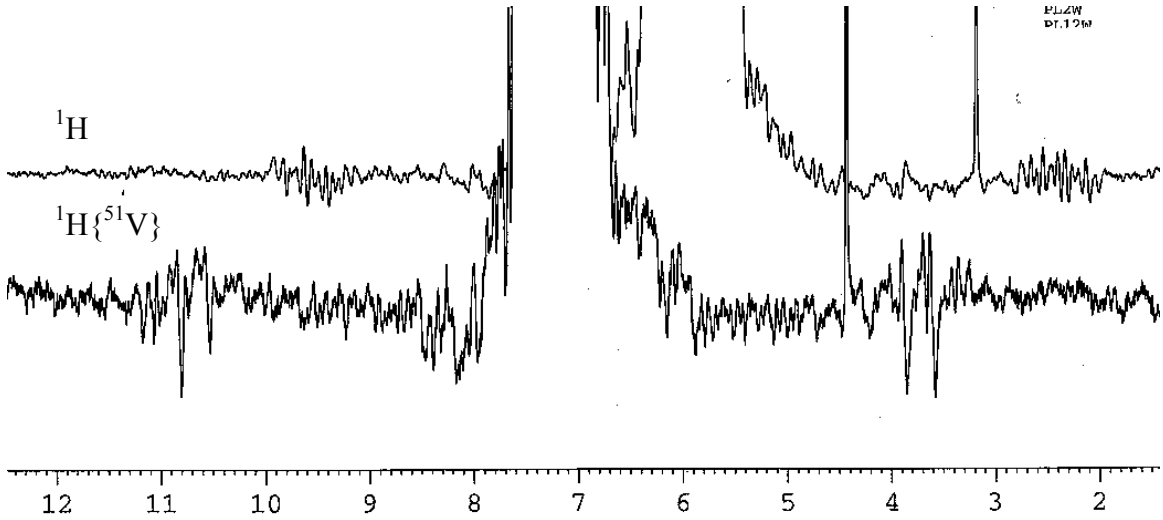

Figure A.1: Stack Plot of ^{1}H and ^{1}H{^{51}V} PHIP-NMR spectra.

(Figure A.1). These signals are broad and express the expected phase/anti-phase pattern. However, as the separation between peaks is on the order of scalar coupling, there is considerable destructive interference. While the ^{1}H{^{51}V} spectrum is considerably simplified, destructive interference persists due to ^{31}P coupling. The large change in the observed coupling in the ^{1}H{^{51}V} spectra clearly indicates that these proton resonances are coupled to V. The chemical shifts observed in these experiments also correlate well with those predicted by DFT calculations, which give for intermediate **A** the V-*H* resonance at 4.03 ppm and the N-*H* resonance at 11.64 ppm referenced to TMS (Figure A.2).

Conclusion

This study provides preliminary evidence that the catalyst **1.10** activates dihydrogen via [1,2]- versus [3+2]-addition, and it is also the first example of the application of PHIP NMR spectroscopy to the study of metal-ligand multiple bond reactivity with dihydrogen. The low enhancement of the signals observed in this case is not unusual for the study metal hydrides generated in equilibrium under para-hydrogen,[14] but the lack of further direct experimental evidence makes definitive assignment difficult. Several approaches have been employed to increase the concentration of the proposed intermediate **A** (Scheme A.1), including the use of Lewis acids BPh_3, $B(Ar^F)_3$, and TlOtf and $^tBuN_3$, in order to consume free PMe_3 under reaction conditions and shift the equilibrium to **A**. Alternatively, the four coordinate cation **1.11** was examined for reactivity with dihydrogen and *para*-dihydrogen. Unfortunately, this complex suffers from competitive, intramolecular decomposition pathways under reaction conditions (see Chapter 1 for synthetic details). Further work on this system should take three paths: (1) use of the heavier group 5 analogs of **1.10**, (2) the use of less reactive phosphine ligands than PEt_3 in complex **1.11**, possibly 1-methyl-phospholane, and (3) the examination of

related systems in which the equilibrium lies toward the hydride and possess less complex NMR active nuclei, such as $Cp^*_2Ti(NPh)$.[15] The latter approach would serve to demonstrate the applicability of PHIP NMR to the study of [1,2]-addition reactions which presumably proceed through a concerted, four-membered transition state.

Experimental

PHIP-PASADENA NMR Experiments:

Parahydrogen Production: A hydrogen mixture enriched in the para spin state (90% *p*-H_2) was produced by passing pure hydrogen gas through a Cu cell, packed with FeO(OH) and immersed in a liquid He-filled dewar. The ortho:para ratio was verified by measuring the NMR signal intensities of H_2 in a cell packed with porous alumina (Al_2O_3).[16,17] An aluminum cylinder was filled with the para-enriched H_2 to 40 psig.

NMR Experiments: A J. Young tube was filled with 2.5 mg of **1.10** (.0018 mmol) in 600 μL of $C_6H_5CF_3$ with a C_6D_6 locking standard inside of a glass capillary tube. The lock and pulse calibration were determined for a Bruker AV-600 probe at 60° C (Typical excitation pulses (π/4) were 6.55 μs in duration). The tube was then removed from the probe and fitted to a Schlenk line and freeze-pumped-thawed three times and filled with 1 atm of parahydrogen-enriched H_2. While keeping the tube chilled at -196 °C in liquid N_2, the NMR tube was carried to the spectrometer and then quickly transferred to the previously warmed probe. After allowing the tube to thermally equilibrate (5 min), double scan ^1H NMR experiments were acquired regularly at 30 s intervals (over the course of ten minutes). At 60° C no enhanced signals were observed. However, on cooling, the probe with the tube inside to room temperature (22° C) over 20 minutes revealed two enhanced signals centered at 3.65 ppm and 10.80 ppm in the ^1H spectrum. Acquiring a $^1H\{^{51}V\}$ spectrum simplified the observed phase/anti-phase pattern to two pseudo doublets (coupling to ^{31}P), but destructive interference was still significant.

Computational Methods

All structures and energies were calculated using the Gaussian03[18] suite of programs and are reported in Chapter 2. Geometry optimizations were converged to at least the default geometric convergence criteria. The use of symmetry was explicitly turned off for all computations. Frequencies were calculated analytically at 298.15 K and 1 atm, and structures were considered true minima if they did not exhibit imaginary modes. Calculated transition state structures exhibited only a single imaginary mode. IRC calculations were performed to ensure the transition state geometries connected the reactant and the product. The hybrid functional used was B3LYP.[17-19] A LANL2DZ small core ECP and its appropriate valence basis set was used for V.[20] The remaining atoms were treated with Pople's 6-31G(d,p) double-ζ split-valence basis using the 5 spherical d orbital functions instead of the default.[21,22] NMR shielding calculations were performed with the GIAO method and referenced to TMS.

Figure A.2: DFT NMR Calculations in $CDCl_3$ referenced to TMS.

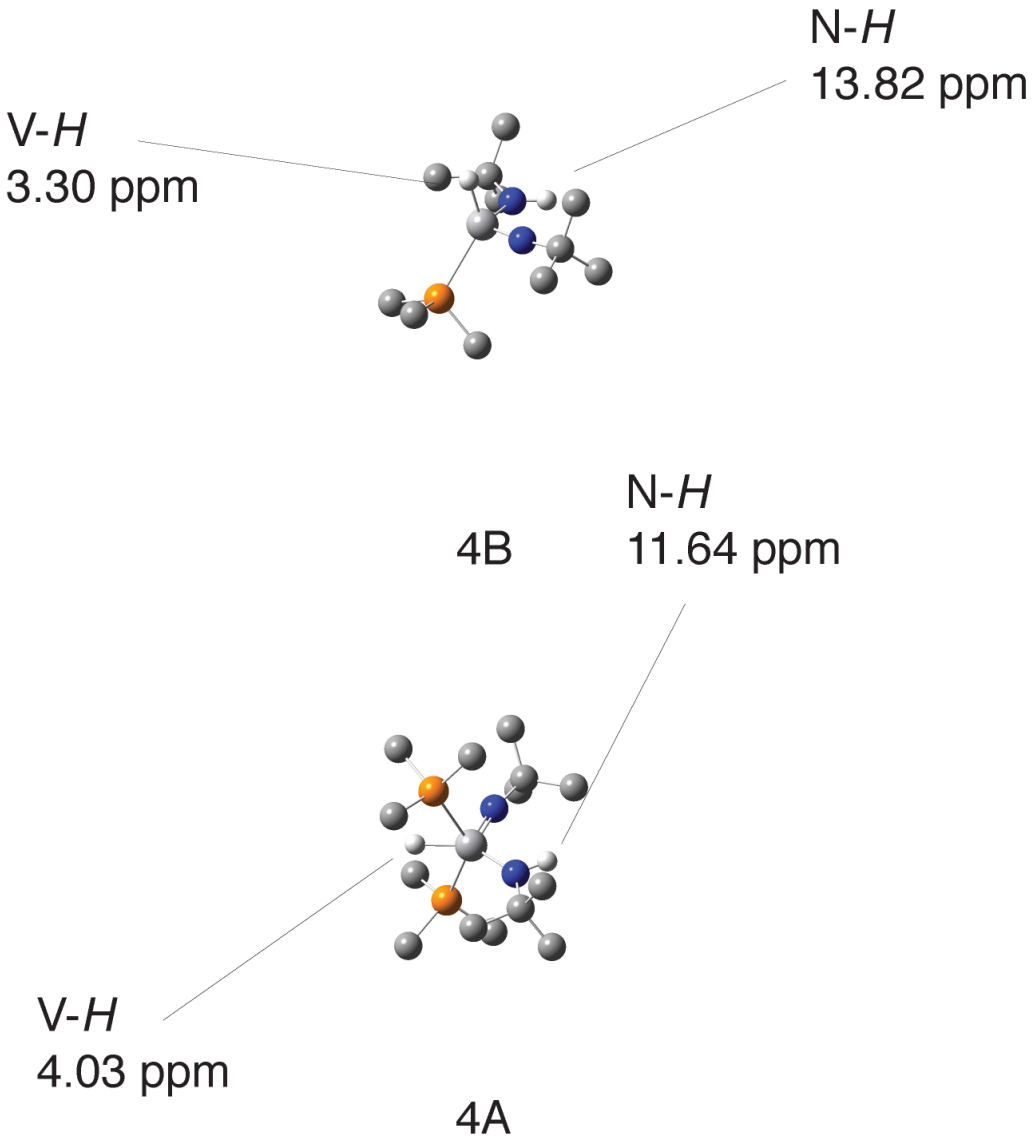

Notes and References

(1) *Handbook of Homogeneous Hydrogenation*; Wiley-VCH Verlag GmbH & Co. KGaA: Weinheim, 2007.
(2) Blazina, D.; Duckett, S. B.; Dunne, J. P.; Godard, C. *Dalton Trans.* **2004**, 2601.
(3) Millar, S. P.; Zubris, D. L.; Bercaw, J. E.; Eisenberg, R. *J. Am. Chem. Soc.* **1998**, *120*, 5329.
(4) Bowers, C. R.; Weitekamp, D. P. *J. Am. Chem. Soc.* **1987**, *109*, 5541.
(5) Duckett, S. B.; Eisenberg, R. *J. Am. Chem. Soc.* **1993**, *115*, 5292.
(6) Duckett, S. B.; Newell, C. L.; Eisenberg, R. *J. Am. Chem. Soc.* **1997**, *119*, 2068.
(7) Duckett, S. B.; Newell, C. L.; Eisenberg, R. *J. Am. Chem. Soc.* **1994**, *116*, 10548.
(8) Eisenschmid, T. C.; Kirss, R. U.; Deutsch, P. P.; Hommeltoft, S. I.; Eisenberg, R.; Bargon, J.; Lawler, R. G.; Balch, A. L. *J. Am. Chem. Soc.* **1987**, *109*, 8089.
(9) Eisenberg, R.; Eisenschmid, T. C.; Mcdonald, J.; Lawler, R. G. *J. Am. Chem. Soc.* **1989**, *111*, 7267.
(10) Sleigh, C. J.; Duckett, S. B.; Messerle, B. A. *J. Chem. Soc. Chem. Comm.* **1996**, 2395.
(11) Duckett, S. B.; Mawby, R. J.; Partridge, M. G. *J. Chem. Soc. Chem. Comm.* **1996**, 383.
(12) Jang, M.; Duckett, S. B.; Eisenberg, R. *Organometallics* **1996**, *15*, 2863.
(13) Carson, P. J.; Bowers, C. R.; Weitekamp, D. P. *J. Am. Chem. Soc.* **2001**, *123*, 11821.
(14) Hasnip, S. K.; Duckett, S. B.; Sleigh, C. J.; Taylor, D. R.; Barlow, G. K.; Taylor, M. J. *Chem. Comm.* **1999**, 1717.
(15) Andersen, R. A. Private Communication.
(16) Koptyug, I. V.; Kovtunov, K. V.; Burt, S. R.; Anwar, M. S.; Hilty, C.; Han, S. I.; Pines, A.; Sagdeev, R. Z. *J. Am. Chem. Soc.* **2007**, *129*, 5580.
(17) Anwar, M. S.; Bouchard, L. S.; Kovtunov, K. V.; Burt, S. R.; Koptyug, I. V.; Sagdeev, R. Z.; Pines, A. *Angew. Chem., Int. Ed.* **2007**, *46*, 4064.
(18) Gaussian 03 Frisch, M. J.; Trucks, G. W.; Schlegel, H. B.; Scuseria, G. E.; Robb, M. A.; Cheeseman, J. R.; Scalmani, G.; Barone, V.; Mennucci, B.; Petersson, G. A.; Nakatsuji, H.; Caricato, M.; Li, X.; Hratchian, H. P.; Izmaylov, A. F.; Bloino, J.; Zheng, G.; Sonnenberg, J. L.; Hada, M.; Ehara, M.; Toyota, K.; Fukuda, R.; Hasegawa, J.; Ishida, M.; Nakajima, T.; Honda, Y.; Kitao, O.; Nakai, H.; Vreven, T.; Montgomery, J., J. A.; Peralta, J. E.; Ogliaro, F.; Bearpark, M.; Heyd, J. J.; Brothers, E.; Kudin, K. N.; Staroverov, V. N.; Kobayashi, R.; Normand, J.; Raghavachari, K.; Rendell, A.; Burant, J. C.; Iyengar, S. S.; Tomasi, J.; Cossi, M. R.; Millam, N. J.; Klene, M.; E., K. J.; Cross, J. B.; Bakken, V.; Adamo, C.; Jaramillo, J.; Gomperts, R. E.; Stratmann, O.; Yazyev, A. J.; Austin, R.; Cammi, C.; Pomelli, J. W.; Ochterski, R.; Martin, R. L.; Morokuma, K.; Zakrzewski, V. G.; Voth, G. A.; Salvador, P.; Dannenberg, J. J.; Dapprich, S.; Daniels, A. D.; Farkas, O.; Foresman, J. B.; Ortiz, J. V., Cioslowski, J., and Fox, D. J. Gaussian, Inc., Wallingford CT, 2009.
(17) Becke, A. D. *Phys. Rev. A* **1988**, *38*, 3098.
(18) Lee, C. T.; Yang, W. T.; Parr, R. G. *Phys. Rev. B* **1988**, *37*, 785.
(19) Stephens, P. J.; Devlin, F. J.; Chabalowski, C. F.; Frisch, M. J. *J. Phys. Chem.* **1994**, *98*, 11623.

(20) Dunning Jr., T. H.; Hay, P. J. In *Modern Theoretical Chemistry*; Schaefer III, H. F., Ed.; Plenum: New York, 1976; Vol. 3, p 1-28.
(21) Hehre, W. J.; Ditchfie.R; Pople, J. A. *J. Chem. Phys.* **1972**, *56*, 2257.
(22) Harihara, P. C.; Pople, J. A. *Theo. Chem. Acta* **1973**, *28*, 213.

Appendix B:

Synthesis of a Three-Coordinate Vanadium Bisimide

Introduction

Three coordinate complexes incorporating homoleptic, hard donors ligands (*i.e.* C, N, or O) have played a central role in organometallic chemistry since the field was developed starting in the 1960's by Burger, Wannagat, Bradley, Lappert, and Andersen.[1] In fact, examples of dramatic reactivity with small molecules continue to be reported. However, isolated, 3-coordinate complexes possessing one,[2] two,[3-6] or even three[7-9] metal-ligand multiple bonds remain rare. In order to explore the reactivity of a low coordinate analog of the phosphine supported cationic vanadium bisimides presented in Chapters 1-3, we sought a sterically bulky ligand in order to kinetically stabilize the bisimide core. Arduengo carbenes have received considerable attention for their ability to stabilize low-coordinate late-metal species and have been widely applied in the development catalytic transformations that require low coordinate metal centers. On the other hand, N-heterocyclic carbene (NHC) complexes of the early metals are uncommon, and few vanadium NHC complexes have been reported. However, we hypothesized that the planarity at the carbene base would facilitate TMSCl elimination from **1.2** in contrast to the large cone angle phophines. Herein we report the synthesis of an IPr (1,3-bis(2,6-diisopropylphenyl)imidazol-2-ylidene) complex of a vanadium bisimide and the observation of a three coordinate bisimide formed by chloride abstraction.

Results and Discussion

Heating a solution of **1.1** and IPr in toluene overnight at 80 °C induces the elimination of TMSCl to give the IPr stabilized bisimide **B.1** (Scheme B.1). Complex **B.1** is defined by a broad ^{51}V NMR resonance at -340.61 ppm. In the solid state, **B.1** is essentially tetrahedral with quite bent imide V-N-C angles of 159.89(18)° and 158.68(17)°. The vanadium imide bond lengths are slightly contracted from those of the five coordinate analogs at 1.667(2) Å and 1.6747(19) Å, as is the V-Cl bond at 2.2776(8) Å (Figure B.1 and Table B.1). Treating **B.1** in PhCl with Li[Al(PFTB)$_4$] results in a shift in color from red to deep red and a distinctive change in the proton NMR with a dramatic upfield shift in the *tert*-butyl resonances to 0.83 ppm. The ^{51}V NMR shifts slightly to -298.65 ppm and broadens dramatically. All attempts to isolate **B.2** have failed to date. In particular, it should be noted that treating **B.2** with diethyl ether leads to bleaching and decomposition to as of yet unidentified products. This transformation may be due to cleavage of diethyl ether C-O and C-H bonds, as has been noted for a few other early metal complexes (Scheme B.1). Further reactivity studies should be directed towards determining the reactivity with ethers as well as unsaturated substrates such as ethylene and alkynes.

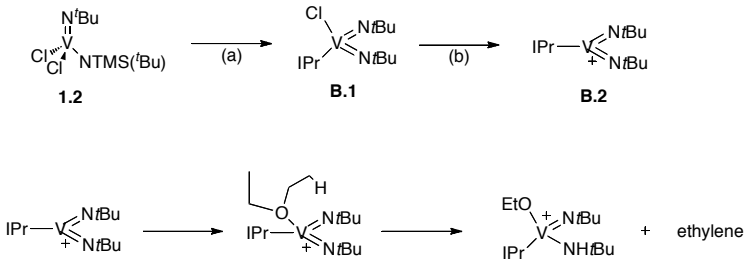

Scheme B.1: Synthesis of B.1 and B.2 and potential decomposition in diethyl ether.

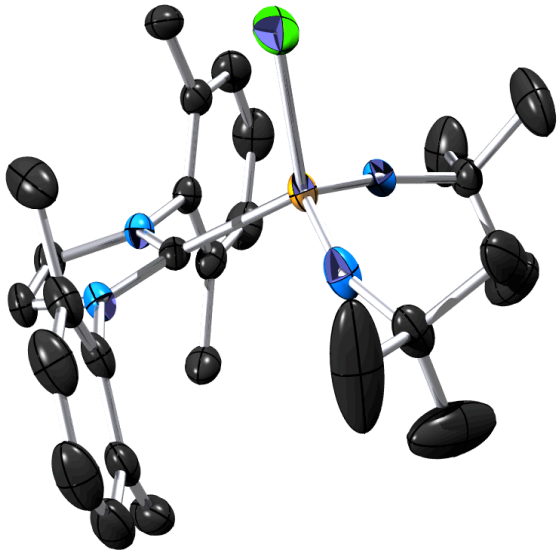

Figure B.1: Molecular structure of **B.1.** Thermal ellipsoids are drawn at 50% probability level. Hydrogen atoms and isopropyl methyl carbons have been removed for clarity. Selected bond lengths (Å) and angles (deg): C(5)-V(1), 2.154(2); N(1)-V(1), 1.667(2), N(4)-V(1), 1.6747(19); Cl(1)-V(1), 2.2776(8); N(2)-C(5)-V(1), 127.77(15); N(3)-C(5)-V(1), 126.95(15); C(1)-N(1)-V(1), 159.89(18); C(32)-N(4)-V(1), 158.68(17); N(1)-V(1)-N(4), 113.51(10); N(1)-V(1)-C(5), 108.05(9); N(4)-V(1)-C(5), 107.49(9); N(1)-V(1)-Cl(1), 107.58(8); N(4)-V(1)-Cl(1), 108.59(7); C(5)-V(1)-Cl(1), 111.69(6).

Experimental Section:

General Considerations. Unless otherwise noted, all reactions were performed using standard Schlenk line techniques or in an MBraun inert atmosphere box under an atmosphere of argon or dinitrogen (<1 ppm O_2/H_2O), respectively. All glassware and cannulae were stored in an oven at ca. 425 K. Pentane, diethyl ether, toluene, tetrahydrofuran, dichloromethane, and dimethoxyethane were purified by passage through a column of activated alumina and degassed prior to use. C_6D_6 was vacuum-transferred from sodium/benzophenone and degassed with three freeze-pump-thaw cycles. 1,2-$C_2D_4Cl_2$ was vacuum transferred from CaH_2 and degassed with three freeze-pump-thaw cycles. NMR spectra were recorded on Bruker AV-300, AVB-400, AVQ-400, AV-500, and AV-600 spectrometers. ^{1}H and ^{13}C chemical shifts are given relative to

residual solvent peaks. ^{31}P, ^{51}V, ^{19}F, and ^{27}Al chemical shifts were referenced to external standards ($P(OMe)_3$ at 1.67 ppm, $VOCl_3$ at 0.00 ppm, $CFCl_3$ at 0.00 ppm, and 1M $Al(NO_3)_3$ in H_2O/D_2O at 0 ppm, respectively). Proton and carbon NMR assignments were routinely confirmed by ^1H-^1H (COSY) or ^1H-^{13}C (HSQC and HMBC) experiments as necessary. Infrared (IR) samples were prepared as Nujol mulls and were taken between KBr disks. The following chemicals were purified prior to use: PhCl, was distilled from P_2O_5 and degassed by bubbling argon through the liquid for 15 minutes. IPrHCl and IPr were prepared using standard literature procedures. All other reagents were acquired from commercial sources and used as received. The X-ray structural determination was performed at CHEXRAY, University of California, Berkeley, on a Bruker SMART APEX diffractometer.

Preparation IPrVCl(N^{t}Bu)$_2$ (B.1) To a solution of VCl_2(N*t*Bu)(NTMS(^{t}Bu) (337 mg, 1.0 mmol) in 10 mL of toluene was added IPr (1.0 equiv., 389 mg) in 5 mL toluene. The reaction mixture was heated to 80 °C for 16 h. It was cooled and reduced to a residue *in vacuo* and extracted with toluene. The solution was transferred to a Schlenk tube *via* a filter cannula, and the filtrate was reduced until the product began crystallize and less than 1 mL solvent remained. The remaining residue and solution was heated to reflux, dissolving all solid material, and allowed to cool. The product was afforded in 47 % (300 mg) in two crops. X-ray quality crystals were grown from hot toluene. ^1H NMR (C_6D_6, 400 MHz, 298 K) δ 7.22 (m, *Ar*, 2H), 7.14 (s, *Ar*, 2H), 7.12 (s, *Ar*, 2H), 6.46 (s, NHC, 2H), 2.86 (septet, *CH*(CH_3)$_2$, 4H, *J* = 6.8 Hz), 1.50 (d, CH(*CH$_3$*)$_2$, 12H, *J* = 6.8 Hz), 1.18 (s, *tBu*, 18H), 1.04 (d, , CH(*CH$_3$*)$_2$, 12H, *J* = 6.8 Hz). $^{13}C\{^1H\}$ NMR (C_6D_6, 100.62 MHz, 298 K) δ 146.44 (s, *Ar*), 138.13 (s, *Ar*), 130.66 (s, *Ar*), 125.10 (s, *Ar*), 124.75 (s, *NHC*), 33.17 (s, β-*t*Bu), 29.24 (s, CH(CH_3)$_2$), 25.80 (s, CH(CH_3)$_2$), 24.43 (s, CH(CH_3)$_2$). The NHC carbene carbon and α-*t*Bu carbon resonances could not be located. $^{51}V\{^1H\}$ NMR (C_6D_6, 105.2 MHz, 298 K) δ -340.61 (br s, $\Delta\nu_{1/2}$ = 1418.03 Hz).

Observation of [IPrV(N^{t}Bu)$_2$][Al(PFTB)$_4$] (B.2). To a solution of IPrVCl(N^{t}Bu)$_2$ (B.1) (6 mg, .01 mmol) in 700 μL of PhCl was added Li[Al(PFTB)$_4$] (1.0 equiv., 9.7 mg). The reaction mixture was transferred via pipette to a J. Young NMR tube along with a sealed C_6D_6 capillary. ^1H NMR (C_6D_6, 400 MHz, 298 K) δ 2.38 (unresolved septet, *CH*(CH_3)$_2$, 4H), 1.12 (d, CH(*CH$_3$*)$_2$, 12H, *J* = 6.4 Hz), 0.85 (d, CH(*CH$_3$*)$_2$, 12H, *J* = 6.4 Hz), 0.83 (s, *tBu*, 18H). Aryl region was obscured by protio-solvent. $^{51}V\{^1H\}$ NMR (C_6D_6, 105.2 MHz, 298 K) δ -298.65 (br s, $\Delta\nu_{1/2}$ = 5402.03 Hz).

General Remarks on the Determination of Molecular Structure by X-ray Diffraction. X-ray diffraction data were collected using either Bruker AXS three-circle or Bruker AXS Microstar kappa-geometry diffractometers with either graphite-monochromated Mo-Kα radiation (λ = 0.71073 Å) or HELIOS-monochromated Cu-Kα radiation (λ = 1.54178 Å). A single crystal of appropriate size was coated in Paratone-N oil and mounted on a Cryo loop. The loop was transferred to a diffractometer equipped with a CCD area detector,[103] centered in the beam, and cooled by an Oxford Cryostream 700 LT device. Preliminary orientation matrices and cell constants were determined by collection of three sets of 40, 5 s frames or three sets of 30, 10 s frames, followed by spot integration and least-squares refinement. COSMO was used to determine an appropriate

data collection strategy, and the raw data were integrated using SAINT.[104] Cell dimensions reported were calculated from all reflections with $I > 10\ \sigma$. The data were corrected for Lorentz and polarization effects; no correction for crystal decay was applied. Data were analyzed for agreement and possible absorption using XPREP.[105] An absorption correction based on comparison of redundant and equivalent reflections was applied using SADABS.[106] Structures were solved by direct methods with the aid of successive difference Fourier maps and were refined on F^2 using the SHELXTL 5.0 software package. All non-hydrogen atoms were refined anistropically; all hydrogen atoms were included into the model at their calculated positions and refined using a riding model. For all structures, $R_1 = \Sigma(|Fo| - |Fc|)/\Sigma(|Fo|)$; $wR_2 = [\Sigma]^{1/2}$. See Table B.1 for integration and refinement details.

Table B.1: Crystal and Refinement Data for complex **B.1**.

	B.1
empirical formula	$C_{35}H_{54}ClN_4V$
formula weight	617.21
temp., K	138(2)
λ	0.71073
crystal system	monoclinic
space group	$P2_1/c$
a, Å	9.898(2)
b, Å	17.685(4)
c, Å	20.758(4)
α, deg	90
β, deg	98.149(3)
γ, deg	90
volume, $Å^3$	3596.9(13)
Z	4
d_{calc}, mg/m^3	1.140
F_{000}	1328
μ, mm^{-1}	0.377
no. rflns measd	49280
no. indep reflns	7152
R_{int}	0.0433
Restr/param	0/384
R_1, wR_2 $[I > 2\sigma(I)]$	0.0453, 0.1093
R_1 (all data)	0.0756
GOF	1.039
Resid peak, hole (e-/$Å^3$)	0.612, -0.360

Notes and References

(1) Cummins, C. C.; John Wiley & Sons, INc.: New York, 1998; Vol. 47.
(2) Warren, T. H.; Dai, X. L.; Kapoor, P. *J. Am. Chem. Soc.* **2004**, *126*, 4798.
(3) Power, P. P.; Ni, C. B.; Fettinger, J. C.; Long, G. J.; Brynda, M. *Chem. Commun.* **2008**, 6045.
(4) Schafer, D. F.; Wolczanski, P. T. *J. Am. Chem. Soc.* **1998**, *120*, 4881.
(5) Schaller, C. P.; Wolczanski, P. T. *Inorg. Chem.* **1993**, *32*, 131.
(6) DeWith, J.; Horton, A. D. *Angew. Chem., Int. Edit.* **1993**, *32*, 903.
(7) Williams, D. S.; Anhaus, J. T.; Schofield, M. H.; Schrock, R. R.; Davis, W. M. *J. Am. Chem. Soc.* **1991**, *113*, 5480.
(8) Williams, D. S.; Schrock, R. R. *Organometallics* **1993**, *12*, 1148.
(9) Schofield, M. H.; Kee, T. P.; Anhaus, J. T.; Schrock, R. R.; Johnson, K. H.; Davis, W. M. *J. Am. Chem. Soc.* **1991**, *30*, 3595.

Appendix C:

Preliminary Studies and Future Work on the Activation and Catalytic Functionalization of Main Group Hydrides *via* [1,2]-Addition to Cationic Vanadium Bisimides

Introduction

In contrast to many *cis*-dioxo and bisimido complexes,[1-3] complex **1.10** is highly reactive with main group hydrides due to a low coordination number and highly polarized metal-ligand multiple bonds. Accordingly, much of our preliminary work has focused on proof of principle systems and extensions to application for this catalytic system and the development of new synthetic methods for group V bisimides. Three important goals for future work are (1) the understanding of the 1,2-addition of readily available main group hydrides, (2) the relation of this elementary step to the development of useful catalytic methodologies, and (3) the elucidation of detailed mechanisms for these transformations.

Scheme C.1: Electropositive main group hydride addition and catalysis.

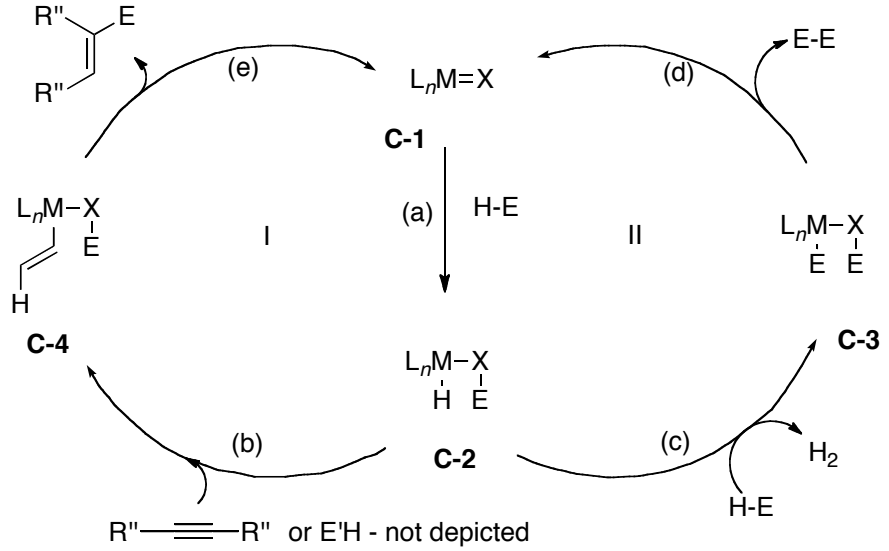

unsaturated substrate; alkyne for visual convenience
Where E = BR'_2, AlR'_2,SiR'_3, GeR'_3,SnR'_3;
R' = any combination of H, alkyl, or aryl groups

The [1,2]-addition of main group hydrides to metal-ligand multiple bonds can occur by two regioisomeric pathways (Schemes C.1 and C.2). The more electropositive and electron deficient main group hydrides (such as BH, AlH, SiH, GeH, *etc*.) are expected to react *via* the formation of a main group element nitrogen bond and a vanadium hydride (Scheme C.1, pathway (a)). On the other hand, the more electronegative and electron rich main group hydrides (such as CH, NH, PH, OH, SH, *etc.*) are expected to add *via* the inverse regiochemistry and generate a main group element vanadium bond and an NH amide (Scheme C.2, pathway (a)). Additions of these substrates are expected based on the previous works by Wolczanski and Bergman.[13,14] The newly generated complexes **C-2** and/or **C-6,** bearing a new metal-element sigma bond or transition metal hydride, can then undergo a functionalization event. This intermediate step can occur by one of two mechanisms: either by sigma-bond metathesis with another equivalent of main group hydride (either homo- or heterodehydrocoupling reactions), or by [1,2]-insertion into an unsaturated inorganic or organic substrate (Schemes C.1 and C.2, pathways (b) and (c)). The catalytic cycle may then be closed by a [1,2]-α-elimination to regenerate the starting complex (Schemes C.1 and C.2, pathways

(d) and (e)). Alternatively, the catalytic cycle may be short-circuited by a sigma-bond metathesis. In this case, the starting complex serves as a precatalyst and the initial [1,2]-addition does not lie on the active catalytic cycle. A third chemically 'degenerate' addition of sigma bonds in which both atoms are equivalent (*e.g.* H-H) is also possible and was demonstrated in Chapter 2.

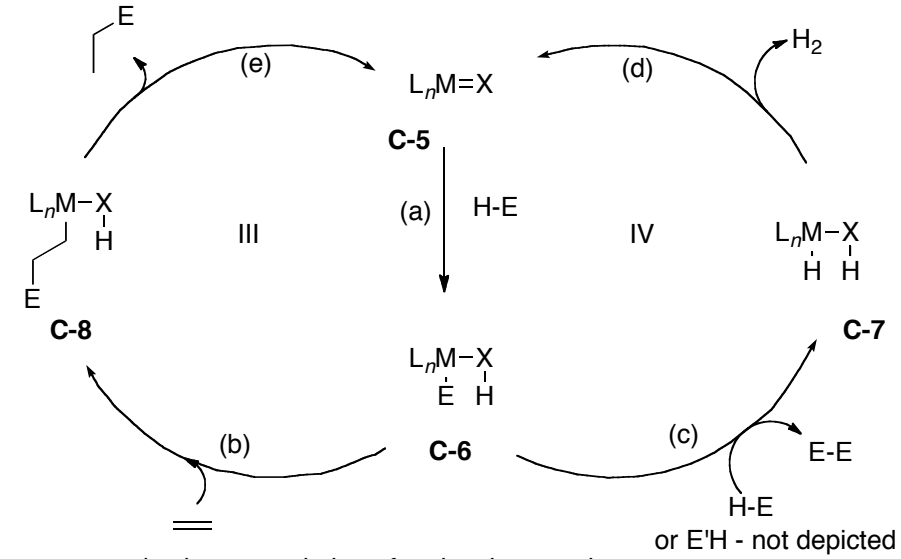

unsaturated substrate; ethylene for visual convenience
Where E = CR'_3, NR'_2, PR'_2, AsR'_2, OR', SR', SeR', TeR'
R' = any combination ofH, alkyl, or aryl groups

Scheme C.2: Electronegative main group hydride addition and catalysis.

Realizing the potential of this alternative approach to catalytically activating and selectively functionalizing main group hydrides presents some fundamental challenges. Complexes must undergo not only this initial [1,2]-addition of a substrate, but also support the subsequent functionalization of the metal-element σ bond ([1,2]-insertion or sigma bond metathesis) and the final [1,2]-elimination of the product to return the active catalyst. The full elaboration of these concepts to application could provide a wide range of interesting and highly useful methodologies and materials. In the case of the homodehydrocoupling/polymerization pathways (Schemes C.1 and C.2, cycles II and IV), depending on the kinetics of [1,2]-addition and sigma bond metathesis of the substrate and the dimer product, these reactions may yield dimers, oligomers, cyclics, or polymers. Attractive synthetic targets for tuning this reactivity pathway include borane and aluminum clusters, diborane reagents for organic synthesis, silicon, germanium, and tin polymers, and linear and cyclic oligomers of group 15 monomers. Under heterodehydrocoupling/polymerization conditions (Schemes C.1 and C.2, cycles I and IV), the synthesis of mixed main group materials such phosphino-borane and phosphino-alane polymers, polysiloxanes, silyl/germyl/stannyl-phosphines and arsines can be achieved. Polymers of this type have several interesting properties including oxidation resistance. Furthermore they may serve as precursors to ceramic materials such as BP.[4] A wide range of organic reactions can be envisioned employing the initial addition of main group hydrides to metal-ligand multiple bonds. Additions of group 13 and the heavier

group 14 hydrides would afford hydroborations, -aluminations, -silylations, -germylations, and -stanylations. Alkynes, alkenes, organic carbonyls and imines are all potential substrates. In particular, the selective addition of the heavier main group species may be especially useful as precursors for cross-coupling reactions. The reactions would proceed *via* pathway (b), cycle I, Scheme C.2. Group 15 and 16 hydrides could afford hydroaminations, -phosphinations, -arsinations, -alkoxylations, and -thioylations. The functionalization of the group 15 hydrides is exciting because of the great need for salt free, catalytic methods for the synthesis alkyl phosphine and arsine ligands. The reactions would proceed *via* pathway (b), cycle III, Scheme C.2.

Results and Discussion

Preliminary work towards these goals has focused on the [1,2]-addition of silanes, borane, and trimethyl aluminum to **1.10**. In an initial screen of stoichiometric reactivity of **1.10**, the complex was found to catalytically, selectively dehydrodimerize phenylsilane under a static vacuum while providing larger oligomers under 1 atm of N_2. It only slowly, stoichiometrically reacts with diphenylsilane which gives a single new complex with a ^{51}V NMR resonance at -650 ppm by small scale reaction in a J. Young NMR tube. (Scheme C.3). Complex **1.10** exhibited no reactivity with tertiary silanes including triphenylsilane and triethylsilane. This kinetic preference to react with smaller, but less reactive (in comparison to disilanes and secondary silanes) monosilanes raises the possibility of developing a selective polymerization catalyst for SiH_4 through rational catalyst design. Furthermore, its stoichiometric reactivity with diphenylsilane is reminiscent of reactivity reported by Nikonov of $Mo(NAr)_2(PMe_3)_2$ with $PhSiH_3$ and may be the basis of catalytic hydrosilylation reactions with unsaturated organic substrates.[5]

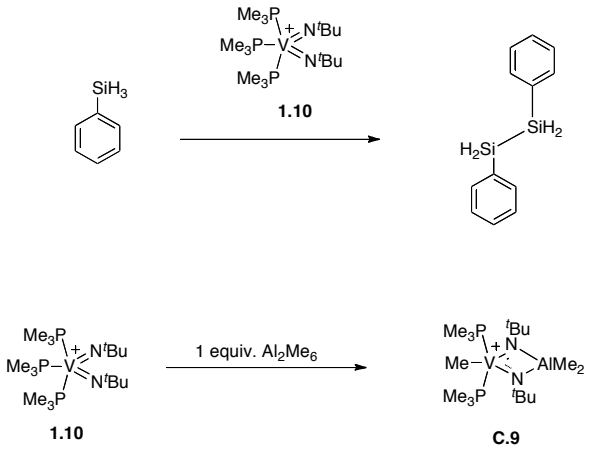

Scheme C.3: Silane dimerization and $AlMe_3$ addition to **1.10**.

Stoichiometric reactivity with group 13 species was also briefly considered. Treating **1.10** with roughly 2 equivalents of DMS•BH_3 in $PHCF_3$ lead to a precipitation of a white solid (presumably BH_3PMe_3) and a color change to green from yellow. Since an excess of barne was employed, the proton NMR was complicated but a single new ^{51}V NMR resonance was observed at -668.10 ppm. In order to clarify the reaction of group 13 species, the addition of trimethyl aluminum was performed on preparative scale which

lead to the isolation of the vanadium methyl cation **C.9** and which is the product of Al-Me addition across an imide. Treatment of solution of **C.9** in PhCF3 with 1 atm ethylene at 45 °C lead to the precipitation of a white waxy solid after 12 h. After isolation of the solid by quenching with 5% HCl in ethanol, it was found to have a broad melting point between 136-140 °C. This melting point suggests that a HDPE was formed, but more detailed experiments are necessary.

Experimental Section

General Considerations. Unless otherwise noted, all reactions were performed using standard Schlenk line techniques or in an MBraun inert atmosphere box under an atmosphere of argon or dinitrogen (<1 ppm O_2/H_2O), respectively. All glassware and cannulae were stored in an oven at ca. 425 K. Pentane, diethyl ether, toluene, tetrahydrofuran, dichloromethane, s dimehtoxyethane were purified by passage through a column of activated alumina and degassed prior to use. C_6D_6 was vacuum-transferred from sodium/benzophenone and degassed with three freeze-pump-thaw cycles. 1,2-$C_2D_4Cl_2$ was vacuum transferred from CaH_2 and degassed with three freeze-pump-thaw cycles. NMR spectra were recorded on Bruker AV-300, AVB-400, AVQ-400, AV-500, and AV-600 spectrometers. ^{1}H and ^{13}C{^{1}H} chemical shifts are given relative to residual solvent peaks. ^{31}P, ^{51}V, ^{19}F, and ^{27}Al chemical shifts were referenced to external standards ($P(OMe)_3$ at 1.67 ppm, $VOCl_3$ at 0.00 ppm, $CFCl_3$ at 0.00 ppm, and 1M Al(NO3)3 in H_2O/D_2O at 0 ppm, respectively). Proton and carbon NMR assignments were routinely confirmed by ^{1}H-^{1}H (COSY) or ^{1}H-^{13}C (HSQC and HMBC) experiments as necessary. Resonances marked with a * were located by HMBC. Infrared (IR) samples were prepared as Nujol mulls and were taken between KBr disks. The following chemicals were purified prior to use: α, α', α''-trifluorotoluene ($PhCF_3$), was distilled from P_2O_5 and degassed by bubbling argon through the liquid for 15 minutes. All other reagents were acquired from commercial sources and used as received. Elemental analyses were determined at the College of Chemistry, University of California, Berkeley.

Preparation of [V(Me)(PMe$_3$)$_2$(μ-N^{t}Bu)$_2$Al(Me)$_2$][Al(PFTB)$_4$]. To a solution of **1.10** (0.275 g, 0.198 mmol) in 15 mL of $PhCF_3$ at 0 °C was added Al_2Me_6 (2.0 M in hexanes, 0.1 mL, 0.0198 mmol) *via* syringe. The reaction mixture was allowed to warm to room temperature and stirred for 3.5 h. It was then reduced to a residue *in vacuo* and extracted with diethyl ether. The solution was transferred to a Schlenk tube *via* a filtration cannula and reduced until the product began to crystallize and stored at -40 °C overnight. The title compound was afforded in an 11% (0.03 g) yield as yellow blocks after decantation. ^{1}H NMR ($PhCF_3$ (C_6D_6 insert), 600.1 MHz) δ 1.185 (t, P*Me$_3$*, 18H, $^1J_{CP}$ = 4.2 Hz), 1.108 (s, N*t*Bu, 18H), 0.957 (t, V(*CH$_3$*), 3H, $^1J_{CP}$ = 17.4 Hz), -.0491 (s, Al(*CH$_3$*)$_2$, 6H). ^{13}C NMR ($PhCF_3$ (C_6D_6 insert), 150.9 MHz), δ 32.57 (pseudo triplet, β-tBu), 14.81(t, PMe_3, $^1J_{CP}$ = 12.07 Hz), -4.54 (m, Al(*Me*)$_2$). The imide β-*t*Bu carbon, the α and the β-$C(CF_3)_3$ and the V(*CH$_3$*) carbon resonances could not be observed. ^{19}F NMR ($PhCF_3$ (C_6D_6 insert), 376.5 MHz), δ -74.54 (s, C(C*F$_3$*)$_3$). ^{27}Al NMR ($PhCF_3$ (C_6D_6 insert), 104.3 MHz), δ 33.96 (s, $\Delta\nu_{1/2}$ = 7.3 Hz). The *Al*(Me_2) resonance could not be observed and may overlap with the aluminate anion as it presents with a slight shoulder. ^{31}P {^{1}H} NMR ($PhCF_3$ (C_6D_6

insert), 242.9 MHz), δ -1.7 (br s, $\Delta\nu_{1/2}$ = 1846.00 Hz). $^{51}V\{^{1}H\}$ NMR ($PhCF_3$ (C_6D_6 insert), 157.9 MHz) δ 214.05 (pseudo triplet, $\Delta\nu_{1/2}$ = 10.1 Hz). Anal. Calcd (%) for $C_{33}H_{45}Al_2F_{36}N_2O_4P_2V$: C, 28.63; H, 3.28; N, 2.02. Found: C, 28.51; H, 3.26; N, 1.91.

Notes and References

(1) Nugent, W. A.; Mayer, J. M. *Metal-Ligand Multiple Bonds*; Wiley: New York, NY, 1988.
(2) Nugent, W. A.; Haymore, B. L. *Coord. Chem. Rev.* **1980**, *31*, 123.
(3) Wigley, D. E. *Prog. Inorg. Chem.* **1994**, 239.
(4) Dorn, H.; Rodezno, J. M.; Brunnhofer, B.; Rivard, E.; Massey, J. A.; Manners, I. *Macromolecules* **2003**, *36*, 291.
(5) Khalimon, A. Y.; Simionescu, R.; Kuzmina, L. G.; Howard, J. A. K.; Nikonov, G. I. *Angew. Chem., Int. Edit.* **2008**, *47*, 7701.

Appendix D:

Carbon Monoxide Oxidation and C-O Bond Cleavage by $[V(PMe_3)_3(N\mathit{t}Bu)_2]^+$

Introduction

Carbon monoxide remains an ideal choice for a C_1 synthetic building block.[1,2] On the industrial scale this takes place most commonly in the heterogeneous Fischer-Tropsch (F-T) process. In order to increase the selectivity of this process, there has been renewed interest in molecular systems that mimic the F-T chemistry and provide access to functionalized CO. Such systems remain rare, but can be broken into 3 classes: (1) direct mimics of the initial steps of F-T that reductively cleave CO to carbides and metal oxides,[3-5] (2) systems that undergo migratory insertion of CO into metal alkyls, silyls, or hydrides followed C-O bond cleavage,[6-12] and (3) systems that generate metal carbides via disproportionation of CO to carbide and CO_2.[13] However no molecular system yet provides access to heterocumulenes utilizing carbon monoxide as the carbon source. Herein we describe the oxidation of CO and the cleavage of the C-O bond by **1.10** to afford carbodiimides.

Results and Discussion

As mentioned in Chapter 3, **1.10** undergoes a dramatic transformation with excess CO. In an initial preparatory scale reaction, a solution of **1.10** was exposed to excess CO. The solution color immediately shifted orange and an orange precipitate formed. Over the course of 24 h this precipitate dissolved and the solution shifted in color to deep red/purple and, on further stirring, shifted green in color. Clearly, simple CO for PMe_3 exchange was not occurring as would be expected based on the isocyanide chemistry described in Chapter 3. In order to learn more about this reaction before attempting to isolate vanadium containing products a ^{13}CO labeling study was undertaken and monitored by ^{13}C NMR (Figure D.1). After twenty minutes under excess ^{13}CO, no ^{13}C containing products are visible. However, on standing for 1 day, *tert*-butylisocyanate is clearly visible at 124 ppm overlapping with the $-CF_3$ quartet of the anion of **1.10**. Further reaction leads to a decrease in intensity of this signal and growth of a new signal at 141 ppm corresponding to 1,3-di-*tert*-butylcarbodiimide. This transformation is illustrated in Scheme D.1.

The oxidative coupling of CO with an imide to give isocyanate was further confirmed by the isolation of **D.1** by treating a solution of **1.10** with excess CO for 1 day. Complex **D.1** is a diamagnetic, octahedral complex with two CO ligands supporting the reduced metal center. While **D.1** clearly has three PMe_3 ligands in a 2:1 ratio and a single imide by NMR, the rest of the coordination sphere is not clear. The presence of two symmetry inequivalent carbonyl ligands was suggested by IR studies that show two sharp stretches at 2016 and 1943 cm^{-1}. While x-ray crystallographic data of sufficient quality remain elusive due both to disorder in the anion and the sensitivity of the complex to light, the connectivity has been confirmed by a preliminary refinement. Further work, however, has been stymied by an inability to accurately assign the Laue group. Nonetheless evidence for the formation of a vanadium oxo product was obtained by treating isolated **D.1** with *tert*-butylisocyanate, which led to the formation of the corresponding carbodiimide as assayed by NMR (further preparative work and GC/MS confirmation is required). It should be noted that similar oxidative coupling of isocyanides does not readily occur. Only in the presence of 3 equivalents of CNXyl and

heating to 105 °C does a new ^{51}V containing product form, albeit in low conversion. This oxidative coupling of CO an early metal is remarkable because such reactivity is usually associated with mid- to late-metal imides such as Fe,[14] Co,[15,16] Ir,[17] and Ni.[18] Only recently has a zirconium imide supported by a redox active ligand been shown to undergo a similar oxidative coupling. Typically reduced early metals react with isocyanates to give imides and carbon monoxide. The exchange of the isocyanate oxygen with the vanadium imide to give the putative vanadium oxo is also quite unusual – there is only one other example a similar reactivity by a tantalum imide.[19]

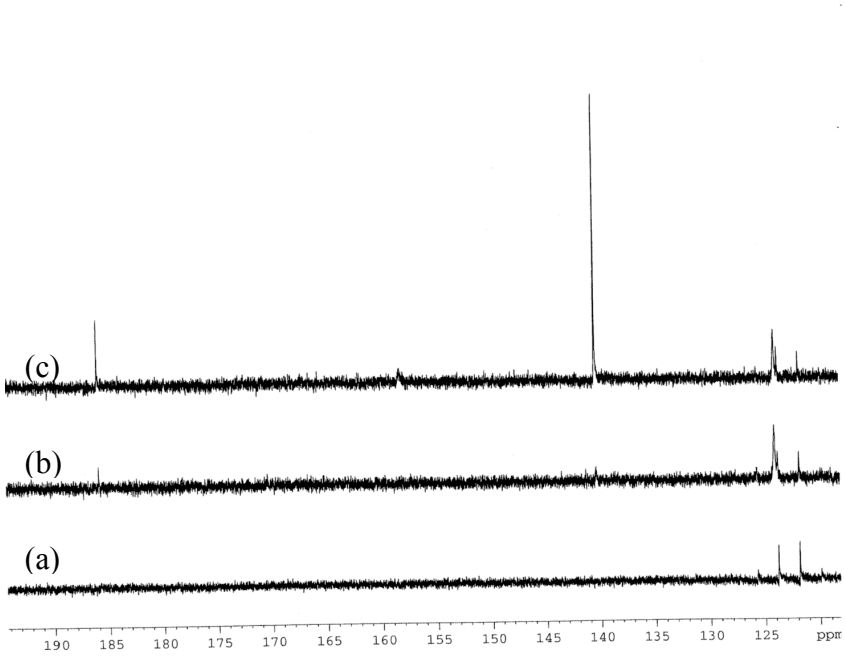

Figure D.1: Stack plot of ^{13}CO labeling experiment at (a) 20 minutes; (b) 1 day; (c) 3 days.

In order to rule out reactivity derived from CO_2 contamination of the CO, **1.10** was examined for its reactivity with CO_2. In the presence of excess CO_2 a solution of **1.10** quickly turned deep red, however no products were able to be isolated. As a result the reactivity of **1.10** with one equivalent of CS_2 was explored. A single product, **D.2**, was isolated (Scheme D.1) in 47% yield. Much like **D.1**, crystallographic data was difficult to acquire. Nonetheless, the NMR data shows two equivalent *tert*-butylimides, two equivalent, axial phosphines, and a single downfield shifted phosphine resonance – suggests the insertion of CS_2 into the equatorial V-P bond as the only product that matches the observed data. This product is intriguing and may imply that the initially observed, sparingly soluble orange material in the CO reaction may be a phosphaacyl complex (Scheme D.1). This hypothesis needs to be tested by direct synthesis with one equivalent of CO.

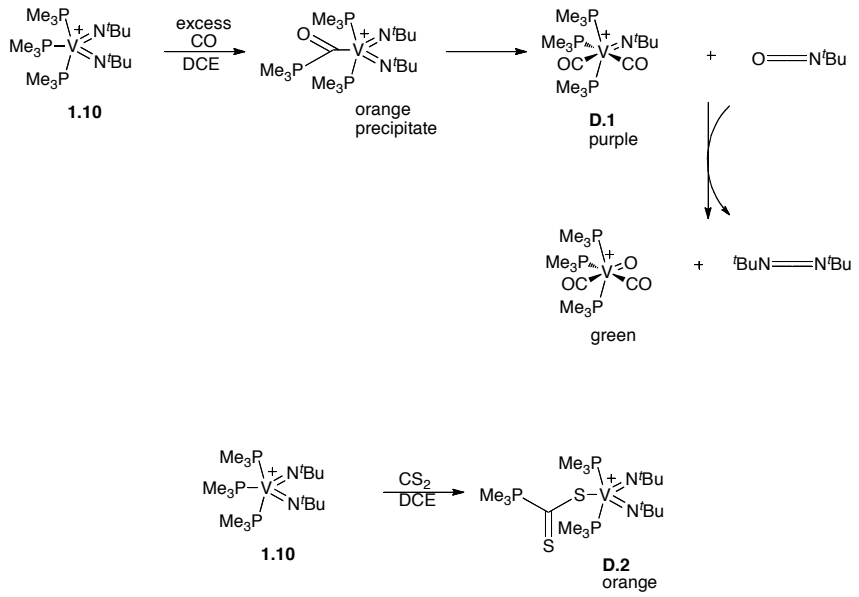

Scheme D.1: Proposed mechanism of CO oxidation and C-O bond cleavage and the synthesis of **D.1** and **D.2**.

Conclusion

This work provides the basis for demonstrating C-O cleavage and functionalization by **1.10**. While further studies are required to confirm the details of the process, this transformation with CO is remarkable in that it demonstrates that complex **1.10** possesses reactivities reminiscent of both prototypical early and late metal imides. Further work will focus on elucidating the initial intermediate and confirming the vanadium oxo product.

Experimental

General Considerations. Unless otherwise noted, all reactions were performed using standard Schlenk line techniques or in an MBraun inert atmosphere box under an atmosphere of argon or dinitrogen (<1 ppm O_2/H_2O), respectively. All glassware and cannulae were stored in an oven at ca. 425 K. Pentane, diethyl ether, toluene, tetrahydrofuran, dichloromethane, and dimethoxyethane were purified by passage through a column of activated alumina and degassed prior to use. C_6D_6 was vacuum-transferred from sodium/benzophenone and degassed with three freeze-pump-thaw cycles. 1,2-$C_2D_4Cl_2$ was vacuum transferred from CaH_2 and degassed with three freeze-pump-thaw cycles. NMR spectra were recorded on Bruker AV-300, AVB-400, AVQ-400, AV-500, and AV-600 spectrometers. ^1H and $^{13}C\{^1H\}$ chemical shifts are given relative to residual solvent peaks. ^{31}P, ^{51}V, ^{19}F, and ^{27}Al chemical shifts were referenced to external standards ($P(OMe)_3$ at 1.67 ppm, $VOCl_3$ at 0.00 ppm, $CFCl_3$ at 0.00 ppm, and 1M $Al(NO_3)_3$ in H_2O/D_2O at 0 ppm, respectively). Proton and carbon NMR assignments were routinely confirmed by ^1H-^1H (COSY) or ^1H-^{13}C (HSQC and HMBC) experiments

as necessary. Resonances marked with a * were located by HMBC. Infrared (IR) samples were prepared as Nujol mulls and were taken between KBr disks. The following chemicals were purified prior to use: DCE was distilled from CaH_2 and degassed by bubbling argon through the liquids for 15 minutes, α, α', α''-trifluorotoluene ($PhCF_3$), was distilled from P_2O_5 and degassed by bubbling argon through the liquid for 15 minutes. All other reagents were acquired from commercial sources and used as received. Elemental analyses were determined at the College of Chemistry, University of California, Berkeley. The X-ray structural determination was performed at CHEXRAY, University of California, Berkeley, on a Bruker APEX II Quazar diffractometer.

Preparation of $[V(N^tBu)(CO)_2(PMe_3)_3][Al(PFTB)_4]$ (D.1). A solution of **1.10** (400 mg, .29 mmol) in 25 mL $PhCF_3$ in a 250 ml round bottom Schlenk flask was degassed by evacuation of the flask for 30 seconds. To this flask was then added 1 atm of CO (excess). Over the course of 24 h the reaction mixture color changed from yellow to purple/red. The reaction mixture was then reduced to a residue, extracted with DCE, and filtered via cannula. The solution was then reduced *in vacuo* until the product began to crystallize and was then placed in a -15 °C freezer overnight. After decantation the desired product was afforded in 79 % (310 mg) yield as dichroic blue/red blocks. Recrystallization by the same method afforded X-ray quality crystals. ^1H NMR ($PhCF_3$ (C_6D_6 insert), 600.1 MHz) δ 1.89 (unresolved t, P*Me*$_3$, 18H), 1.10 (s, N*tBu*, 18H), .95 (d, PMe_3, 9H, J_{PH} = 6.6 Hz). ^{13}C NMR ($PhCF_3$ (C_6D_6 insert), 150.9 MHz) δ 72.6* (α-N*t*Bu), 30.62 (s, β-N*t*Bu), 18.72 (t, PMe_3, J_{CP} = 13.7), 15.60 (d, PMe_3, J_{CP} = 18.26). The α and β-$C(CF_3)_3$ carbon resonances could not be observed. $^{31}P\{^1H\}$ NMR ($PhCF_3$ (C_6D_6 insert), 242.9 MHz) δ -12.07 (vbr s, $\Delta\nu_{1/2}$ = 1929.08 Hz, rel. int. 2), -36.04 (s, rel. int. 1). $^{51}V\{^1H\}$ NMR ($PhCF_3$ (C_6D_6 insert), 157.7 MHz) δ -690.13 (pseudo t, $\Delta\nu_{1/2}$ = 15.15 Hz). ^{19}F NMR ($PhCF_3$ (C_6D_6 insert), 376.5 MHz, 298 K) δ -74.40 (s). ^{27}Al NMR ($PhCF_3$ (C_6D_6 insert), 104.3 MHz, 298 K) δ 33.80 (s, $\Delta\nu_{1/2}$ = 4.13 Hz). Anal. Calcd (%) for $C_{30}H_{36}AlF_{36}NO_6P_3V$: C, 26.47; H, 2.67; N, 1.03. Found: C, 26.41; H, 2.56; N, 1.36. IR (KBr, cm^{-1}): 2016 (s), 1943 (s), 1352 (s), 1169 (s), 946 (s), 832 (w), 560 (w), 537 (w), 471 (w), 445 (m). Mp = 186-188 °C (dec.).

Preparation of $[V(N^tBu)_2(CS_2PMe_3)(PMe_3)_2][Al(PFTB)_4]$ (D.2). Carbon disulfide (13 μL, 1 equiv.) was added to a solution of **1.10** in DCE *via* syringe. The reaction mixture was stirred at room temperature overnight (12 h). It was then reduced to a residue *in vacuo*, extracted with DCE, and filtered *via* cannula. The filtrate was then reduced in volume until the product began to crystallize and was then placed in a -15 °C freezer overnight. After decantation the desired product was afforded in 47 % (150 mg) yield as orange plates (beige powder after drying under vacuum). ^1H NMR ($PhCF_3$ (C_6D_6 insert), 600.1 MHz) δ 1.66 (pseudo t, P*Me*$_3$, 18H), 1.27 (d, PMe_3, 9H, J_{PH} = 8.4 Hz), 1.16 (s, N*tBu*, 18H). ^{13}C NMR ($PhCF_3$ (C_6D_6 insert), 150.9 MHz) δ 68.2* (α-N*t*Bu), 33.95 (d, β-N*t*Bu, J_{CP} = 2.8 Hz), 18.69 (d, PMe_3, J_{CP} = 24.24 Hz), 14.09 (unresolved dd, PMe_3). The α and β-$C(CF_3)_3$ and CS_2 carbon resonances could not be observed. $^{31}P\{^1H\}$ NMR ($PhCF_3$ (C_6D_6 insert), 242.9 MHz) δ 26.74 (s, rel. int. 1), 11.05 (vbr s, $\Delta\nu_{1/2}$ = not measurable, rel. int. 2). $^{51}V\{^1H\}$ NMR ($PhCF_3$ (C_6D_6 insert), 157.7 MHz) δ -845.24 (pseudo d, $\Delta\nu_{1/2}$ = 390.45 Hz). ^{19}F NMR ($PhCF_3$ (C_6D_6 insert), 376.5 MHz, 298 K) δ -

74.51 (s). ^{27}Al NMR ($PhCF_3$ (C_6D_6 insert), 104.3 MHz, 298 K) δ 33.74 (s, $\Delta\nu_{1/2}$ = 3.81 Hz). Anal. Calcd (%) for $C_{34}H_{45}AlF_{36}N_2O_4P_3VS_2$: C, 27.88; H, 3.10; N, 1.91. Found: C, 28.06; H, 2.82; N, 1.95. IR (KBr, cm^{-1}): 1353 (s), 1169 (s), 1101 (m), 897 (w), 867 (w), 833 (w), 815 (w), 755 (w), 583 (w), 561 (m), 537 (m), 446 (m). Mp = 101-103 °C (dec.).

^{13}CO Labeling Experiment. A solution of **1.10** (30 mg, .02 mmol) in d_4-DCE in a J. Young NMR tube was degassed with three freeze-pump-thaw cycles filled with 1 atm 99% ^{13}CO. The reaction was followed by ^{13}C NMR over the course of three days.

Notes and References

(1) Arnold, J.; Tomson, N. C.; Yan, A.; Bergman, R. G. *J. Am. Chem. Soc.* **2008**, *130*, 11262.
(2) Kuhlmann, E. J.; Alexander, J. J. *Coord. Chem. Rev.* **1980**, *33*, 195.
(3) Lapointe, R. E.; Wolczanski, P. T.; Mitchell, J. F. *J. Am. Chem. Soc.* **1986**, *108*, 6382.
(4) Neithamer, D. R.; Lapointe, R. E.; Wheeler, R. A.; Richeson, D. S.; Vanduyne, G. D.; Wolczanski, P. T. *J. Am. Chem. Soc.* **1989**, *111*, 9056.
(5) Miller, R. L.; Wolczanski, P. T.; Rheingold, A. L. *J. Am. Chem. Soc.* **1993**, *115*, 10422.
(6) Marsella, J. A.; Huffman, J. C.; Folting, K.; Caulton, K. G. *Inorg. Chem. Acta* **1985**, *96*, 161.
(7) Marsella, J. A.; Folting, K.; Huffman, J. C.; Caulton, K. G. *J. Am. Chem. Soc.* **1981**, *103*, 5596.
(8) Wood, C. D.; Schrock, R. R. *J. Am. Chem. Soc.* **1979**, *101*, 5421.
(9) Planalp, R. P.; Andersen, R. A. *J. Am. Chem. Soc.* **1983**, *105*, 7774.
(10) Arnold, J.; Tilley, T. D.; Rheingold, A. L.; Geib, S. J.; Arif, A. M. *J. Am. Chem. Soc.* **1989**, *111*, 149.
(11) Kropp, K.; Skibbe, V.; Erker, G.; Kruger, C. *J. Am. Chem. Soc.* **1983**, *105*, 3353.
(12) Erker, G.; Kropp, K.; Kruger, C.; Chiang, A. P. *Chem. Ber.* **1982**, *115*, 2447.
(13) Horwitz, C. P.; Shriver, D. F. *J. Am. Chem. Soc.* **1985**, *107*, 8147.
(14) Peters, J. C.; Brown, S. D.; Betley, T. A. *J. Am. Chem. Soc.* **2003**, *125*, 322.
(15) Arnold, J.; Chomitz, W. A. *Chem. Comm.* **2008**, 3648.
(16) Arnold, J.; Chomitz, W. A. *Inorg. Chem.* **2009**, *48*, 3274.
(17) Glueck, D. S.; Hollander, F. J.; Bergman, R. G. *J. Am. Chem. Soc.* **1989**, *111*, 2719.
(18) Hillhouse, G. L.; Mindiola, D. J. *Chem. Comm.* **2002**, 1840.
(19) Royo, P.; Sanchez-Nieves, J. *J. Organomet. Chem.* **2000**, *597*, 61.

Appendix E:

Tables of Atom Cartesian Coordinates for DFT studies in Chs. 2 and 3

Table E.1: B3LYP Energies and Cartesian Coordinates
For Chapter 2 DFT Studies
Compound $[V(PMe_3)_3(N\textit{t}Bu)_2]^+$ (1)
E (a.u.) = -1879.78098784
ZPE (a.u) = 0.602371

V 0.18276700 0.24457200 0.08135600
P 0.06156300 -0.00234700 2.59869700
P -1.14005100 -2.23059800 0.07092400
P 0.00523100 0.05119200 -2.43577500
N -0.53430700 1.74801000 0.10982900
N 1.85077800 0.21744700 0.05891200
C -1.00919700 3.12287800 0.13289500
C 3.25548100 0.58881700 0.04196700
C -0.46160900 3.86138200 1.37144800
H -0.78081900 4.90797400 1.35089600
H -0.84606200 3.41943600 2.29467900
H 0.63140300 3.83659600 1.38908100
C -2.55359000 3.10044600 0.18287200
H -2.95332700 4.11948000 0.20371300
H -2.96130000 2.58855500 -0.69380600
H -2.90430500 2.57563300 1.07643200
C -0.54446000 3.87118200 -1.13327600
H 0.54596300 3.86301000 -1.21378600
H -0.97512400 3.42452400 -2.03360600
H -0.87725000 4.91293400 -1.09151500
C 3.95202600 -0.03118800 1.27512800
H 5.02629800 0.17420000 1.23848100
H 3.56751700 0.38631800 2.20774000
H 3.81142500 -1.11603900 1.29231800
C 3.91712600 -0.01503400 -1.21839200
H 3.50570600 0.41239300 -2.13499800
H 4.99175600 0.19148300 -1.20993700
H 3.77736400 -1.09982700 -1.24441500
C 3.41052000 2.12163500 0.04974600
H 2.95741600 2.55081700 0.94791000
H 4.46805100 2.40429600 0.02923000
H 2.91906800 2.56295900 -0.82194300
C 0.77018000 -1.52171900 3.38237200
H 0.73439300 -1.44303500 4.47325700
H 0.23891300 -2.42555900 3.08187600
H 1.81226700 -1.61907500 3.06783500
C -1.58955300 0.20593400 3.40256500
H -2.30904700 -0.52740600 3.03971500
H -1.50493400 0.11533500 4.48988800
H -1.97022900 1.20098300 3.15910200
C 1.02944900 1.29308900 3.48830700
H 0.69441300 2.28573300 3.19351000
H 0.89673900 1.17343400 4.56815000
H 2.08910300 1.20355100 3.25093300
C 0.12284500 -3.58496500 0.06034000
H 0.76852300 -3.49773300 0.93713300
H -0.35507700 -4.56944300 0.06307900
H 0.75413800 -3.49605000 -0.82684700
C -2.25364800 -2.74921200 1.46373800
H -2.57440400 -3.78443700 1.31200000
H -1.76416200 -2.68075500 2.43496500
H -3.14122600 -2.11084400 1.47504500
C -2.26475700 -2.74303900 -1.31542300
H -3.15904400 -2.11406900 -1.30859700
H -1.78747100 -2.65807300 -2.29139400
H -2.57328300 -3.78318400 -1.17216100
C -1.66307800 0.24940700 -3.20652300
H -2.05335900 1.23541500 -2.94217500
H -1.59678600 0.17607400 -4.29646300
H -2.36588000 -0.49925700 -2.84239000
C 0.71759900 -1.44985400 -3.25004600
H 0.65935000 -1.36102300 -4.33914600
H 1.76657500 -1.53556100 -2.95607600
H 0.20503900 -2.36383400 -2.94777200
C 0.94027300 1.36926100 -3.32805900
H 2.00283100 1.30515900 -3.09506100
H 0.80598900 1.24602100 -4.40731600
H 0.58265600 2.35426500 -3.03364600

Compound $[V(PMe_3)_2(N\textit{t}Bu)_2]^+$ (2A)
E (a.u.) = -1418.65838625
ZPE (a.u.) = 0.484952

V 0.10819100 -0.70197400 0.28296800
P 0.83334000 -3.03380600 -0.18822100
P 0.68581200 0.88672500 2.10909000
C 0.51440100 -4.22263100 1.18375000
H 0.82351600 -5.23372500 0.90183000
H 1.06792800 -3.92373800 2.07834700
H -0.55179400 -4.22381700 1.42240600
C 2.62930700 -3.22768900 -0.55012900

H 2.87302400 -4.27191800 -0.76808100
H 2.89385000 -2.60685300 -1.40927800
H 3.22337400 -2.89916200 0.30724300
C -0.00826200 -3.78106100 -1.64197000
H 0.35055900 -4.80165500 -1.80608900
H -1.08643000 -3.79991200 -1.46972600
H 0.19030000 -3.17951300 -2.53131600
C 0.27522500 0.29419900 3.80545000
H 0.82192200 -0.62701100 4.02532200
H 0.53960700 1.04668600 4.55462500
H -0.79483500 0.08261900 3.86797700
C 2.47147200 1.33177600 2.20519200
H 2.78743800 1.77085000 1.25595200
H 2.65049100 2.04755500 3.01325100
H 3.07394000 0.43771800 2.38808300
C -0.17791900 2.50306100 1.96772200
H -1.25797100 2.34384600 1.97082000
H 0.09698000 3.15638500 2.80128900
H 0.09933800 2.98166200 1.02619100
N 0.59395000 0.11205000 -1.06992700
N -1.52758800 -0.87372900 0.44159400
C -2.96109100 -0.81243900 0.21479900
C 0.59264000 0.84394800 -2.32485800
C 0.18429900 -0.11680900 -3.46124800
H 0.17627600 0.41336800 -4.41854500
H 0.89626700 -0.94440100 -3.54118600
H -0.81357100 -0.52665000 -3.28438100
C -0.39534800 2.02462100 -2.24091500
H -0.11137200 2.71229100 -1.43851900
H -0.39384300 2.58448900 -3.18122100
H -1.41244800 1.67252700 -2.05173400
C 2.02450400 1.36935900 -2.56791400
H 2.32976000 2.05061300 -1.76795800
H 2.74031800 0.54327900 -2.60937800
H 2.07142800 1.91335700 -3.51648000
C -3.61576000 -1.95075100 1.02823200
H -3.38638100 -1.84996200 2.09291900
H -4.70303300 -1.92564200 0.90545100
H -3.25678000 -2.92692300 0.68788900
C -3.47981200 0.55404900 0.71050200
H -3.00610800 1.37163900 0.15965300
H -4.56194600 0.62184800 0.56250900
H -3.27604300 0.68166700 1.77826000
C -3.27367000 -0.98661600 -1.28431700
H -4.35604100 -0.97932300 -1.44588800
H -2.83449200 -0.17714500 -1.87256000
H -2.88160400 -1.93778000 -1.65627800

Compound $[V(PMe_3)(N\mathit{t}Bu)_2]^+$ (2B)
E (a.u.) = -957.480152226
ZPE (a.u.) = 0.369773
V 0.20434900 0.29821500 0.75127800
P 1.27999800 -1.90272000 0.87987300
C 0.92598500 -2.78595800 2.45379500
H 1.43095400 -3.75651000 2.47346500
H 1.27188000 -2.19286200 3.30494300
H -0.15157400 -2.93528000 2.55245100
C 3.11542100 -1.80663700 0.78315000
H 3.55389000 -2.80738100 0.84295800
H 3.40851800 -1.33965800 -0.16001500
H 3.50751600 -1.20296800 1.60643600
C 0.78695800 -3.06059800 -0.45417000
H 1.28570800 -4.02509100 -0.32040700
H -0.29498000 -3.20417900 -0.43573500
H 1.06693900 -2.63941000 -1.42187800
N 0.59005600 0.71063600 -0.79390400
N -1.37051400 -0.14031400 0.93588300
C -2.78635600 -0.36432600 0.69308700
C 0.50681800 1.06586300 -2.20018100
C 1.93769300 1.00322200 -2.77942900
H 1.92414000 1.29935600 -3.83254200
H 2.60695200 1.67873200 -2.23985800
H 2.34116400 -0.01216600 -2.71747200
C -0.41995200 0.09256500 -2.95234100
H -1.43599800 0.12801200 -2.55258800
H -0.46012400 0.36490100 -4.01108000
H -0.05219200 -0.93546100 -2.88305500
C -0.03900700 2.50933700 -2.28392700
H -1.04967300 2.56989600 -1.87091700
H 0.60643200 3.20292900 -1.73752400
H -0.07440600 2.82789300 -3.33003500
C -3.46153500 -0.56050000 2.06905500
H -3.33527900 0.32715300 2.69492700

H -4.53296700 -0.73651700 1.93373000
H -3.03596000 -1.42011000 2.59459400
C -3.37766300 0.87074300 -0.01772000
H -2.91516500 1.02185700 -0.99622900
H -4.45314300 0.73324200 -0.16388100
H -3.22876800 1.77300900 0.58269500
C -2.96178800 -1.62953600 -0.17155100
H -4.02556500 -1.80296800 -0.35857700
H -2.45749100 -1.52381200 -1.13554700
H -2.56532500 -2.51048000 0.34297300

TS H_2 + $[V(PMe_3)_2(NtBu)_2]^+$ (TS - 3A)
E (a.u.) = -1419.80555363
ZPE (a.u.) = 0.499352
V 0.06005400 -0.73344300 0.30777800
P 0.79675200 -2.99693800 -0.32902300
P 0.68772400 1.11898300 1.79833600
C 0.41786400 -4.33607100 0.87665000
H 0.77884900 -5.29984400 0.50535000
H 0.89196300 -4.11701700 1.83572000
H -0.66237700 -4.39579500 1.03092200
C 2.62120900 -3.11126100 -0.55163600
H 2.91137200 -4.12923700 -0.82905900
H 2.94189400 -2.41956400 -1.33377800
H 3.12564600 -2.84136700 0.37998300
C 0.09706500 -3.64133400 -1.90424200
H 0.45954500 -4.65610600 -2.09494000
H -0.99355200 -3.65913600 -1.83834100
H 0.38189000 -2.99409200 -2.73469500
C 0.13573500 0.97957300 3.54931300
H 0.53515000 0.06428100 3.99140800
H 0.48112300 1.84153600 4.12784800
H -0.95528000 0.93788500 3.59099700
C 2.51618100 1.29665300 1.93157700
H 2.94562900 1.47092400 0.94259300
H 2.77428300 2.13226100 2.58944200
H 2.94460100 0.37842700 2.34198600
C 0.09538600 2.78801200 1.29993800
H -0.99684700 2.79573800 1.26590900
H 0.43470200 3.54407600 2.01454200
H 0.47232300 3.03611200 0.30638500
N 0.48513300 0.03660500 -1.10368900
N -1.57838800 -0.97794000 0.69712400
C -3.03286400 -1.02326400 0.74363900
C 0.83176400 0.75130700 -2.31603800
C 0.96820200 -0.27217600 -3.46471100
H 1.22104300 0.24740100 -4.39383500
H 1.76353100 -0.99405000 -3.25525600
H 0.02812900 -0.80890700 -3.61838600
C -0.29667300 1.75035700 -2.65134800
H -0.42743100 2.47850500 -1.84592600
H -0.05985200 2.29724400 -3.56945700
H -1.24447500 1.22464500 -2.79493000
C 2.17199300 1.49247800 -2.12462800
H 2.10014100 2.23467100 -1.32373100
H 2.97242600 0.78897100 -1.87568900
H 2.45141700 2.01930100 -3.04224700
C -3.48358500 -2.49039600 0.89929800
H -3.09576700 -2.92597300 1.82585500
H -4.57568000 -2.54502700 0.93286200
H -3.13902100 -3.09400500 0.05459700
C -3.52234500 -0.18432600 1.94231400
H -3.20682700 0.85836500 1.84148500
H -4.61491400 -0.20555100 1.99271600
H -3.13389300 -0.58190900 2.88548600
C -3.56037300 -0.43355200 -0.57910400
H -4.65441500 -0.43477900 -0.57333000
H -3.21581000 0.59548900 -0.71183700
H -3.21995600 -1.02546500 -1.43306200
H 0.30251800 -1.55699800 1.93600000
H -0.75570000 -1.46350700 1.69699600

TS H_2 + $[V(PMe_3)(NtBu)_2]^+$ (TS - 3B)
E (a.u.) = -988.655488877
ZPE (a.u.) = 0.383206
V 0.25833500 0.04677500 0.68223900
P 1.56661900 -2.06740400 0.85482900
C 1.49029700 -2.91590900 2.48622200
H 2.08147800 -3.83646800 2.46565800
H 1.88551900 -2.26143700 3.26798800
H 0.45347600 -3.16041500 2.73009600
C 3.35927700 -1.84108500 0.51615100
H 3.88671300 -2.79734900 0.58403100
H 3.49107700 -1.42250400 -0.48405000
H 3.79315500 -1.14692600 1.24109000

C 0.98650300 -3.30896500 -0.36855300
H 1.59058700 -4.21896700 -0.30445100
H -0.05936400 -3.55835300 -0.17445400
H 1.06469200 -2.89296100 -1.37535100
N 0.66533400 0.58289800 -0.80413800
N -1.40027200 -0.19308400 0.93016300
C -2.85669600 -0.14891200 0.79902900
C 0.62916700 1.04966100 -2.17963800
C 2.07182200 0.98500700 -2.72785700
H 2.09031400 1.35718100 -3.75635800
H 2.74578000 1.60044100 -2.12611600
H 2.44376700 -0.04416700 -2.73290300
C -0.30615000 0.14743900 -3.00770800
H -1.32646700 0.17648700 -2.61665000
H -0.32707800 0.49023600 -4.04628900
H 0.04107000 -0.89025200 -3.00101000
C 0.12448400 2.50867300 -2.17281500
H -0.89193400 2.56929500 -1.77538900
H 0.77568400 3.14301700 -1.56576800
H 0.11901100 2.89699800 -3.19557700
C -3.47153400 -0.20433300 2.21263900
H -3.18471500 0.67185000 2.80306600
H -4.56286000 -0.21768600 2.14000200
H -3.14945100 -1.10357000 2.74461700
C -3.28999200 1.13388200 0.06564800
H -2.85752800 1.17899300 -0.93706000
H -4.37934800 1.15470300 -0.02921700
H -2.98504200 2.02772400 0.61943600
C -3.25077200 -1.40147400 -0.01171000
H -4.33777800 -1.42818900 -0.12841700
H -2.79661700 -1.38302800 -1.00613300
H -2.94100700 -2.31518600 0.50341300
H 0.05024600 1.47155500 1.59226400
H -0.90007400 0.93439900 1.54518400

Compound
$[VH(PMe_3)_2(NH\mathit{t}Bu)(N\mathit{t}Bu)]^+$ (4A)
E (a.u.) = -1419.86003077
ZPE (a.u.) = 0.504171
V 1.25510900 0.11029700 0.33317500
N 1.12415500 0.05439800 1.95699100
H -0.26821800 0.25034600 -0.31018600
N 3.02662100 -0.00903300 -0.16456800
H 3.62616800 -0.09853500 0.65835200
C 3.87317600 -0.02288400 -1.37775300
C 2.98285200 0.13569900 -2.61702200
H 2.24830500 -0.67336700 -2.68253400
H 2.44823200 1.09048900 -2.59880700
H 3.58329300 0.11103600 -3.53055900
C 4.87944400 1.14261000 -1.29499500
H 5.51406400 1.05413000 -0.40669000
H 5.53291700 1.14745100 -2.17278300
H 4.36095000 2.10516500 -1.25045300
C 4.63572100 -1.36186000 -1.43859000
H 5.29594100 -1.38664500 -2.31101900
H 5.25537200 -1.50366700 -0.54670300
H 3.94267700 -2.20560700 -1.51156900
C 1.32362000 -0.02560500 3.40001500
C 2.83242300 -0.15701800 3.68770100
H 3.37777600 0.71424500 3.31173100
H 3.00851000 -0.22716900 4.76543200
H 3.24003800 -1.05818900 3.21896600
C 0.76257400 1.25503100 4.04996800
H -0.31025900 1.34966800 3.86123100
H 0.91576400 1.21803400 5.13271000
H 1.27101500 2.14482400 3.66769400
C 0.56587000 -1.25639100 3.93703000
H 0.94255400 -2.17798200 3.48416100
H 0.70391000 -1.33218000 5.01981600
H -0.50554300 -1.17281100 3.73499900
P 0.26316800 -2.05769600 -0.15125600
P 0.59906000 2.43242400 0.03739400
C -0.95470400 2.87551300 0.91329600
H -1.18344500 3.93624900 0.77390100
H -1.77534000 2.27035700 0.52243400
H -0.84841600 2.66641000 1.97907800
C 1.82374000 3.66688200 0.65162400
H 2.76182600 3.55284100 0.10329500
H 1.45232100 4.68827900 0.52360900
H 2.02397900 3.48830400 1.71071600
C 0.27817800 2.97271000 -1.69534100
H -0.08515600 4.00492200 -1.70484500
H 1.19302900 2.92179900 -2.29026500
H -0.47387200 2.32481800 -2.15130500
C -1.36879500 -2.32648700 0.65042700
H -2.07314900 -1.57101900 0.29615900
H -1.75179100 -3.32364800 0.41368400
H -1.27010400 -2.22635700 1.73271200

C -0.07866600 -2.40003700 -1.93034400
H 0.85273000 -2.43396000 -2.50048600
H -0.58510200 -3.36447800 -2.03467100
H -0.71613600 -1.61519900 -2.34395900
C 1.25948400 -3.51841400 0.37577600
H 1.44894800 -3.46521400 1.45030100
H 0.73378800 -4.45165700 0.15125100
H 2.22185600 -3.51476500 -0.14159200

Compound
[VH(PMe$_3$)(NH*t*Bu)(N*t*Bu)]$^+$ (4B)
E (a.u.) = -988.695129819
ZPE (a.u.) = 0.387739
V -1.19983100 -0.00700400 0.43215600
N -0.56018000 1.06601500 1.44091200
N -2.90478400 -0.15406600 0.99523500
P -0.67063000 1.10778400 -1.78918700
H -0.47447500 -1.27814700 1.09920400
H -3.31599700 0.37428900 1.76126400
C -3.81781500 -1.19919800 0.46864800
C -5.06447000 -0.51331500 -0.12190300
H -4.79301400 0.15706600 -0.94331000
H -5.76395500 -1.26334100 -0.50324700
H -5.58660400 0.07360900 0.64036900
C -3.06929000 -1.98701700 -0.62080900
H -2.80361000 -1.34505300 -1.47137700
H -2.16742400 -2.46918300 -0.21863000
H -3.69965800 -2.78521500 -1.02123500
C -4.21154900 -2.13408100 1.62774700
H -3.33021500 -2.62150500 2.05299500
H -4.71617200 -1.57618300 2.42343900
H -4.90171000 -2.90537400 1.27243000
C -1.21732900 2.86295600 -1.79363700
H -0.74432600 3.39546900 -0.96570900
H -0.94817700 3.34696900 -2.73711900
H -2.30111800 2.91094500 -1.66186100
C -1.35010900 0.40548700 -3.35064800
H -0.98903000 0.97982000 -4.20915500
H -1.03872900 -0.63599200 -3.46668500
H -2.44231800 0.44483300 -3.33571200
C 1.14949700 1.16190900 -2.06459500
H 1.63740000 1.65073400 -1.21830100
H 1.54625300 0.14694200 -2.15513000
H 1.37944700 1.71313300 -2.98134900
C -0.02249000 1.92234500 2.48781200
C -1.02345000 3.06985500 2.73127800
H -0.63572300 3.73468200 3.50860300
H -1.17791000 3.65937400 1.82298700
H -1.98996200 2.68343900 3.06666400
C 0.15221000 1.06244000 3.75666900
H 0.83769800 0.23190400 3.57188200
H 0.56021200 1.68228700 4.56063100
H -0.80659400 0.65454400 4.08707100
C 1.33779800 2.47060900 2.01015900
H 2.03681200 1.65563600 1.80317100
H 1.22318600 3.08122900 1.10905300
H 1.77047800 3.10185100 2.79173300

Compound PMe$_3$
E (a.u.) = -461.107455925
ZPE (a.u.) = 0.113026
P -0.70997500 0.15708600 -0.12536900
C 0.26587200 1.09058900 -1.41342400
H 0.17970900 0.58010900 -2.37761300
H -0.15251200 2.09482500 -1.53222600
H 1.32784700 1.18004900 -1.15658100
C -0.16278000 1.08133600 1.40077100
H -0.59965700 2.08472500 1.39607000
H -0.53100900 0.56472400 2.29252000
H 0.92722500 1.17284900 1.47207100
C 0.36499100 -1.35996500 0.03243500
H 0.01675600 -1.96754500 0.87345200
H 0.27433700 -1.96713900 -0.87358500
H 1.42255800 -1.11692000 0.18808800

Compound H$_2$
E (a.u) = -1.17853933615
ZPE (a.u.) = 0.010174
H -1.47072700 1.04037300 -0.05609300
H -2.21351900 1.04037300 -0.05609300

Table E.2: Atom Cartesian coordinates and energies for Chapter 3.

Compound 9
E (a.u.) = -1531.558382
ZPE (a.u.) = 0.493224

V -0.01702611 0.44835414 0.00000000
P 0.26308189 -1.89433386 -0.81236500
P 0.33759689 2.42477814 1.47751500
C -0.23072011 -3.20603686 0.38420700
H -0.11701711 -4.19748986 -0.06440800
H 0.39100689 -3.15416386 1.28180200
H -1.27243711 -3.06107986 0.67738800
C 1.96629289 -2.38603386 -1.31593200
H 1.97042489 -3.40596486 -1.71210500
H 2.33339289 -1.70107986 -2.08326200
H 2.64342789 -2.34064686 -0.45895100
C -0.75006511 -2.26118486 -2.30354800
H -0.67952011 -3.32417686 -2.55415400
H -1.79217111 -1.99896186 -2.11605000
H -0.39035911 -1.67009286 -3.14716200
C -0.18244211 2.22220214 3.23339200
H 0.38318689 1.41448614 3.70524100
H -0.00983611 3.14595914 3.79392000
H -1.24380511 1.96975614 3.27404500
C 2.07329389 3.03077714 1.60809200
H 2.46611789 3.23578714 0.61014500
H 2.11607489 3.94479014 2.20803300
H 2.70488889 2.27360414 2.07999600
C -0.59447811 3.90784214 0.91379700
H -1.65882211 3.67593114 0.85293100
H -0.44272511 4.73658814 1.61225300
H -0.24877611 4.20506614 -0.07779300
N 0.50572689 1.20824214 -1.39288700
N -1.66217611 0.31947614 0.26407100
C -3.11190011 0.33559714 0.22700700
C 0.67246789 1.92630214 -2.64122900
C 1.24711489 0.95585914 -3.69698300
H 1.43627889 1.49268714 -4.63143400
H 2.19157789 0.52287114 -3.35474700
H 0.54207489 0.14853614 -3.91189000
C -0.67941311 2.48986014 -3.12177800
H -1.10741911 3.16365114 -2.37410400
H -0.54778611 3.04951514 -4.05314100
H -1.39280411 1.68172814 -3.30221300
C 1.68360589 3.07343314 -2.41363900
H 1.30554889 3.79569914 -1.68452800
H 2.64030289 2.68186914 -2.05564500
H 1.85994589 3.60773114 -3.35209000
C -3.62238211 -1.11164386 0.41091100
H -3.26288211 -1.53318386 1.35418100
H -4.71648611 -1.12310986 0.42491500
H -3.29230511 -1.75372686 -0.41066100
C -3.62342011 1.19852114 1.40235300
H -3.29308211 2.23606414 1.30270300
H -4.71746411 1.19581114 1.41809400
H -3.26708111 0.80315914 2.35802600
C -3.61503511 0.91142114 -1.11170300
H -4.70923111 0.93269214 -1.12659800
H -3.24799011 1.93023314 -1.25936500
H -3.27493111 0.30029514 -1.95277200
C 1.37319089 -0.31783386 1.39274100
O 2.12440189 -0.73206386 2.14526600